DOE/ER/61916--T1

Reconciling Uncertainties in Integrated Science and Policy Models: Applications to Global Climate Change

A DISSERTATION SUBMITTED

IN PARTIAL FULFILLMENT OF THE REQUIREMENTS

for the degree

DOCTOR OF PHILOSOPHY

in the Department of

ENGINEERING AND PUBLIC POLICY

Milind Kandlikar

Carnegie Mellon University

Pittsburgh, PA 15213

December 1994

DISCLAIMER

Abstract

Uncertainties are endemic to science and policy models of global climate change. Although it is impossible to make accurate predictions of future socio-economic outcomes, characterizing the relevant scientific and economic uncertainties could provide important insights for policy. Integrated assessments provide the platform for analyzing the role of these uncertainties. In this thesis tools of data reconciliation are used to integrate available information into scientific and policy models of greenhouse gases. The role of uncertainties in scientific and policy models of global climate change is examined, and implications for global change policy are drawn.

Methane is the second most important greenhouse gas. Global sources and sinks of methane have significant uncertainties. A chance constrained methodology was developed and used to perform inversions on the global methane cycle. Budgets of methane that are consistent with source fluxes, isotopic and ice core measurements were determined. While it is not possible to come up with a single budget for CH_4, performing the calculation with a number of sets of assumed priors suggests a convergence in the allowed range for sources. In some cases -- wetlands (70-130 Tg/yr) , rice paddies (60-125 Tg/yr) a significant reduction in the uncertainty of the source estimate is achieved. Our results compare favorably with the most recent measurements of flux estimates. The approach also constrains fossil CH_4 flux estimates as well as other anthropogenic emissions from biomass burning and landfills. For comparison, a similar analysis using bayes monte carlo simulation was performed.

The question of the missing sink for carbon remains unresolved. Two analyses that attempt to quantify the missing sink were performed. First, a steady state analysis of the carbon cycle was used to determine the pre-industrial inter-hemispheric carbon concentration gradient. The analysis shows that the value of the missing sink could be reduced by 0.6 GT/yr, although that number depends critically on the covariance between seasonality of the carbon concentration and seasonality of atmospheric transport. Second, a full blown dynamic inversion of the carbon cycle was performed. An advection diffusion ocean model with surface chemistry, coupled to box models of the atmosphere and the biosphere was inverted to fit available measurements of ^{12}C and ^{14}C carbon isotopes using Differential- Algebraic Optimization. The biospheric uptake inferred from the calibrated dynamic mode of the carbon cycle is about 1.9 GT/yr for 1990. This implies a net oceanic uptake of 2.2 GT/yr. The model effectively suggests that the "missing" sink for carbon is hiding in the biosphere. These results are in fair agreement with a number of recent estimates of the biospheric uptake. The inferred biospheric uptake trajectory for the past 200 years indicates that the biosphere has been responsible for almost as much uptake of atmospheric carbon as the oceans.

Comprehensive control strategies would be facilitated by the formulation of indices that allow for an evaluation of tradeoffs between greenhouse gases. An optimal control formulation was set up to determine values for such indices that incorporate the scientific and economic aspects of the greenhouse gas abatement. Scenario dependent trace gas indices were calculated for CH_4, N_2O, HCFC-22. Trace gas indices were found to be far more sensitive to the level of non-linearity in the greenhouse damages than to costs of abatement. The indices were also found to be reasonably robust over a wide range of possible outcomes of energy supply futures but depended critically on the choice of a discount rate. In the case of methane, scientific and economic uncertainties can cause the value of the index to vary by a factor of three.

Acknowledgements

My sincere thanks for all the support and help I received during the past four years. My debts are manifold and various.

To my family. My parents, Radha and Prabhakar, and my siblings, my sister Ratna and brother Sunil for everything they have given me. For their constant support and undemanding love. For their quiet confidence in my ability to fulfill my choices.

To Alexia Bloch for her warmth that sustains me, her sparks of encouragement in times of difficulty, her laughter and free spirit that makes my step lighter.

Looking back, none of this would have been possible without EPP's commitment to research and training unfettered by formal labels. Otherwise, I would surely have become another victim of the narrow intellectual labeling that pervades academia. An electrical engineer wanting a Ph.D. in environmental policy is just the kind of oddball that thrives in EPP. My time here has been one of intense intellectual growth, and I have learnt much from the people with whom I had the opportunity to interact.

Granger Morgan gave me the freedom to explore research topics and placed few restrictions on my early explorations. Later, he helped me crystallize ideas into specific research questions and tasks. Interaction with him has molded my view of policy research and his impact on my problem structuring and solving skills is immense.

Hadi Dowlatabadi has taught me much of what I know about energy & environmental economics and integrated policy modeling. As a co-advisor, he gave me just the right amount of guidance, providing advice and suggestions without cramping my style. His intellectual and personal support has been invaluable.

Urmila Diwekar aided and encouraged me in several ways. I constantly drew upon her expertise in various aspects of numerical modeling - optimization, optimal control, system identification. She spent long hours working with me despite her busy schedule; her encouragement and unsurpassed modeling skills helped me tackle some difficult problems.

Jayant Kalagnanam has been a wonderful teacher and friend. I have learnt an enormous amount from regular discussions with Jayant on a wide range of topics -- from system identification & non linear dynamics to behavioral decision theory & economics. His cutting intellect constantly forces me to clarify my thoughts, and his excitement over new ideas is infectious.

Indira Nair has been a source of inspiration and provided comfort and advice during difficulty. She patiently listened to my mundane and existential worries, and helped me sort through dilemmas. Indira was an anchor in the otherwise stormy world of graduate school.

Mitch Small helped me sort out some issues with bayes monte carlo simulation. His warm smile and encouragement were always reassuring.

Anand Patwardhan has been a genuine colleague and friend. Anand often helped me think through the scientific questions I was grappling with. Our continuing discussions on the limitations of quantitative policy analysis and sevral research collaborations have been very fruitful.

Despite my limited interaction with them Bob Ayres and Greg McRae have had a great influence on my fledgling academic career. Working with Greg taught me that any limits to analytical problem solving are mostly self-imposed. Bob's fundamental work in many different areas will continue to be a remarkable resource to draw upon.

EPP grads, particularly Pete A., Garrick L., Stu S., Elena S., Joe M., Tom A., Bill W., Jean C., Lucien R., Karen J., made life interesting and fun.

Priti Shah and Jim Hoeffner have been wonderful friends. I will miss the warmth and vitality of their company when we move on. Vibhu Mittal and Sujata Bannerjee welcomed me to their house when I needed to get away, particularly, after a distasteful brush with ivy league arrogance. Eileen Kraus was a supportive roommate and friend despite the vast gulf in our political views.

Ram has been a close friend for the past decade; his generosity and good humor have been a source of inspiration. Gopi's joy for life and music heartened me when I was homesick. Manu, Varun and Prasad cheered me on from the other side of the academic - corporate divide. Deba's solemn irreverence and Sanjeev's light headed banter provided much needed relief from academic sobriety.

Table of Contents

Chapter 1. Modeling, Uncertainty, and Climate Change

Concentrations of trace gases in the atmosphere have increased significantly in the past 100 years due to human activity. The rise in concentration of RITS (Radiatively Important Trace Substances) results in an increased atmospheric radiative forcing.[1] Water vapor is the most important greenhouse gas currently contributing to about 96% of the greenhouse effect. However, the change in radiative forcing is being *driven*[2] by the anthropogenic emissions of CO_2, CH_4, N_2O and other trace substances, including atmospheric aerosols which tend to offset a portion of the increase in radiative forcing. An enhancement of the greenhouse effect may, over time scales of a century or more, impact human and natural systems through a change in the Earth's climate. These changes include a rise in the Earth's mean surface temperature, a reduction in the equator to pole temperature gradient, changes in global and regional precipitation, and sea level rise. There are significant uncertainties associated with future predictions -- both in the inputs to and components of the physical climate system, as well as in the resulting impacts on human and natural systems. As a result no clear policy picture has emerged.

There have been some studies that attempt to characterize these uncertainties and rank their importance with respect to future outcomes (Dowlatabadi and Morgan, 1993; Peck and Teisberg, 1991). These studies have consistently shown that the impacts of climate change, given current state of knowledge, depend more upon future socio-economic variables--such as population and technological change and social discount rate--than upon the geophysical variables that are the focus of most current global change research. While these studies may be useful, the results should be

---

[1] Radiative forcing is defined as the change in the net heat flux to the atmosphere

[2] An increase in the global average temperature could increase atmospheric concentration of water vapor, which in turn would lead to increased surface temperature. This is the water vapor positive feedback.

treated with caution, because they tend to espouse a particular expectation of future outcomes, and a particular valuation of these outcomes. As Lave and Dowlatabadi (1993) note in their analysis on the role of personal belief and scientific uncertainty in climate change policy:

> ...The analysis suggests that scientific uncertainty is not the most important obstacle to decision making, the degree of optimism of the decision maker is moderately important, but the most important is the *decision criteria.*

If socio-economic factors and technological change are the key determinants of the effects of climate change, then making accurate forecasts about the variables that represent them in models of future worlds is an important requirement for predictive modeling. While models of socio-economic phenomena based on statistical extrapolations of past behavior are reasonably good predictors in the very short-term, they show poor performance and make noticeably overconfident predictions for longer time periods (Shlyakter et al., 1993), partly because they do not seem to capture long term "weak" feedback relationships. The "Limits to Growth" Models of the 1970s epitomize much that is wrong with long term predictive modeling; most models of the systems dynamics genre suffer from an inherent inability to characterize and parameterize long term interactions between the economy, society and environment. Even if we were able to somehow qualitatively describe all the interactions between model variables, we would still need to parameterize the model. Alas, a non-linear world with long term feedbacks is more complicated than the modeler's limited imagination. As shown by Smale (1974) a non-linear dynamic system of more than four variables can show essentially any behavior; the form of the model does not significantly constrain its behavior. The devil is in the mathematical details, i.e., the parameters and initial conditions of the assumed model form. Additionally, individual choice and co-evolution may make socio-economic models inherently unpredictable at the macro-level. In his excellent paper on long range modeling Ayres (1984) notes that long range models may never be able to make meaningful predictions; the goal should instead be to achieve qualitative realism without imposing assumptions of causal determinism between variables. Echoing similar ideas Herbert Simon (1987) suggests an approach to modeling for achieving prescriptive (as opposed to predictive) goals.

Despite the difficulties mentioned above, modelers of the world and the world(s) of modeling continue to predict in an undaunted manner, partly due to policymakers' demand for numbers and partly due to modeling being an alluring and self-fulfilling exercise. The recent explosion in models attempting to solve the Climate Change problem using a desktop computer is a case in point.[3] While little faith can be placed in model outputs that calculate "optimal global paths",[4] such as those from the DICE model, integrated models are useful for getting an overall understanding of the problem. They allow policy analysts to navigate in a systematic manner through a sea of uncertainties and may provide prescriptive information for use in research prioritization and resource allocation.

The limitations that plague the predictive capabilities of long term socio-economic models are present in the modeling of geophysical phenomena as well, particularly because natural systems are never closed and because model results may be non-unique (Oreskes et al., 1994). Feedbacks in geophysical models are also difficult to characterize because of a lack of historical analogs to rapid climate change and a poor understanding of coupled feedback processes; in some ways this is akin to the problem of weak feedbacks that plague socio-economic models.

However, models of geophysical phenomena may be easier to confirm and calibrate for two reasons. First, scientists can draw upon paleo-climatic information and laboratory studies to establish the nature of some of these feedbacks. Second, and more importantly, unlike for economic models, individual[5] choice and response ("co-evolution") may not affect the outcome of these models.[6] It must be stressed, however, that in the face of limited scientific evidence some aspects of geophysical modeling may suffer from these very same drawbacks. In particular, the response of

---

[3] At last count there were 14 such efforts underway.

[4] This "Optimality" is of course, limited by the assumption of the modeler. Experts have been known to make very poor predictions for extensively studied fundamental constants (Fischoff and Henrion, 1986). Given overwhelming evidence to the contrary it is hard to believe that any expert alive can make model-based reliable predictions of socio-economic variables for the year 2100.

[5] The "individual" is broadly defined to include decision-making entities such as firms, organizations and societies.

[6] Recent insights from complex systems regarding technological "lock in" arising from increasing returns to scale/positive feedbacks provide examples of how individual choices, which are inherently unpredictable, may affect long term economic outcomes (Arthur, 1990).

ecosystems to climate change and the resulting feedbacks into the climate system are poorly known. Observation and modeling of the geophysical phenomena have received significant attention in the past decade. Geophysical phenomena have been the focus of most federally funded research on global environmental change in the US and elsewhere. An important goal of this research has been to narrow the considerable scientific uncertainties in the predictions of future climatic variables. While observing that these scientific uncertainties may not be the most important in terms of understanding the effects of climatic change on human and natural systems, I will duck the question of efficient allocation of research dollars. That topic is beyond the scope of this thesis.

In this thesis an attempt is made to integrate available information with all its uncertainties into a consistent framework(s) for use in greenhouse scientific and policy debates. There are two reasons for such an effort. First, systematic analyses of uncertainties may provide new insights from already available data. This is by no means guaranteed, but given the lack of formal approaches for dealing with uncertainty in some aspects of the greenhouse scientific debate, it is an exercise well worth undertaking. The second reason stems from the enormous uncertainties that exist in the greenhouse policy debate. Building formal models helps characterize the role of each relevant scientific and economic uncertainty and thereby glimpses of their relative importance are provided. Such insights cannot be gained by focusing on scientific or economic aspects alone.

1.1 Scientific Uncertainties in Greenhouse Gas Cycles

The IPCC (Houghton et al., 1990) has identified the following as the most critical areas of scientific research:

- Control of greenhouse gases by the earth system
- Control of radiation by clouds
- Precipitation and evaporation
- Ocean transport and storage of heat
- Ecosystem processes

More recent scientific work suggests that anthropogenic aerosols may alter Earth's albedo enough to cause significant reduction in excess radiative forcing of the atmosphere (Charlson et al.,

1993; Penner, 1994). The uncertainties in aerosol effects affect predictions of global temperature change by *at least* as much as each of the above five categories.

That the atmospheric concentration of most greenhouse gases have increased since pre-industrial times is, perhaps, the single irrefutable piece of scientific evidence in current understanding of climate change. However, the problem of accurately determining the sinks and sources of greenhouse gases is a difficult one because of the global scale of the phenomena at hand. Uncertainties in the quantification and prediction of the sources and sinks of CO_2 and CH_4 can arise out of natural variability, lack of measurements and/or measurement error, and incomplete understanding of scientific phenomena. From a public policy viewpoint explicit characterization and reduction of the uncertainty is important because:

- It can affect predictions of future greenhouse concentrations, and consequently affect predictions of future impacts.
- Cost-effective mitigation strategies might require a more precise quantification of sources and sinks than currently available.
- Allocation of responsibility for greenhouse emissions on a nation by nation basis will require that estimates of greenhouse gas releases have low uncertainties.

Sources of greenhouse gases, (CO_2, CH_4 in particular), have large natural components and their sinks are controlled by natural processes. In addition, the amount of carbon in terrestrial and oceanic reserves is far greater than the amount in the atmosphere. The steady fluxes between these natural reserves are very much larger compared to anthropogenic release. Therefore, small changes in the factors controlling these fluxes can have a large affect on atmospheric concentrations. Conversely, minor perturbations to the parameters in models of biogeochemical cycles can lead to a large deviation in future predictions. Measurements of fluxes from natural sources[7] and sinks are fraught with uncertainties. Another way to obtain better estimates of sources and sinks and the interactions of greenhouse gases is by using concentration measurements to calibrate models of

[7] In the case of methane release from rice paddies, for example, there are several reasons that play a role in source flux uncertainty. There is significant seasonal, and geographical variability in source emissions (Matthews and Fung, 1991). Data from field measurement sites is scant, and scientific understanding of mechanisms of methane production by methanogens (as well as methane consumption by methanotropic bacteria) is insufficient (Nueu and Rogers, 1993)

biogeochemical cycles. However, the problem of determining sources and sinks of atmospheric species given measurements of concentrations in the atmosphere is an ill-posed inverse problem where small errors in the measured data can lead to significant errors in the estimates of sources and sinks. The ill-posed nature of the inverse problem may arise either due to lack of data in under-determined problems or because the problem structure is itself ill-posed. Therefore, inferred "best" estimates and percentile ranges for sources, sinks, and parameters could depend upon the choice of the inversion methodology. As pointed out by Enting (1990), this argues for the use of a wide range of techniques, and an examination of the trade-offs involved in these techniques. Additionally, inverse techniques could point to data gathering exercises and measurement strategies to answer questions regarding data worth.

Sources and sinks of greenhouse gases, particularly carbon dioxide, have been extensively studied. Nonetheless, there continues to be debate in scientific circles regarding uncertainties in greenhousegas cycles of both carbon dioxide and methane. Much of the recent debate on atmospheric carbon has been driven by the conclusions of a detailed study of meridional measurements of the atmosphere-ocean CO_2 flux (Tans et al., 1990). Tans et al. used the measured fluxes in conjunction with a model for atmospheric transport and distribution of carbon dioxide to compare source/sink scenarios for carbon dioxide. They concluded that the observed North-South inter hemispheric gradient of CO_2 could only be explained by a large northern biospheric sink. This conclusion is not supported by measurements of biospheric flux into the atmosphere and the meridional ^{13}C isotopic ratio. In response to Tans et al. (1990), several modifications and corrections to their budget have been suggested. Although these modifications serve to reduce the discrepancy, the puzzle of the "missing sink" is yet to be completely resolved; however, some recent literature (Sarmiento and Pacala, 1994) and work by the author indicate that the interpretation of a "missing" sink may in fact result from the inter-annual variability of the biospheric uptake.

Unlike CO_2, which is released mostly from the burning of fossil fuel, the sources of methane are mostly biogenic. Concentrations of methane have more than doubled since pre-industrial times. Agricultural activity and land use change have, to a large extent, contributed to this

increase. Because of the diffuse nature of the sources of methane, extrapolations of field measurements to a global value for each representative source type, e.g., release from rice paddies, have wide uncertainty bands. Additionally, the chemistry involving the hydroxyl radical, which is the main sink of atmospheric methane, is complicated and involves several hundred chemical species. As a result, the concentration of the OH radical is typically inferred from global cycles of anthropogenic chemical species not involved in complex tropospheric chemistry. The sink for atmospheric methane from such inverse calculation is far less uncertain than the source uncertainty.

1.2 Uncertainties in the Economics of Greenhouse Gas Emissions

A key element of possible policy responses to global climate change is the abatement of emissions of radiatively active gases, primarily CO_2. There is much debate in policy circles about the true cost of carbon abatement. Engineers and "bottom up" modelers have constructed supply curves for the costs of carbon abatement which show 30-50% reduction in CO_2 emissions at zero cost from unavailed energy efficiency opportunities. Energy economic "top down" modelers, on the other hand, predict that such a "free lunch" does not exist and that carbon abatement policies, especially those calling for stringent abatement measures, can be implemented only at very high cost. Most economic approaches to climate abatement attempt to quantify the costs and benefits (damages avoided) of carbon abatement and compare them in search of a rational policy response. Damages from climate change, or more precisely, the benefits of greenhouse abatement, may be the most poorly understood area of climate change research. This gets worse as one tries to quantify catastrophic, low probability, high consequence events. Most studies (Pearce et al., 1994) peg their numbers to one or two of the more detailed calculations carried out early in the game (Nordhaus, 1992; Cline, 1992) giving rise to serious questions about assumptions that could lead to systematic biases in damage estimates. While it is not expected that damage estimates will get sufficiently clarified in the near future, using quantitative damage estimates in scenario analyses may be one way

of explicating the range of future outcomes. Another approach that has recently gained currency in the greenhouse debate is the use of optimal control techniques that attempt to provide "optimal" global economic pathways, primarily due to the work of Nordhaus (1993). As mentioned earlier, these methods are highly suspect in terms of assigning any confidence to the optimal outcome, but when used judiciously for policy analysis they may provide some valuable insights.

Though much of the discussion and policy debate has focused on CO_2, there has been considerable recent interest in viewing the emissions abatement problem as one involving multiple gases and not CO_2 alone. Comprehensive abatement strategies were proposed by the US Government (USDJ, 1991) based on the rationale that all greenhouse gases, some more than others, contribute to climate change. Under a comprehensive plan greenhouse gas abatement must be carried out where "it costs least to do so" (Stewart, 1992). In such an approach a minimum cost solution would require the control of multiple gases, including Methane, Nitrous Oxide, and CFCs.

1.3 Description of Thesis

The foregoing discussion sets out the role of greenhouse gas cycles in the larger context of modeling for associated socio-economic and for geophysical phenomena, and prescriptions for policy responses. In the remainder of this chapter I will describe the goals of this thesis and the analyses accomplished to meet those goals. This will be followed by a chapter by chapter description of this document.

Integrating all available information in a consistent manner is a requirement for most problems of interest in global change; since uncertainty is endemic in this field, the modeler has to explicitly include it in his/her models. This thesis attempts to bring together tools of modeling and data reconciliation for attacking science and policy problems where uncertainty plays an important role. The thesis focuses on two problem areas. The first, global biogeochemical cycles, is a well studied topic of scientific research. Nonetheless, this thesis shows that building consistent frameworks for analysis and performing careful reinterpretations of available data may provide new

insights. The second problem area that the thesis considers is greenhouse gas abatement policy. Combining scientific and economic concerns effectively into policy analyses of global change problems is an important requirement for integrated assessments. Additionally, the role of time dynamics is key in global climate change policy formulation and hence has to be explicitly incorporated into policy analyses (Morgan and Dowlatabadi, 1994). This thesis brings together scientific and economic concerns in a dynamic framework for the assessment of multiple gas abatement policies.

The area of research in global biogeochemical cycles is enormous in terms of scope, complexity, and the size of the scientific community involved in the work so a single dissertation thesis can only nibble away at the issues. The attempt here is not to build elaborate, regionally disaggregated models of greenhouse gas cycles, but instead to focus on models that are small enough to provide meaningful interpretation of the available data. The thesis contains several coupled analyses that involving different inversion techniques for examine different parts of the problem.

In chapter 2 a description of the various inverse methods used, along with their advantages and disadvantages, is provided. The topic of inverse methods is vast and the literature spans a variety of disciplines. Although a comprehensive survey of inverse methods has not been attempted, the chapter intends to provide an overview of inverse methods and associated difficulties. In particular, a detailed description of each of the methods used in this thesis is provided.

In Chapter 3 the global cycle for methane is analyzed using two different inversion techniques. First the problem of inferring source uncertainties of methane is cast as a chance for a constrained programming problem, where uncertainties in sources and sinks are propagated directly through the global mass balance equations for the isotopes of methane and the pre-industrial ice-core record (Section 3.1). The mass balance equations serve as constraints in a least squares optimization problem used to determine the ranges on sources of methane that are consistent with atmospheric observations. The second part of the analysis uses the Bayes Monte Carlo technique to

find a consistent budget for methane. Prior distributions based on field measurements are provided for the sources of methane and sinks of methane. A Monte Carlo simulation of mass balance equations is used to determine the distribution on the atmospheric concentration for isotopes of methane. Atmospheric measurements for the different isotopes are used to determine a likelihood function for the model output. Using the Bayes rule, an updated posterior distribution for the model input and output variables and implications for the global budget of methane are determined (Section 3.2) .

Chapter 4 addresses the question of the missing sink in the global carbon cycle and contains two separate analyses. The first is an analysis of the pre-industrial carbon cycle and the insights that it can provide for resolving the missing sink controversy. The second is a full-blown inversion of a dynamic model of the carbon cycle where the time trajectory of the biospheric "missing" sink is estimated from pre-industrial times to the present. The steady-state analysis uses a simple hemispherically disaggregated box model of the carbon cycle. The model is posed as a non-linear programming problem with the objective of obtaining bounds on the pre-industrial inter-hemispheric asymmetry of atmospheric CO_2 concentrations.

The dynamic inversion uses a box representation of the ocean carbon cycle coupled with atmospheric and biospheric models. The model has N and S (North and South) hemispheric boxes for the atmosphere, well-mixed northern and southern (N and S) low and high latitude ocean surface boxes, well mixed high latitude (N and S) deep water boxes, an advective-diffusive interior box, and N and S hemispheric young/old biospheric boxes. The analysis seeks to determine the time trajectory of biospheric uptake, as well as model parameters for the ocean uptake and circulation. Atmospheric and oceanic measurements of Carbon-12 and -14 and a priori estimates of parameters determined from the steady-state analysis are used to perform the inversions. The analysis is done by posing the time dependent inversion as a Differential-Algebraic Optimization problem with an objective function that seeks to minimize the difference between model predictions and atmospheric and oceanic measurements.

Although much has been written on comparing emissions of different greenhouse gases, this literature is marred by an insensitivity to policy and economic issues as well as by poor science. Comprehensive control strategies would be facilitated by the formulation of indices that allow for an evaluation of tradeoffs between greenhouse gases in the abatement contexts described above. Such a greenhouse gas index would require the dynamic representation of the greenhouse forcings, as well as the global cycles of individual gases. Additionally, for most cases of interest to policy it is impossible to derive a purely scientific metric for comparing greenhouse gases. The economics of climate damages and abatement costs have to be explicitly included to make a meaningful comparison between the emissions of different gases.

A simple way of integrating the scientific and economic issues is by devising indices which compare the eventual economic impacts of unit emissions of different greenhouse gases. If greenhouse damages are a function of global mean temperature change, then the indices would depend on the future emissions of trace gases. Future emissions of trace gases are intrinsically linked to economic growth and abatement policies, which in turn, are governed by expectations of greenhouse damages. Trace gas indices that depend upon future emissions can be calculated either on the basis of emissions scenarios, such as those devised by IPCC, or using optimal control techniques where the trade off between damages and abatement costs is made explicit. In chapter 5 of this thesis the author attempts to comprehensively address the scientific and economic issues of multiple gas abatement policies and trace gas indices by performing these calculations. Conclusions and implications of this work are provided in Chapter 6.

Chapter 2: Inverse Methods and Applications to Greenhouse Gas Cycles

2.1 Introduction

The inverse problem is best understood in the linear form and clear discussions of this are provided by Enting and Newsam (1990) and Gelb (1988). The description below draws upon these references and attempts to :

1. Clarify the alternative approaches to inversion -- particularly for the under-determined inverse problem.

2. Make explicit the similarities between the linear form of the inverse problem and the inversion methodologies used in this thesis.

Let us assume that the set of n measurements, y, can be expressed as a linear combination of the m elements of a constant vector x, plus a random, additive measurement error, v. That is, the measurement process is modeled as

$$y = Ax + v \tag{2.1}$$

where A is an nxm vector. We term this the "forward" problem. For example, this could be the problem of obtaining concentrations, given sources, where y is the vector of observed concentrations, x is a vector of properties that can be observed only indirectly (source/sink terms), and the matrix A represents a model that predicts the observations given x. A is usually a discretized representation of some general operator, such as a continuous system represented by a system of differential equations.

The inverse problem of the above linear form involves determining the set of vectors x, given y and A. The linear form of the inverse problem in atmospheric sciences is often encountered in source receptor modeling (See e.g., Cass and McRae, 1983). If the number

of measurements m of y exceeds the number of terms n in x (m>n) then the measurement set contains redundant information, and the problem of estimating x is termed an overdetermined problem. However, if, m < n, then it is impossible to uniquely determine x for the given set of measurements and the problem is an under-determined inverse problem.

In least squares estimation, one chooses as the best estimate $\hat{x}$ that value which minimizes the weighted sum of squares of the deviations, $y_i - \hat{y}_i$, i.e. minimizes the quantity

$$S = (y - A\hat{x})^T W^{-1}(y - A\hat{x}) \qquad (2.2)$$

where W (mxm) is a weighting matrix. The solution to the equation $\frac{\partial S}{\partial \hat{x}} = 0$, gives the weighted least squares estimate $\hat{x}$.

$$\hat{x} = (A^T W^{-1} A)^{-1} A^T W^{-1} y \qquad (2.3)$$

The result in equation 3 holds for overdetermined problems. The estimate $\hat{x}$ in (2.3) can be determined if the inverse $(A^T W^{-1} A)^{-1}$ exists. If $(A^T W^{-1} A)^{-1}$ is ill-conditioned, i.e., its value is large or unbounded, then small errors in the measurement of y lead to large errors in inferred values of x. Such problems are called ill-posed inverse problems. In many practical problems $(A^T W^{-1} A)^{-1}$ may not exist and it is necessary to form an approximate inverse H, so that, x= Hy. This approximate inverse should have certain desirable properties:

- the solution is as close as possible to unique,
- the estimated parameters x provide a good fit to the data,
- the uncertainties in the estimates of x should not be too large.

The goal of any inversion is to satisfy the desired properties for the approximate inverse H. Although ill-posedness arises in both over and under-determined problems, the

discussion in this chapter will focus on under-determined problems because inversions of global biogeochemical cycles are typically under-determined.

If the problem is an under-determined one, then the solution for least squares inverse problem

$$\min\ (y - A\hat{x})W^{-1}(y - A\hat{x})^T \quad \text{is given by:}$$

$$\hat{x} = A^T W^{-1}(AW^{-1}A^T)^{-1}\mathrm{y} \tag{2.4}$$

Typically, since an under-determined problem has infinite solutions[8] the solution to (2.4) is unbounded. Unique solutions to under-determined inverse problems can be obtained by the use of external information through the following conditions:

Condition 1. Defining ranges on the allowed values of x.

Condition 2. Incorporating external information directly into the inversion in a least squares sense.

Defining ranges on the allowed values of x, is the simpler approach that weighs all elements in the vector x equally within the prescribed range. The least squares approach proceeds by defining a set of priors x_0 on variables x and adding the term $(\hat{x} - x_0)V^{-1}(\hat{x} - x_0)^T$ in the weighted least squares minimization equation (2.2), where V is a weighting matrix. The problem of finding the best fit $\hat{x}$ is no longer an under-determined one. The solution to the least squares problem in (4) can now be rewritten as:

$$\hat{x} = x_o + W^{-1}A^T(A^T W^{-1}A + V)^{-1}(y - Ax_o) \tag{2.5}$$

These results have no direct probabilistic interpretation; they were derived through deterministic argument only. Equations 2.3 and 2.5 can also be derived alternatively using statistical arguments based on Maximum Likelihood and Bayesian approaches respectively. In the Maximum Likelihood approach we choose the best estimate of x as that value which

---

8 The problem of fitting a line through a single data point is an example of an under-determined linear inverse problem.

maximizes the probability of the measurements y, taking into account the properties of noise v. Here x is still treated as a deterministic variable. The conditional probability density for y, given x, is the density for v centered around Ax. If v is normally distributed with mean zero and a covariance matrix W, then

$$p(y/x) = \frac{e^{-(\frac{1}{2}(y-Ax)^T W^{-1}(y-Ax))}}{(2\pi)^{m/2}\sqrt{det(W)}} \qquad (2.6)$$

To maximize p(y/x) the exponent in brackets is minimized--which is equivalent to minimizing equation 2.2 -- the over-constrained least squares inverse problem; the best estimate of x is given as in equation 2.3. Although it is possible to justify the incorporation of prior information in a Maximum Likelihood formulation[9] (See Enting, 1985), the probabilistic interpretations of under-determined inverse problems are best done using a Bayesian estimation approach.

In order to incorporate prior information about x, which we need to if the problem is under-determined, one can define both x and y as random variables and seek to maximize a chosen cost functional of the posterior conditional density function, p(x/y). From Bayes rule

$$p(x/y) = \frac{p(y/x) * p(x)}{p(z)} \qquad (2.7)$$

where p(x) is the prior probability density function of x and p(y) is the probability density function of the measurements. Depending on choice of the cost function, one can compute x from p(x/y). Two such cost functions are illustrated; the first is a maximum posterior objective and the second is the generalized minimum variance objective.

In the maximum posterior case, the objective is to maximize the probability that $\hat{x}$= x. The best estimator for x is $\hat{x}$ = mode(x) which is given by the condition $\frac{\partial p(x/y)}{\partial(x)} = 0$.

---

9 If x is defined to lie within allowable limits, then the maximum likelihood estimate in (2.6) is equivalent to condition (1) for the solution of under-determined inverse problems.

From this we can make the following observations about the under-determined inverse problem. :

1. When p(x) is uniform the above Bayes estimator is equivalent to the maximum likelihood estimator, within the prescribed range for x. This is equivalent to solving the under-determined problem using bounds on variables.

2. When p(x) is normal with mean x_0 and covariance V, the above Bayes estimator is equivalent to solving the under-determined inverse problem using the least squares estimator with prior information, using the solution given in (2.5).

The minimum variance objective is given by $(x-\hat{x})^T R(x-\hat{x})$,

The cost function to be minimized is $C(x/y) = \int (x-\hat{x})^T R(x-\hat{x}) p(x/y)dx$ (2.8)

where R is an arbitrary weighting matrix. It is easily shown that the minimum cost estimate is the condition mean estimate:

$$\hat{x} = \int x p(x/y)dx \qquad (2.9)$$

Assuming normal distributions for x (mean x_0, covariance V) and v (mean 0, covariance W), equation 9 results in an estimate :

$$\hat{x} = x_o + W^{-1}A^T(A^TW^{-1}A+V)^{-1}(y-Ax_o). \qquad (2.10)$$

This is exactly equal to the estimate derived from equation (2.5). Therefore, under assumptions of normality, the weighted least squares approach, the maximum posterior approach, and the minimum variance approach give the same results.

The earlier laid out the various approaches to carrying out inversions of under-determined linear inverse problems. A brief description of research on inverse modelling applied to global biogeochemical cycles is now provided.

Although inverse problems are very important to our understanding of the sources and sinks of greenhouse gases and other important species, relatively little work has been done in

systematically applying inversion techniques to problems in atmospheric chemistry, and evaluating their efficacy. There is, however, a rich literature on computational approaches to inverse problems in other areas such as hydrology,[10] Ocean Circulation (Bolin et al., 1983), and Systems Theory and Electrical Engineering. Kalman filtering has been used extensively in systems theory for the parameter estimation of dynamic systems and the first application of this technique in atmospheric chemistry is found in the recent work by Hartley and Prinnn (1993) for determining the surface emissions of trace gases.

Atmospheric inverse problems are often under-determined and ill-posed and the same is true of carbon cycle modeling. This actually involves a sequence of inverse problems (Enting, 1985a) corresponding to each of the different isotopes of carbon, as well as to steady-state conditions derived from ice core data. Other inverse problems in atmospheric chemistry are reviewed by (Enting, 1990a). Carbon cycle modeling studies have usually dealt with the inverse problem in an ad-hoc sense in that it has been typically treated as a part of the calibration of the steady-state. Little work has been done to simultaneously estimate parameters as well as time-varying sources and sinks. Explicit inversion studies have been performed by Enting and coworkers (Enting 1985, Enting and Newsam 1988, Enting and Newsam 1990b). Peng et al. (1983) have performed a deconvolution of the tree-ring based $\delta^{13}C$ record. Though little work has been done to explicitly invert the methane cycle, inverse methods have been used by (Spivakovsky et al., 1990; Prinn et al., 1992) to determine the atmospheric concentration of the OH radical from atmospheric circulation models and the measurements of methyl chloroform in the atmosphere.

In the following section (2.2) I will provide some details about the different techniques that can be used for inversion of global cycles, as well as a discussion of the limitations of the techniques.

---

[10] An excellent review of the inverse methods applied in hydrology is provided in Ginn and Cushman (1990).

2.2 Techniques of Inversion

This section provides a brief description of a variety of techniques that can be used for inversion of global biogeochemical cycles. In particular, an explanation of the inverse techniques used in this thesis is provided and linked to the discussion on inverse methods in the previous section. Additionally a description of other techniques not used in this thesis but applied to global biogeochemical cycles is provided for completeness. It should be noted that the solution of an inverse problem may be obtained either by the formulation of an inverse relation, i.e., the error minimization condition is explicitly specified as in equations 2.3 and 2.5, or by the (repeated) use of the forward model itself, as part of an optimization. I refer to the two techniques as, respectively, Filtering approaches and Optimization approaches. Both these approaches are applicable in the two contexts of interest -- inversions of steady-state models and inversions of dynamic models. The discussion below on the methodologies for inversion is certainly not comprehensive, but instead attempts to provide a more descriptive perspective of the techniques. A basic text or paper is cited where appropriate.

2.3 Optimization Approaches

Optimization approaches are commonly used for model calibration and inversion of steady-state as well as dynamic models. Here I will describe three such techniques in terms of their applicability to the inversion of global cycles. The first is chance constrained programming which can deal with steady-state or quasi steady-state inversions. The other two methodologies--the sensitivity equations approach and the differential algebraic optimization (DAOP) approach--can be used for the inversion of dynamic systems. The sensitivity equations approach is the more traditional approach to carrying out dynamic inversions; the DAOP approach is a new technique which has only recently gained attention in chemical engineering and has not been applied in the context of global biogeochemical cycles.

2.3.1 Chance Constrained Programming

Chance constrained programming (Charnes and Cooper, 1963; Vajda, 1970) can be used to perform constrained inversion under assumptions of linearity.[11] Uncertainties are directly propagated through the model. A typical CCO problem can be stated as follows:

$$\text{Optimize} \quad Z = C(X) \quad \text{(Cost Function)}$$

$$\text{Subj. to.} \quad P(A_i X \leq b_i) \geq \alpha_i \quad \text{(Constraint)}$$

X is a vector of independent random variables representing source and sink terms. The linear constraints define mass balances for different isotopes of the greenhouse gas. The approach involves stipulating the probability of a constraint violation ($1-\alpha_i$) due to uncertainty in measurements. The probabilistic constraints are converted into deterministic ones under the assumption that the distribution of random variables X is normal. The deterministic constraints are in terms of the moments of X. The problem is then solved using routine constrained optimization techniques. The cost function $C(X)$ is a least squares error function which seeks to minimize the difference between model variables and their observations. Additionally, if the problem is under-determined additional statistical information about the variables X can be incorporated into $C(X)$. In terms of the discussion in section 2.1, the chance constrained technique is equivalent to using the maximum posterior approach of section 2.1 where the variables X are its *moments*. Thus, the method attempts to find normal distributions for model variables X, that provide the best fit to the observations. This method has been applied to the global cycle of methane to arrive at consistent budgets for the methane cycle. A more detailed description of the approach and the results is provided in chapter 3.1.

---

[11] The use of linear mass balance relations for some gases is not unrealistic. For example, if the dependence of OH on levels of the methane in the atmosphere is ignored, the global mass balance for methane can be represented by a linear relationship. This is the approached followed by Fung et al (1991).

2.3.2 Sensitivity Equations Approach

This approach requires the numerical integration of the model of the equations corresponding to the sensitivity of the state variables to the model parameters, and of initial conditions. The numerical integration is performed in an "inner" loop while an optimization algorithm computes the updated initial conditions and parameter values in an "outer" loop. This process continues until the weighted least squares objective function--derived from the mean values--and a covariance matrix for the measured data (and/or parameters) is minimized (Bard,1974). Enting and Pearman (1987) have applied this technique to the calibration of a one-dimensional carbon cycle model. The ill-posed nature of the inverse problem was handled by imposing additional constraints. Enting and Pearman (1987) refer to this as "constrained inversion". Their approach to inversion involves the use of priors for parameter values as a part of the objective function. The sensitivity approach is restricted to the estimation of parameters which are not time-dependent, although it is possible to handle a time-dependent profile by assuming a functional form and estimating the (time-invariant) coefficients of that function. Furthermore, these techniques require the repeated solution of the forward problem and also of the sensitivity equations--which can be computationally intensive and can cause numerical difficulties in the case of stiff and non-linear systems.

2.3.3 Differential-Algebraic Optimization

An alternative to the sensitivity equations approach is to pose the inversion as a differential algebraic optimization problem (DAOP) where the sources are treated as time-varying parameters and the inversion is treated as a parameter estimation problem (Cuthrell and Beigler, 1987). In addition to source terms, the inversion also calculates optimal values of other parameters. The solution technique proceeds by discretizing the set of differential-algebraic equations and defining

the model using orthogonal collocation on finite elements. The resulting set of non-linear algebraic equations are treated directly as constraints in the minimization of the weighted least squares objective function. The optimization is performed using a Hybrid Successive Quadratic Programming (SQP) method, which gives a faster convergence compared to other methods. In addition, the SQP method readily provides sensitivity information. The weighted least squares parameter estimates obtained from this solution technique correspond to maximum likelihood estimates under the assumption that measurement errors are normally distributed with known covariance.

For under-determined problems external information can be readily provided by either specifying bounds on model parameters to the optimizer -- which is a practical requirement for most optimization algorithms or by incorporating them in the least squares objective function. One problem with this approach is the increase in dimensionality of the optimization problem for non-smooth data, i.e., when a large number of finite elements are required. The DAOP approach was applied to perform a dynamic inversion of the global carbon cycle. The model estimates the time trajectory of the biospheric and oceanic sinks of carbon from pre-industrial times to the present. Details of the analysis, the resulting estimates of sources and sinks, and implications for the "missing" sink of the carbon cycle are discussed in chapter 3. 2 of this thesis.

2.4 Filtering Approaches

In filtering approaches a direct inverse relationship is used to estimate the inputs. Equations 3 and 5 are examples of explicit inverse relationships. Both the approaches described in this section can be used for dynamic as well as steady-state inversions.[12]. This section provides a description of two such techniques--Bayes Monte Carlo simulation and Kalman Filtering.

---

12 Although Kalman Filtering is a dynamic filter, it is a general framework that can be easily adapted to the (trivial) steady state-case.

2.4.1 Bayes Monte Carlo Simulation

Bayes Monte Carlo Simulation is a technique that combines Monte Carlo Simulation with the Bayesian formulation discussed in section 2.1 but with a key difference. The approach simply provides posteriors distributions for the model input given assumptions on the priors x and observations on the model output y. In other words, Bayes Monte Carlo simulation provides distribution of the p(x/y) (equation 7, in section 2.1). The update distribution can be used as is to provide updated bounds/fractiles on the model variables. If the objective is to provide a best fit the updated posterior distribution can be used to either calculate the minimum variance Bayes estimator, using equation (8), or the mode of the updated posterior distribution to determine the maximum posterior estimate.

The advantage of the Bayes Monte Carlo approach is twofold. First, it can be used sequentially to update model input and output distributions as new information comes in. Second, the restrictions of normality can be removed. The price to be paid for the approach arises from the requirement of sampling. Bayes Monte Carlo approaches can be computationally expensive for large models and errors introduced from sampling in parameter estimates could be quite large if the problem is ill-posed. Bayes Monte Carlo Simulation was applied to the global methane cycle and consistent budget for methane was determined.

2.4.2 Kalman Filtering

As discussed above the Bayes Monte Carlo simulation approach uses the Bayes rule in conjunction with direct sampling of the parameter space. Kalman Filtering takes the idea one step forward. In Kalman filtering the updated Bayes minimum variance estimator is evaluated sequentially as measurements are made; it is written explicitly in a recursive form using a state space formulation assuming a normal error structure on model priors and observations. Kalman Filtering does not use sampling; instead, assumptions of normality make it possible to write state

space equations for the best estimate without the need for repeated measurements. The method is more computationally efficient than sampling and has a long history of use in engineering problems. In the context of Biogeochemical cycles the goal is to use a state space model to determine source strengths and parameter values that best reproduce measured concentration profiles using the recursive algorithm. In addition to the measurements, the approach requires a priori estimates of source distributions. The measured data, along with a state space representation of the inverse model, are used to refine these priors. Hartley and Prinn (1993) have recently carried out an inversion of atmospheric tracer data to obtain the source distributions for $CFCl_3$. Kalman Filtering explicitly provides estimates of error around the optimal parameters and time trajectories of state variables and, therefore, allows one to perform uncertainty analyses. Gelb(1988) and Papoulis (1974) are excellent basic texts on the topic.

Chapter 3: Inverse Methods Applied to the Global Methane Cycle

In this chapter two of the inverse methods described in the previous section -- Chance constrained Programming (Section 3.1) and Bayes Monte Carlo simulation (Section 3.2) are applied to the global cycle of methane. Methane is the second most important greenhouse gas contributing close to 15% of current radiative forcing. Abatement of methane could also provide a cheap short-term abatement option. The understanding of methane is plagued by some major uncertainties in its sources and sinks. This chapter deals with methodologies for providing consistent ranges on the estimates for sources of methane by using two different approaches described in chapter 2 -- Chance Constrained Programming (3.1) and Bayes Monte Carlo Simulation (3.2).

In section 3.1 a more detailed discussion of the role of methane in global climate change is provided (3.1.1). A description of Chance constrained Programming (CCP) is provided in section 3.1.2. Literature on measurements of individual sources and sinks of CH_4 is used to arrive at prior ranges for the same (Section 3.1.3). Constraints on the global budget of CH_4 derived from ^{12}C, ^{13}C, and ^{14}C isotopic mass balances and ice core data are described (section 3.1.4). A detailed description of the chance constrained programming formulation and the equivalent deterministic problem with minimum mean squared error objective function is provided (Section 3.1.5). An optimal budget(s) that is consistent with observations of atmospheric concentrations and fluxes is provided for CH_4 and compared with others in the literature. The results of sensitivity analysis are discussed (Section 3.1.6) and conclusions are provided in section (3.1.7).

Section 3.2 builds on section 3.1 in that the details of a global cycle for methane are not discussed in 3.2. Monte Carlo approaches (3.2.1) and its Bayesian variant (3.2.2) are described.

The application of the Bayes Monte Carlo approach to the global cycle of methane is discussed in section 3.2.3. Results and a brief comparison of the two inversion approaches used in this chapter are provided.

3.1 Inversion of the Methane Cycle using Chance Constrained Programming

3.1.1 Introduction

A better understanding of how the Earth System controls greenhouse gases has been identified by the IPCC as one of the five most critical areas in the study of climate (Houghton et al., 1990). Much of the initial focus has been on CO_2 and the role of methane frequently has been overlooked (Hogan et al., 1991; Harris et al., 1992). Methane (CH_4), currently contributes 15% to the overall radiative forcing--relative to 60% for CO_2--and is increasing at a rate of 0.8 - 1.0% per year (Steele et al., 1988). CH_4 also plays an important role in tropospheric chemistry and is involved in the series of chemical reactions that regulate concentrations of OH radical, the primary oxidizing agent in the atmosphere (See e.g., Hough 1991; Thompson and Cicerone, 1986; Logan et al., 1981).

Recently CH_4 has also been the focus of debate on comprehensive abatement of greenhouse gas emissions (USDJ, 1991). Hogan et al. (1991) assert that reductions in CH_4 emissions will be 20-60 times more effective in reducing potential warming to the Earth's surface temperature. Other studies have noted that CH_4 provides an attractive short-term abatement option (EPA, 1990) with negligible costs of abatement of some sources such as landfill emissions (Rubin et al., 1992). Despite the importance of CH_4 in the Earth's radiative and chemical balance, as well as its importance to a comprehensive abatement regime, its budget is not well known (Khalil and Rasmussen, 1983; Cicerone and Oremland, 1988). Uncertainties in CH_4 budget can significantly affect long term predictions of tropospheric chemistry models (Guthrie and Yarwood, 1991), as reflected in the current debate on slowing down of the atmospheric increase (Steele et al., 1992; Khalil and Rasmussen, 1993).

There is also a concern that uncertainties in emissions, particularly those of CH_4 and N_2O will make it very difficult to adopt comprehensive abatement strategies in the context of a global climate treaty (Victor, 1991; Grubb et al., 1992). Citing CH_4 sources from rice paddies and biomass burning as examples, Cicerone (1991) states that further research is needed to reduce "some very troubling" uncertainties in the current knowledge of greenhouse gas flow. Therefore, the explicit characterization and reduction of this uncertainty is an important task because it can both affect predictions of future greenhouse concentrations, and also impact mitigation and abatement policies.

The foregoing discussion summarizes the role of source/sink uncertainties of CH_4 as they relate to science and abatement policy. The rest of section 3.1 will focus on using inverse methods to address the issue of uncertainties in a global biogeochemical cycle of CH_4. We employ a specific inversion method using chance constrained programming to arrive at budget(s) for CH_4 which are consistent with observations and we also use sensitivity analysis to determine the key parameters in the mass balance of CH_4.

3.1.2 Chance Constrained Programming

Chance constrained programming (Charnes and Cooper, 1963; Vajda, 1970) can be used to perform constrained inversion under assumptions of linearity. This method involves

- Dealing explicitly with the uncertainties by attributing probability distributions to the individual source and sink terms using the available uncertainty bounds.
- Formally applying the constraints on the source and sink components and using optimization techniques to determine a budget with consistent values for source and sink ranges.

A typical CCP problem can be stated as follows:

$$\text{Optimize} \quad Z = C(X) \quad \text{(Cost Function)}$$

$$\text{Subj. to} \quad P(A_i X \leq b_i) \geq \alpha_i \quad \text{(Constraint)} \qquad (3.1.1)$$

is a vector of independent random variables representing source and sink terms. The linear constraints are mass balances for different isotopes of the greenhouse gas. The approach involves stipulating the probability of a constraint violation $(1-\alpha_i)$ due to uncertainty in measurements. The probabilistic constraints are converted into deterministic ones under the assumptions that the distribution of random variables X is a stable distribution.[13] The deterministic constraints are in terms of the moments of X. The cost function $C(X)$is a least squares error function, which seeks to minimize the difference between model parameters/variables and their prior/observed values. The deterministic problem can be then solved using routine constrained non-linear optimization techniques.

If $A_i(X)$is a weighted sum of independent normal random variables $X\{x_i\}$ the constraint $P(A_iX \le b_i) \ge \alpha_i$ is equivalent to the deterministic constraint,

$$\mu(A_iX-b)+q\sigma(A_iX-b) \le 0. \qquad (3.1.2)$$

where $q = F^{-1}(\alpha)$ μ and σ are the expected value and standard deviation operators and $F^{-1}(\,)$ corresponds to the inverse cumulative function of the normal N (0,1).

3.1.3 Characterization of Source Uncertainties

Most budgets of CH_4 provide bounds on individual sources and on the global source. However, there has been little effort in assigning statistical measures such as confidence intervals or standard deviations to these bounds. By assigning statistical meaning to individual sources of trace gases Khalil (1992) has shown that the unconstrained global source has less uncertainty than that derived from merely adding the upper and lower bounds of the individual source terms. This

---

13 Stable distributions are such that the convolution of two distribution functions, $F(x-u_1/v_1)$ and $F(x-u_2/v_2)$ is of the form $F(x-u)/v$, where u_i and v_i are two parameters of the distribution (Lukacs, 1972). Normal, Cauchy, Chi-square, and Poisson are all stable distributions and allow for the conversion of probabilistic constraints into deterministic ones

is equivalent to stating that the standard deviation of a sum of independent random variables is lesser than the sum of the individual standard deviations.[14] Khalil (1992) assumes a uniform, non-informative prior for source distributions with ranges that are symmetric around a median value. In our analysis we assume that the sources and sinks are normally distributed and we find the set of source distributions that best fit available flux and mass balance measurements. The choice of normal distributions was driven by the stability property.

For each source we prescribe upper and lower bounds U and L which are interpreted statistically in terms of fractiles. Source E_i is assumed to satisfy the probabilistic constraints

$$\begin{aligned} P(E_i \geq L_i) &\geq \alpha \\ P(E_i \leq U_i) &\geq \beta. \end{aligned} \tag{3.1.3}$$

For example, if $F^{-1}(\alpha) = F^{-1}(\beta) = 1$, then U_i and L_i define at least 1σ bounds on E_i.
U_i and L_i represent "worst case" unconstrained bounds in the sense that the range on the source i consistent with mass balance constraints is expected to be lower than that defined by U_i and L_i.[15] The choice of upper and lower bounds on individual sources is made on the basis of recent literature. In general, our choice of source ranges is more conservative than recent estimates in the literature, i.e., we tend to ascribe larger uncertainty bounds to the source values. A brief description for each source follows.

Wetlands

Wetlands represent the largest natural source of CH_4 and have large uncertainties associated with them. Detailed studies using classification of wetland and soil types were carried out by Matthews and Fung (1987), who estimated a global source of 100 Tg/yr, and by Asselman and Crutzen (1988), who estimated a range of 40-160 Tg/yr with a most likely value of 80 Tg/yr. Bartlett and Harris (1993) provide a detailed analysis of global sources from wetlands

---

14 For independent random variables x_i with standard deviation σ_i, the standard deviation of Σx_i is $\sqrt{\Sigma\sigma_i^2}$. Since $\sigma_i > 0$, this is always lesser than $\Sigma\sigma_i$.

15 In any case, the effect of selecting U_i and L_i can be determined by sensitivity analysis.

incorporating recent advances; they estimate a global source range from 80 to 115 Tg/yr. Although independent estimates of wetland emissions seem to cluster around 100 Tg/yr, the convergence may hide some major and systematic uncertainties related to the quantification of methane release from wetlands. In particular, uncertainties about the periods of seasonal methane production and the relative importance of climate--ecosystem interactions for different types of ecosystems have been cited as being major contributors to the uncertainty (Matthews, 1993). Additionally, there are few measurements of methane emissions from areas of major wetland emissions--particularly from Russia, which contains 30% of total global wetland area (Matthews, 1993; Bartlett, 1990). A similar lack of measurements plagues estimates of release from wetlands in Asia, as well as flooded wetlands of Africa. To account for these uncertainties, we chose a relatively large range of 70-150 Tg/yr.

Termites

Termites also represent a source of methane with a considerable variation in estimates of emissions. One early source cites an amount of 150 Tg/yr (Zimmerman, 1982), although recent studies cite much lower values--20 Tg/yr (Khalil and Rasmussen, 1990) and 26 Tg/yr (Martius et al., 1993). Other recent estimates also provide ranges for the emissions of 10-35 Tg/yr (Bachelet and Nueu, 1993) and 15-35 Tg/yr (Rouland et al., 1993). The uncertainties pertain mostly to the abundance of termites and their mode of nutrition. The difficulty in estimating the population of termites in each of the nutrition groups (e.g., wood feeding vs. soil feeding) is the reason for much of this uncertainty (Judd et al., 1993). For the purposes of this analysis we chose a range of 15-30 Tg/yr.

Oceans

Ehhalt (1974) was the first to include oceanic sources of methane in a global budget and suggested a value of 5-20 Tg/yr. Subsequently others (Khalil and Rasmussen, 1983; Fung et al., 1991) have used this value in their budget. More recent measurements by Lambert and Schmidt (1993) conclude that while the open ocean emits 3.6 TG/yr, emissions from coastal oceans--which

are high in methane--are 6.1 Tg/yr. This amounts to a total of about 10 TG/yr for the emissions of methane. For our analysis we chose a range of 5-20 TG/yr.

Geological Sources

Very large deposits of methane exist in crystalline form in and near the permafrost regions of the world. Kvenvolden (1988) estimates that this reservoir may hold between two thousand and two million Tg of carbon as methane. The estimated annual release for methane from CH_4 hydrate destabilization is expected to be low. Kvenvolden (1988) estimates a source of 3 Tg/yr from hydrate destabilization. Other minor geological sources of methane have only recently been estimated (Lacroix, 1993; Judd et al., 1993). Emissions from Volcanic (0.8-6.2 Tg/yr), Hydrothermal sources (0.9-3.7 Tg/yr), and other release pathways such as natural gas seepages (1 Tg/yr) all contribute to this category (Judd et al., 1993) which is broadly termed in this paper as geologic sources of methane. We specify a range of 5-15 Tg/yr for this category.

Agriculture

Agricultural sources followed by emissions from the energy sector are the largest contributors to anthropogenic sources of CH_4. Rice paddies, mostly from Asia represent some of the major source uncertainties. The uncertainties in rice paddies can be attributed to local environmental conditions, such as soil properties, temperature and rainfall, as well as traditional and modern agricultural techniques, including fertilizer application, irrigation, and choice of cultivars. A recent comparison of rice paddy emissions by Shearer and Khalil (1993) presents point estimates ranging from 50 Tg/yr (Bachelet and Nueu, 1993) to 82 Tg/yr (Matthews et al., 1987).[16] Another recent compilation provides ranges for rice paddy related emissions for a number of different studies whose estimates are typically in the range of 50-150 Tg/yr. (Renneberg et al., 1992; Wassman et al., 1993). Additionally, recent work by Wasmann et al.

[16]The calculation was done by Bachelet and Nueu (1993) using the Matthews et al. (1987) database.

(1993) estimates a global emissions range of 50-150 Tg/yr. Accordingly, we chose a range of 50-150 Tg/yr for the purposes of this analysis.

Ruminants

Although emissions from ruminants are among the best understood sources of CH_4, there are several contributing factors to uncertainties in their calculation. These include the uncertainty in the number of animals in a country, the amount of daily feed consumed, and methane yield per unit consumption (Johnson et al., 1993). Early estimates by Crutzen (1983) of 60 Tg/yr have been pushed upward to 65-100 Tg/yr (IPCC, 1990). A more recent and detailed calculation by Johnson et al. (1993) yielded a value of 79 Tg/yr (Johnson et al., 1993). Our choice of 60-100 Tg/yr is intended to reflect a 25% uncertainty in the value determined by Johnson et al. (1993).

Coal Mining

Coal mining contributes to emissions of CH_4 mostly via release underground mines, although surface and abandoned mines also contribute to the emissions inventory. The amount and rate of release depends upon the type of coal and local geology of the mine. Cicerone and Oremland (1988) use a synthesis of some of the early estimates of release from coal mining to come up with annual range of 25-45 Tg/yr. More recent calculations by Boyer et al. (1990) and Kirchgessner et al. (1993) have slightly higher values of 47 and 45.6 Tg/yr, respectively. In their recent work Beck et al. (1993) synthesize a number of studies and suggest a range of 35 - 48 Tg/yr. We chose a range of 25-50 Tg/yr for the purposes of our analysis.

Natural Gas

The production and transmission/distribution of natural gas contributes to emissions of CH_4 from venting at production sites or from fugitive emissions from leaking components. There is considerable uncertainty in the global value of these emissions resulting from a lack of hard data on a country specific basis (Beck et al., 1993). Some of the earlier estimates, such as those by Crutzen (1987) and Bolle (1986), are close to 35 Tg/yr. More recent estimates peg the actual value

to lie between 25-50 Tg/yr (Beck et al., 1993). Additionally, minor industrial sources of methane could contribute close to 10 Tg/yr to the global budget (Lacroix, 1993; Beck et al., 1993). To reflect this we chose a range of 35-60 Tg/yr for our range on methane emissions from natural gas.

Waste Management

Previous estimates of landfill emissions of 30-70 Tg/yr (Bingemer and Crutzen, 1987) may be higher than suggested by subsequent modeling analyses primarily because the earlier work assumed that no oxidation of CH_4 took place inside the landfill. Recent analyses suggest a far lower figure with uncertainties arising from estimates of amounts of refuse landfilled, the CH_4 generating potential of the refuse and the oxidation of released CH_4 by methanotropes (Peer et al., 1993; Augenstein, 1990). The recent analyses by Thorneloe et al. (1993) calculate a far lower number of 21 Tg/yr. Additionally other waste management practices, particularly waste water treatment (Orlich, 1990) and emissions from livestock waste (Safley, 1992), may contribute up to 40 Tg/yr, although very few studies exist on those sources and the numbers are highly uncertain. To accommodate for this uncertainties we chose a range of 30-80 Tg/yr .

Biomass Burning

Biomass burning represents a large anthropogenic source of CH_4 that has recently received much attention.[17] The actual amount of CH_4 released in the atmosphere depends on the mass of annual burned biomass for each ecosystem type, the carbon content of the biomass, and the emission factor that links the carbon content to CH_4 emissions. Much of the uncertainty in the biomass emission source is contributed by the uncertainty in the total mass of the burned biomass. Levine et al. (1993) estimate the amount of methane released from biomass burning to be 51.9 Tg/yr with a range of 29-75 Tg/yr. In accordance with their numbers we chose an annual range of 30-80 Tg/yr CH_4 emissions.

---

17 See Levine et al. , 1991, for details.

Sources (Tg/yr)	Lower bound(L)	Upper bound (U)
Wetlands	70	150
Rice	50	150
Landfills+	30	80
Biomass	30	80
Coal Mining	25	50
Natural gas	30	65
Oceans	5	20
Ruminants	65	100
Geologic*	5	15
Termites	15	30

Table 3.1.1. Range of CH_4 source emission by type of sources
(* includes hydrates, volcanic and hydrologic emission / seepage of methane
+ including other waste management practices)

Sources (Tg/yr)	R	Q
Wetlands	0.939	1.16
Rice	0.939	1.12
Landfills	0.947	1.15
Biomass	0.975	1.37
Coal Mining	0.959	0
Natural gas	0.935	0
Oceans	0.96	1.16
Ruminants	0.95	1.2
Hydrates	0.938	0
Termites	0.94	1.24

Table 3.1.2: Prior values for isotopic fractionation ^{13}C (R), and ^{14}C (Q) isotopes for sources of CH_4.

Chemical destruction in the atmosphere by reaction with the hydroxyl (OH) radical is the primary mechanism for removal of CH_4 from the atmosphere. Soil absorption and loss to the stratosphere, the other reported sinks of CH_4, were not considered. The levels of OH are inferred from measured concentrations of methylchloroform and atmospheric tracer models. Methylchloroform has no natural sources and OH is its primary sink. Concentrations of OH radical in the atmosphere are determined to an accuracy of 20% from tracer studies of CH_3CCl_3 (Prinn etal., 1987; Spivakovsky et al., 1990; Prinn et al., 1993). The range for the concentration of the OH radical was chosen to be $(8.1\pm 0.9)* 10^5$ radical /cm^3 in accordance with Prinn et al. (1993)

3.1.4 Mass Balance Constraints

Constraints on the global budget of methane are provided by isotopic mass balances and ice-core data. ^{13}C and ^{14}C mass balances make it possible to discriminate between sources because different sources have differing isotopic ratios. Ice core data provides clues regarding pre-industrial emissions.[18]

^{12}C Mass Balance

Concentration of the main isotope of CH_4 (^{12}C) in the atmosphere has been increasing at the rate of about 0.8-1%/yr, over the past decade (Trends, 1990; Khalil and Rasmussen, 1991). This corresponds to an increase in the atmosphere of between 40-48 Tg/yr (IPCC, 1990).[19] If the dependence of OH on levels of the CH_4 in the atmosphere is ignored--a reasonable assumption for time scales of one year--the global mass balance for isotopes of CH_4 can be represented by a linear relationship. The mass balance for ^{12}C is written as:

$$\frac{dC}{dt} = \sum_{i=i}^{10} E_i - K * OH * C \qquad (3.1.4)$$

---

18 Although pre-industrial anthropogenic sources of methane were not considered in this study, Kammen and Marino (1993) suggest that they may have been as high as 10 Tg/yr.

19 Recent data suggests that the build up of methane has slowed considerably (Khalil and Rasmussen, 1993).

The probabilistic mass balance constraint is:

$$P[\sum_{i=1}^{10} E_i - K*OH*C \geq I_l] \geq \alpha$$

$$P[\sum_{i=1}^{10} E_i - K*OH*C \leq I_u] \geq \beta \qquad (3.1.5)$$

Where E_i represent the individual source terms (i=1,10), K is the rate constant for the reaction between CH_4 and OH, OH represents the atmospheric concentration of the OH radical, and C is the amount of CH_4 present in the atmosphere (4650±100 Tg). The recent reduction in the rate constant K by 25% (Vaghjiani and Ravishankara, 1991), suggests a lower sink term for the OH radical than previously accepted. I_u and I_l are the values of the upper and lower bounds on I, the measured annual increase in the amount of atmospheric CH_4. The values for α and β were picked such that the upper and lower bounds define at least the 1σ bound on the observed atmospheric increase.

^{13}C Mass balance

Differences in ^{13}C isotopic concentrations in different sources arise because anaerobic bacteria which produce CH_4 show a marked preference for ^{12}C over ^{13}C during CH_4 production (Stevens, 1987). The isotopic fractionation of a sample R is defined with respect to the Pee Dee Belemnite standard as $R = \frac{(^{13}C/^{12}C)_{sample}}{(^{13}C/^{12}C)_{standard}}$ in terms of $\delta^{13}C$, R can be written as $R = \frac{\delta^{13}C_{sample}}{1000} + 1.$

The mass balance for ^{13}C is written as:

$$R_g \frac{dC}{dt} + C\frac{dR_g}{dt} = \sum_{i=1}^{10} R_i * E_i - K * Kj * OH * Rg * C \qquad (3.1.6)$$

In equation (8), the isotopic fractionation ratio for atmospheric CH_4 is denoted by R_g, $\frac{dC}{dt}$ is the annual increase in atmospheric CH_4, and $\frac{dR_g}{dt}$ is the annual change in the ^{13}C isotopic fractionation, henceforth referred to as R_g'. Additionally, the ^{12}C isotope reacts slightly faster than ^{13}C isotope with the OH radical. The kinetic fractionation ratio, K_j, is the ratio of reaction rates for the reaction of OH with the two isotopes (K_{13}/K_{12}). Quay et al. (1991) provide isotopic fractionation ratios for sources taken from the literature and measured isotopic fractionation values for atmospheric CH_4 (Table). They also provide corrections provide a new estimate of K_j--0.993±0.002. The ^{13}C isotopic fractionation ratio has been observed to be increasing in the atmosphere (Stevens, 1993). On an average the increase $\delta^{13}C$ fractionation in the Northern Hemisphere in the years 1983 to 1988 was 0.112±0.008 $^{o}/_{oo}$ per year. During the same period the trend in the Southern Hemisphere was observed to be 0.14 $^{o}/_{oo}$ per year (Stevens, 1993).[20] We used an average of the two quantities to determine the global trend R_g'. The probabilistic constraint for equation (3.1.6) can be derived analogously from equation (3.1.5).

^{14}C mass balance

The measurement on ^{14}C content of CH_4 provides an additional constraint on the source term for CH_4 since the fossil sources of CH_4 contain little or no radiocarbon. This is in opposition to the recent biogenic sources which contain background levels of radiocarbon. The fraction of atmospheric CH_4 that is depleted in ^{14}C is a measure of the fossil sources. Natural gas, coal mining, and release from hydrates are the known sources of CH_4 depleted in ^{14}C (Cicerone and Oremland, 1988). The isotopic fractionation of a sample, Q, is defined with respect to an oxalic acid standard as

$$Q = \frac{(^{14}C/^{12}C)_{sample}}{(^{14}C/^{12}C)_{standard}} \text{ in terms of pMC, } Q = \frac{pMC}{100}..$$

20 A more detailed discussion of the problems associated with the interpretation of hemispheric trends is provided in Stevens (1993). A second study by Lassey et al. (1993) shows no observed trend.

The mass balance equation for $^{14}C\ CH_4$ is :

$$Q_g * \frac{dC}{dt} + C * \frac{dQ_g}{dt} = \sum_{i=1}^{10} Q_i * E_i + \frac{E_{nuc}}{A_{abs}} - K * K^{2_i} * Q_g * OH * C \qquad (3.1.7)$$

Nominal ^{14}C fractionation values Q and associated uncertainties were taken from data summarized by Quay et al. (1991). $^{14}C\ CH_4$ released from water pressurized nuclear power plants has to be accounted for in the mass balance; one estimate of the global release of this source is $8*10^{24}$ molecules (Quay et al., 1991). A_{abs} is the $\frac{^{14}C}{^{12}C}$ ratio for the standard and is equal to $1.176*10^{-12}$ (Stuiver and Pollach, 1977) and the annual increase in the value of atmospheric fractionation ratio Q_g' is 1.4±0.5 PM/yr as measured by Quay et al. (1991). The probabilistic constraint for equation (3.1.7) can be derived analogously from equation (3.1.6).

Ice core data

Ice cores from different locations in polar regions give historic information regarding CH_4 concentrations. The measurements provide strong evidence that concentrations of CH_4 in a pre-industrial atmosphere were stable at around 650 ppbv (Khalil and Rasmussen, 1982; Pearman and Fraser, 1988; Raynaud et al., 1988). These concentrations reflect emissions of CH_4 from historic sources that were primarily natural. After accounting for changes in the global sinks from pre-industrial times Khalil and Rasmussen (1990), conclude that the fraction of anthropogenic CH_4 emissions should be between 40%-70% of total emissions, which is equivalent to the 30-60% range for natural emissions. This translates into a constraint on the natural sources of CH_4 as follows:

$$P[\sum_{n=1}^{N} E_n - f_1 * \sum_{i=1}^{10} E_i \geq 0] \geq \alpha$$

$$P[\sum_{n=1}^{N} E_n - f_2 * \sum_{i=1}^{10} E_i \leq 0) \geq \beta \qquad (3.1.8)$$

where f_1 and f_2 are the minimum and maximum values of the natural fraction of CH_4 emissions and equal to 0.3 and 0.6, respectively.

3.1.5 Model Formulation

The objective function is a mean square error function of the form $e^T We$, where the vector e is the difference between variables and their observed values and parameters and their priors and W is a weighting matrix. The probabilistic constraints translate to a deterministic feasible region in the space defined by means and standard deviations of the source and sink distributions. The objective function is minimized within this feasible region. The formulation is given by:

$$\begin{aligned} &\text{Minimize} && e^T We \ \text{(Cost Function)} \\ &\text{Subj. to.} && F(\mu, \sigma) \geq 0 \end{aligned} \qquad (3.1.9)$$

where $F(\mu, \sigma) \geq 0$ is the set of deterministic equivalents of the chance constraints for the isotopic mass balances and ice-core data constraints. Deterministic equivalents of the chance constraints are easily obtained using equation 4, with α and β set uniformly to 1.

The least squares objective function $e^T We$ is given by:

$$\sum_i \frac{(x_i - x_{i(obs)})^2}{\gamma_{x_i}^2} + C_1 \sum_i \frac{(y_i - y_{i(obs)})^2}{\gamma_{y_i}^2} \qquad (3.1.10)$$

The variables x_i are the model variables and parameters that can be directly observed or inferred. The observations used for calibration are the annual increase in the global concentrations of ^{12}C, ^{13}C, and ^{14}C isotopes and the concentration of CH_4 and OH in the atmosphere. In addition x_i includes measured parameters such as the isotopic fractionation ratios for individual sources and reaction rates. The weights γ_x can be interpreted either as the variance of a parameter with normal

distributions or as describing half the range on an unknown parameter to be determined by the optimization. For each x, γ_x was chosen to reflect this variability.

The problem of determining sources and sinks is under-determined and thus requires the use of additional information in its solution. The variables y_i in equation (3.1.10) provide additional information regarding the sources and sinks of methane through the use of *prior* values for means (μ_i) and standard deviations (σ_i) of sources for CH_4 and ^{14}C CH_4 from nuclear reactors. The specification of priors on source μ_i and σ_i is equivalent to assigning prior distributions on sources. The optimization procedure then determines the posteriors on μ_i and σ_i given the prior values, the model, and measurements. By choosing plausible sets of priors, the optimization allows us to determine a set of plausible budgets for CH_4 which are *consistent* with observations and *optimal* for the assumptions on the priors.[21]

Normalizing factors γ_y are used to make the optimization independent of the units chosen in calibration. Because there is no clear method to decide on the actual value of weights γ_y, we used weights that are equal to 20% of the assigned prior for the elements. If the values for γ_y are small then the optimizer tends to pick posterior values close to the priors. For large values of γ_y the optimal values are equivalent to those determined by an unweighted least squares technique (Bard, 1974). A multiplying factor C_1 was used to test the sensitivity of the solution to the assumed value of γ_y[22]. The estimated value of the parameters was found to be relatively insensitive to C_1 over a wide range of values. Therefore C_1 was set to one in all model runs.

The inversion was carried out for three sets of prior values on the means and standard deviations of source terms. The priors on the means in each set are equal to the source terms in the scenarios used by Fung et al. (1991). The three sets we chose were the most likely budget (scenario 7 of Fung et al., 1991), the high fossil emissions scenario (scenario 5), and the high biomass emissions scenario (scenario 6). The specified priors on the means and standard deviations are

---

21 In terms of Bayesian inference, minimizing the least squares objective function is equivalent to maximizing the posterior likelihood of the estimated parameter.

22 In particular if $C_1 > 1$, then the normalizing weights used are overestimates. Conversely, $C_1 < 1$ implies that the normalizing weights are underestimated.

provided in table 3. The constraints on source flux of natural gas and biomass burning (Section 3, table 1) were relaxed for set 2 and set 3, respectively. Priors are also specified on the parameters that are independently measured, such as isotopic fractionation ratios (see table 3.1.2).

3.1.6 Results of the Inversion and Sensitivity Analysis

The non-linear optimization formulation was solved using the General Algebraic Modeling Software (GAMS) package (Brook et al., 1988) with successive quadratic programming (SQP). For each of the formulations an optimal feasible solution was found and the posteriors on the distribution of sources of CH_4 were obtained. Table 3.1.4 gives the posterior (1σ) ranges of sources and sinks in a global budget of CH_4.

The available information does not allow us to uniquely specify a global budget of CH_4 because different specifications on the prior values of the source distributions in general lead to different posterior distributions. Since the prior information is subjectively provided, the analysis was carried out on a scenario basis. For some of the sources, noticeably wetlands, the analysis yielded similar values for each of the scenarios. For others, particularly rice paddies, biomass burning, and natural gas there was significant variation in the estimated source range across the scenarios. It is not possible to determine the "best " set of priors from this exercise alone. Some other criteria, preferably one that uses new information has to be used to make possible the judgment of a best guess budget. Since seasonal and latitudinal constraints were not applied in this analysis but were a part of the 3D model synthesis done by Fung et al. (1991), we pick the budget that uses priors from the most likely scenario in Fung et al. (1991) as our "best guess" budget. However, each of the budgets in table 3.1.4 is consistent with measurements of atmospheric concentration, source flux measurements, and other relevant geophysical data such as reaction rates and fractionation ratios. While one study has checked previous budgets for consistency (Khalil and Rasmussen, 1990), no other study has presented budgets that are consistent with all

available globally averaged data where the uncertainty is explicitly characterized. The optimization formulation guarantees that constraints on the global budget are satisfied.[23] A comparison of the best guess budget with other recent budgets is provided in table 3.1.5.

The global source of CH_4 for each of the above budgets is 425-525 Tg/yr. Prinn et al., (1993) calculate a source of 420-520 Tg/yr. The discrepancy arises from the fact that the posteriors on the mean and variability of the atmospheric OH concentration are slightly different from the assigned prior values. Global emissions of methane for most other budgets in Table 3.1.5 lie within this range. There have been suggestions in the literature that a missing source of CH_4 might be required to explain the mass balance adequately, especially after the revision of the reaction rate with OH (Crutzen, 1991). However, we observe that there is no need to invoke a missing source as Crutzen (1991) does. Uncertainties in the CH_4 budget are adequate to accommodate even the 25% reduction in the rate constant OH-CH_4 reaction. If a missing source was required to explain the data, the optimization would have yielded an unfeasible solution.

Sources of ^{14}C depleted carbon are constrained by the analysis, despite the significant uncertainty in the source of ^{14}C CH_4 released from water pressurized nuclear reactors. In figure 3.1.1, we show the relationship between the global and fossil sources of methane. The point values of the fossil fraction presented in the literature lie well within the range shown in figure 3.1.1.

The model-determined range for wetland sources is close to 70-130 Tg/year for each of the scenarios. This is in agreement with a number of recent point estimates cited by Bartlett and Harris (1993), all lying in the range of 85-115 Tg/yr, as well as with the NATO-ARW's estimate of 100 Tg/yr. Our analysis shows that the higher end of 200 Tg/yr provided by Crutzen et al. (1993) and IPCC (1990) for the emissions range of wetlands is likely to be an overestimate. Due to the large variation in prior distributions for rice paddies, the posteriors were different for the high biomass and high fossil scenarios. The lower bound of the range is between 50 and 60 Tg/yr for the

---

[23] In fact, the formulation does lead to unfeasible solutions if the source ranges are fixed at values specified in the IPCC budget.

threescenarios, while the upper bound of about 130 Tg/yr is less than 150 Tg/yr suggested by Seiler and Schutz (1990). Neue and Bachelet (1993) have compared results of several studies with and without the inclusion of soil characteristics. They suggest that emission from Asian rice paddies which accounts for 90% of global emissions, may be overestimated by up to 25% and they cite a revised range of 57-82 Tg/yr. Our results agree with theirs in that the high biomass burning scenario gives results very close to this estimate.

It is not surprising that given their small amounts and ranges some of the minor sources -- oceans, termites and hydrates--were essentially unconstrained by the analysis. In contrast, emissions from landfills and other waste management practices were consistently in the range of 30-50 Tg/yr. This is lower than recent estimates of 54-95 Tg/yr where a significant proportion of emissions arise from emissions from waste water and livestock waste (Thorneloe et al., 1993). These emissions need to be better quantified in order to reconcile this discrepancy.

Biomass burning source ranges from 40-60 Tg/year to 55-90 Tg/year for the high biomass burning scenario. The 40-60 Tg/yr range corroborates with other recent estimates by Levine et al., (1991) who estimate a flux of 51 Tg/yr and Quay et al. (1991) who infer a biomass burning source that is 11% of the global source.[24] The high biomass burning scenario is consistent with the low values for rice paddy emissions in the range of 50-80 Tg/yr.

Emissions from coal mining are in reasonable agreement with recent estimates of 45 Tg/yr for each of the scenarios, with the exception of the high natural gas scenario, where coal mining emissions are smaller to accommodate the increase in the natural gas fraction of the budget. Natural gas emissions estimates from our analysis are in close agreement with those of Quay et al. (1991) for the high biomass and most likely scenarios.

A high fossil range of 45-75 Tg/yr is consistent with the observations, but seems unlikely. However, if the definition of a natural gas source is expanded to include minor industrial emissions, then the high fossil range of 45-75 Tg/yr is plausible.

---

24 For a global source of 475±50 Tg/year this amounts to a range of 45-55 Tg/yr.

Sources (Tg/yr)	Set 1		Set 2		Set 3	
	μ	σ	μ	σ	μ	σ
Wetlands	105	30	80	20	90	25
Rice	100	30	50	10	100	25
Landfills	40	10	20	5	20	5
Biomass	55	10	100	25	50	10
Coal Mining	35	5	40	5	40	5
Natural gas	50	10	60	10	95	25
Oceans	10	5	10	5	10	5
Ruminants	80	10	80	10	80	10
Geologic	10	5	5	2.5	5	2.5
Termites	20	10	15	10	20	5

Table 3.1.3. Specified priors on the distributions of sources and sinks (Tg/yr).

Sources (Tg/yr)	Set 1 Best Guess	Set 2 High Biomass	Set 3 High Fossil
Wetlands	70-130	70-140	70-130
Rice	60-125	50-80	60-120
Landfills	30-50	30-50	30-40
Biomass	40-60	55-90	40-60
Coal Mining	30-40	35-45	25-35
Natural gas	35-55	35-55	45-75
Oceans	5-15	5-15	5-15
Ruminants	65-85	65-85	65-85
Geologic	5-15	5-10	5-10
Termites	15-25	15-25	15-25

Table 3.1.4. Constrained budget(s) of CH_4 for Most likely, High Fossil, and High Biomass burning scenarios.

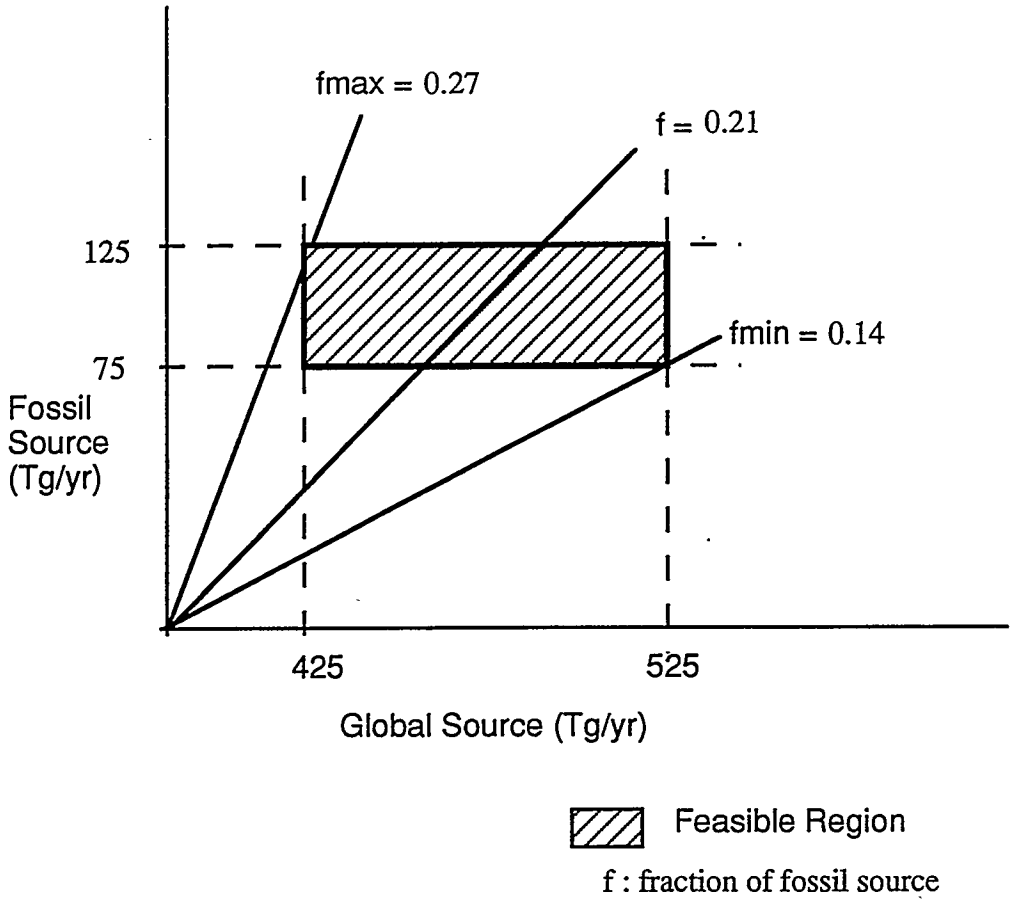

Figure 3.1.1. ^{14}C depleted sources as a fraction of the global source.

The optimal values of model parameters, such as fractionation ratios and global OH concentration, are calculated as a part of the optimization. The priors and the derived optimal posteriors are given in Tables 3.1.6 and 3.1.7. In our analysis each of the mass balances act as binding constraints depending on the scenario. In addition, bounds on some of the fractionation ratios act as binding constraints. Other binding constraints include the bounds specified on sources-- specifically, termites, oceans, and hydrates. This implies that the budgets we have

Sources (Tg/yr)	This Study	Crutzen et al. (1993)	NATO-ARW+	IPCC- 1990
Wetlands	70-130 (100)	60-200	110	100-200
Rice	60-125 (90)	95	65 (55-90)	60-170
Landfills‡	30-50(40)	25-75	63 (27-80)	30-70
Biomass	40-60(50)	15-45	50	20-80
Coal Mining	30-40(35)	25-45	46 (25-50)	25-40
Natural Gas	35-55(45)	30-110	43 (37-60)++	25-50
Oceans	5-15(10)	5-15	5-15	5-55
Ruminants	65-85(75)	60-100	79	65-100
Geologic	5-15(10)	5	10	0-100
Termites	15-25(20)	15-25	20	10-100
Marine Sediments	-	-	? (8-65)	-
Low Temperature Fuels	-	-	17	-
Wild Fire	-	-	3	-
TOTAL	425-525(475)	520 (440-600)	510	525

+ Point estimates with available ranges provided in brackets. The NATO-ARW budget is summarized in Shearer and Khalil (1993).
‡ Including Waste Management
++ Includes mean value and range for other industrial anthropogenic sources. Point value for natural gas source alone is 30 Tg/yr.

Table 3.1.5. A comparison with recent budgets

Sources (Tg/yr)	R	Q
Wetlands	0.939	1.16
Rice	0.939	1.12
Landfills	0.947	1.15
Biomass	0.95	1.37
Coal Mining	0.959	0
Natural Gas	0.935	0
Oceans	0.96	1.16
Ruminants	0.975	1.2
Hydrates	0.938	0
Termites	0.94	1.24

Table 3.1.6. Posterior values for isotopic fractionation ^{13}C (R), and ^{14}C (Q) isotopes for sources of CH_4.

Parameter	Prior Value	Optimal Value
Kj	0.993	0.993
C	4650 Tg	4650 Tg
μ_{OH}	$8.1*10^5$ rad/cm^3	$8.143*10^5$ rad/cm^3
σ_{OH}	$0.9*10^5$ rad/cm^3	$0.903*10^5$ rad/cm^3
μ_{nuc}	$8.1*10^{24}$ mol.	$8.08*10^{24}$ mol
σ_{nuc}	$1.22*10^{24}$ mol	$1.21*10^{24}$ mol
R_g	0.9646	0.955
R_g'	0.112	0.112
Q_g	1.22	1.221
Q_g'	1.5 pM/yr	1.52 pM/yr

μ and σ refer to mean values and standard deviations of the variables

Table 3.1.7 Prior and Posterior values for parameters for the best guess budget.

derived are appropriate only if the bounds specified for these sources in Table 3.1.1 are reasonable. If the ocean source, for example, is about 65 Tg/year as suggested by Lambert and Schmidt (1993), then the analysis will have to be redone after relaxing the constraint on the oceanic source.

An important part of this analysis involves quantifying the sensitivity $\frac{dF}{dp}$ of the objective function F to changes in values of the model parameters p. The optimization allows us to estimate the sensitivity of the objective function to the constraints C by providing a non-zero marginal value $\frac{dF}{dC}$ when the constraint is binding. In order to calculate the sensitivity of the objective function to a model parameter the sensitivity $\frac{dC}{dp}$ of each binding constraint to model parameters p is determined. Using chain rule $\frac{dF}{dp} = \frac{dF}{dC} * \frac{dC}{dp}$, a normalized sensitivity measure $\left(\frac{dF}{F} * \frac{p}{dp}\right)$ can then be used to compare the relative importance of each model parameter. The key estimated model sensitivities are provided in table 3.1.8. From table 3.1.8 it is clear that all the most important model parameters--the atmospheric concentration of methane and OH and the rate of reaction of OH with CH_4--pertain to the calculation of the atmospheric sink for methane. Atmospheric isotopic fractionation ratios and the kinetic fractionation ratio are more important than isotopic fractionation ratios of individual sources. It is intuitively straight forward--the global averages affect the sink processes for all the sources and, hence, have a greater impact on the model sensitivity. The objective function is also sensitive to changes in the source of nuclear $^{14}CH_4$.

3.1.7 Conclusions

We have shown that it is possible to construct consistent budgets of CH_4 using a chance constrained programming based inversion technique. The budgets are consistent with available isotopic mass balance information, flux measurements, and independent estimates of model parameters. While it is not possible to come up with a single budget for CH_4, performing the calculation with a number of sets of assumed priors suggests a convergence in the allowed range

Parameter	Sensitivity
C (CH_4 Concentration)	1.0
k_1 (CH_4 -OH Reaction rate)	0.96
OH (OH Concentration)	0.96
Q_g (CH_4 ^{14}C fractionation)	0.32
K_j (Kinetic fractionation)	0.26
R_g (CH_4 ^{13}C fractionation)	0.14
^{14}C Nuclear source	0.1
^{14}C fractionation (Wetlands)	0.07
^{14}C fractionation (Rice)	0.065
^{14}C fractionation (Biomass)	0.05
^{13}C fractionation (Wetlands)	0.06
^{13}C fractionation (Rice)	0.095

Table 3.1.8 Normalized senstitivities for model parameters.

for sources. In some cases (for, e.g, wetlands, rice paddies) a significant reduction in the uncertainty of the source estimate is achieved. Our results compare favorably with the most recent measurements of flux estimates. The approach also constrains fossil CH_4 flux estimates as well as other anthropogenic emissions from biomass burning and landfills. Sensitivity analysis shows that the key model parameters are the atmospheric concentration of methane and OH, the rate of reaction of OH with CH_4 along with global isotopic fractionation, and kinetic fractionation ratios.

3.2: Inversion of the Global Methane Cycle using Bayes Monte Carlo Simulation

3.2.1 Introduction

In this section the Bayes Monte Carlo simulation technique will be used to determine a consistent global budget for methane. The results of the analysis will be compared to the results from the chance constrained approach of the previous section (3.1).

Monte Carlo simulation is a powerful technique used for modeling in the presence of uncertainty. The applications of Monte Carlo span over a wide range of problem areas. Early methodological uses of Monte Carlo included Multi-dimensional Integration (Hammersley and Hanscomb, 1964), error analysis of parameter estimates (Bevington, P.R., 1969; Bard, 1974). More recently Monte Carlo methods have contributed to robust optimization techniques--Simulated Annealing and Genetic Algorithms

Apart from having a major impact on numerical analysis methods, Monte Carlo techniques have found applications in a wide variety of substantive problem areas where uncertainty in the model parameters plays a key role. Policy analysis has greatly benefited from the use of Monte Carlo techniques. Morgan and Henrion (1990) have shown how Monte Carlo simulation can be used as a framework for policy analyses. Applications in policy analysis include models for nuclear reactor safety (Rasmusson, 1975), Integrated Assessment of Acid Rain (Rubin et al., 1992) and Climate Change (Dowlatabadi and Morgan, 1993). Applications of Monte Carlo techniques to the mathematical modeling of environmental systems are also widespread. Examples include models of acid rain (Rubin et al., 1992), water quality modeling (Beck et al., 1987), and air quality modeling (Freeman et al., 1986). Surprisingly few analyses of greenhouse gas cycles employ the Monte Carlo simulation techniques.

Monte Carlo simulation proceeds by randomly sampling the joint distribution of model parameters and calculating the model output for each sample of this distribution. The resulting distribution provides a statistical representation of uncertainty in the model output. In terms of the discussion in section 2 this corresponds to the probability density function for the model output p(y).

3.2.2 Bayes Monte Carlo Simulation

A recent refinement to Monte Carlo simulation is the Bayes Monte Carlo Method, which incorporates new information regarding model output. The model output from the Monte Carlo run is compared to a "real world" observation of the model output. The model output and the observation are reconciled using Bayes rule to determine a posterior for the model output. Similarly, the prior distribution of model inputs can be updated to determine the posterior. In other words, Bayes Monte Carlo simulation provides the distribution the p(x/y) (equation 2.1.7, in section 2.1). The algorithm proceeds as follows (Patwardhan and Small, 1992):

1. Define a prior (joint) distribution on model parameters
2. Sample from this distribution using a Monte Carlo or Stratified Sampling Scheme.
3. Run the model for each set of input samples to determine a distribution of model output
4. Evaluate the likelihood function for model output using the error structure on measurements.
5. Reconcile the model output and observation using Bayes Rule--obtain posteriors for model output.
6. Reconcile the model inputs and observation using Bayes' Rule--obtain posteriors for model input.

The two key steps in proceeding with the analysis, and where care need to be taken, are steps 1 and 4. The selection of prior distributions for model parameters/variables is typically based on values presented in the literature. If a best estimate and corresponding error structure for all or a

subset of model parameters is available, then these would form the priors. Often such information is not available. In such cases, the modeler's subjective distribution gleaned from a careful reading of the literature is used. Typically, but not always,[25] these subjective distributions tend to be uniform, and hence, termed as "non-informative" priors.

The likelihood function is ideally determined by the error structure on the measurement process. Depending on the level of aggregation in the model, the measured quantity may only be linked to the model output of interest. For example, Patwardhan and Small (1992) aggregate local sea level rise data and determine the likelihood function for global sea-level rise. Therefore, care has to be taken to account for variability in the measurement not associated with the model output of interest.

The actual simulation proceeds as detailed below. Consider a function $y = f(x_1,x_2,.....x_N)$. Let j (j = 1 to M) be the index for sample runs of the model, and i (i = 1 to N) be the index for model inputs. For each of the j model runs a probability mass function $p_j(x_i)$ is associated with run j of the input model variable x_i. Similarly, a probability mass function $p_j(y)$ is associated with each output y_j. The likelihood function for the measurement ym, given a given a model output y_j is evaluated. If the error (ε) on y_m is normally distributed with mean zero and variance σ_y, then the likelihood function

$$L(y_m / y) \text{ is given by } L(y_m / y_j) = \frac{e^{\frac{-1}{2\sigma_y^2}(y_m - y_j)^2}}{\sqrt{2\pi}\sigma_{ym}}. \qquad (3.2.1)$$

The posterior mass function for the sample model output y_j is determined by Bayes rule as:

$$P(y_j / y_m) = \frac{P(y_j) * L(y_m / y_j)}{\sum_{j=1}^{M} P(y_j) * L(y_m / y_j)} \qquad (3.2.2)$$

Similarly the posterior mass function for model input x_i for each model run j is determined by

---

25 For an example on the use of non-uniform priors see Enting and Newsam (1987).

$$P_j(x_i / y_m) = \frac{P_j(x_i) * L(y_m / y_j)}{\sum_{j=1}^{M} P_j(x_i) * L(y_m / y_j)} \qquad (3.2.3)$$

Since $P_j(x_i) = \frac{1}{M}$, equation (3.2.3) readily reduces to

$$P_j(x_i / y_m) = \frac{L(y_m / y_j)}{\sum_{j=1}^{M} L(y_m / y_j)} \; . \qquad (3.2.4)$$

The process can be repeated sequentially for each measurement of y and the model variables are updated for each measurement.

3.2.3 Application to Methane Cycle

Bayes Monte Carlo simulation can easily be applied to a model of mass balance calculations, given their prior values and concentration measurements of species, with the objective of deducing posterior ranges on sources and model parameters. The equation $\frac{dC}{dt} = \sum_i Sources - \sum_k Sinks$ represents the mass balance equation for one species in a single, well-mixed reservoir. If the model has more than one reservoir then C(t) is a vector and the R.H.S.of the equation may contain source, transport, and chemical loss terms. A Monte Carlo simulation of the model output C(t) can be performed given the initial conditions C(0) and prior distributions for the source and sink terms. Observations of the concentration C(t) at time t can be used to determine posteriors on the source and sink terms. An alternative approach would be to treat the change in the concentration $\frac{dC}{dt}$ as the observed quantity. This allows us to update the source and sink terms from flux considerations alone. In such a formulation source and sink

variables for methane correspond to the model inputs x_i. The change in annual concentration corresponds to the model output y_i.

In the case of atmospheric methane there are three mass balance conditions, one for each of the carbon isotopes $^{12}C, ^{13}C, ^{14}C$. The corresponding equations are given below. Details for each are provided in section 3.1.

$$\frac{dC}{dt} = \sum_{i=i}^{10} E_i - K * OH * C$$

$$R_g \frac{dC}{dt} + C\frac{dR_g}{dt} = \sum_{i=1}^{10} R_i * E_i - K * Kj * OH * Rg * C$$

$$Q_g * \frac{dC}{dt} + C * \frac{dQ_g}{dt} = \sum_{i=1}^{10} Q_i * E_i + \frac{E_{nuc}}{A_{abs}} - K * K^{2_i} * Q_g * OH * C \qquad (3.2.5)$$

A fourth condition is provided from ice-core data which helps distinguish natural sources from anthropogenic one. This condition is given by:

$$f_1 \leq \sum_i S_{nat} \Big/ \sum_i S_i \leq f_2 \qquad (3.2.6)$$

The allowed ranges on the sources of methane were determined from a reading of the literature Two sets of prior distributions on the sources of methane were used. The first assumed source distributions to be uniform in the allowable range given in table 3.1.1. The second assumed the source distributions to be normally distributed with the range specifying 1σ bounds (See table 3.1.1) . Globally averaged values of concentrations and the corresponding error structures were used to determine the likelihood function for each isotope. For example, the likelihood function for the 13C isotope is evaluated from the RHS of equation (3.2.5), assuming that R_g, C, $\frac{dC}{dt}$, and $\frac{dR_g}{dt}$ are normally distributed random variables with mean values and standard deviations taken from the literature (See section 3.1). In cases where the likelihood function had to be constructed

from a number of observed variables, as in the case of ^{13}C and ^{14}C isotopes, the likelihood function can be determined either analytically or be generated using random sampling. In this work the latter was used.

The probability mass function for each sample j is determined from the likelihood functions for each isotope as follows:

$$P_{j,k}(x_i / y_m) = \frac{P_j(x_i) * L_k(y_{m,k} / y_{j,k})}{\sum_{j=1}^{M} P_j(x_i) * L_k(y_{m,k} / y_{j,k})} \qquad (3.2.7)$$

where the subscript k (k = 1,2,3) corresponds to the isotopes ^{12}C, ^{13}C and ^{14}C, and L_k is the joint likelihood function for the model output of each isotope $y_{j,k}$ given atmospheric measurements $y_{m,k}$. The posterior distributions for methane are determined by the probability mass functions and associated values for the variables $x_{i,j}$. The minimum variance Bayes estimate, which is a measure of the best estimate x is given by the expected value of the posterior distribution of x_i:

$$\hat{x}_i = \sum_j P_j(x_i / y_m) * x_{i,j} \qquad (3.2.8)$$

3.2.4 Results and Discussion

The analysis was carried out for methane assuming that the ranges given in table 3.1.1 capture 1σ (68%) of the distribution. This can be used to derive appropriate uniform and normally distributed priors. The likelihood function for each of the isotopes was constructed from the L.H.S. of equation 3.2.5. Mean values and standard error of quantities in equation 3.2.5.taken from literature are described in section 3.1.4. The constrained annual global budget of methane determined from the posterior distributions for sources is shown in table 3.2.2. The normally distributed priors give tighter bounds than the uniformly distributed priors. For normally

distributed priors the probability mass functions $P_j(x_i)$ tend to bias the posteriors toward the mean value of the prior. In section 3.1, a comparison with other budgets of methane and implications for the global methane cycle is provided. A similar discussion in this section would prove repetitious. The reader is therefore referred to that section for a detailed discussion on the implications of this analysis for the global methane cycle. Note that the budget for normally distributed priors on source distributions is very similar to the budget obtained from chance constrained programming.

Sources (Tg/yr)	CCP Budget	Bayes M.C. (Uniform)	Bayes M.C. (Normal)
Wetlands	70-130(100)	65 -145 (100)	70-130(100)
Rice	60-125(90)	55-140(80)	60-125(90)
Landfills	30-50(40)	30-70(50)	30-50(40)
Biomass	40-60(50)	30-80(50)	40-60(50)
Coal Mining	30-40(45)	25-50(35)	30-40(45)
Natural gas	35-55(45)	30-65(45)	35-55(45)
Oceans	5-15(10)	5-20(15)	5-15(10)
Ruminants	65-85(75)	65-95(80)	65-85(75)
Geologic	5-15(10)	5-15(10)	5-15(10)
Termites	15-25(20)	15-25(20)	15-25(20)

Table 3. 2. 2 A comparison of ranges(best estimates) on the sources of methane from bayes monte carlo and chance constrained approaches. All answers rounded to the nearest multiple of 5.

The similarities and differences between Chance Constrained Inversion and the Bayes Monte Carlo approaches require some more discussion. The two approaches have several similarities. Specification of prior distribution on model variables is required in both. Chance Constrained programming requires one to specify normal distributions. The Bayes Monte Carlo approach, on the other hand, is more flexible and there are no such restrictions on the input priors.

Thus, the Bayes Monte Carlo approach allows for the use of uniform "non-informative" priors. A second difference arises from the way priors are specified. In Chance Constrained programming the specification is done by incorporating priors into the objective function, while in the Bayes Monte Carlo method the input distribution restricts the sampling.

Chapter 4: Inverse Methods Applied to the Global Carbon Cycle

Concentrations of atmospheric carbon dioxide have increased in the past 200 years much of this increase may be attributed directly to emissions of fossil fuels that have steadily risen since pre-industrial times (See figure 3.2.1). As described in section 1 of this thesis, increased carbon concentration may lead to global climate change. The longest observational record of atmospheric CO_2 has been gathered by C.D. Keeling at Mauna Loa in Hawaii. Between 1951 and 1990, the mean atmospheric CO_2 level as measured at Mauna Loa and at the South Pole increased from 313.6 to 353 ppmv (Figure 3.2.2). This increase corresponds to approximately 50% of all fossil carbon released in that period. There are indications that the biosphere has been an additional *net* CO2 source. However, inventories of biospheric releases and uptake have significant uncertainties and the sign of net biospheric release is disputed. Existing models of the global carbon cycle in general predict that the ocean has taken up less than the 45% of all fossil carbon. This has led to the hypothesis of a "missing sink" that is presumably hiding in the biosphere.

This chapter explores the question of the missing sink of carbon using two different approaches. In section 4.1 an analysis of a steady-state carbon cycle is used to explore the constraints imposed by the pre-industrial atmospheric inter-hemispheric gradient of carbon on this "missing sink". The model is a simple non-linear programming model that attempts to find the allowable range on the inter-hemispheric gradient subject to various assumptions about oceanic uptake of the carbon cycle. This can then be used to make inferences about net biospheric uptake/release.

In section 4.2 a full blown dynamic inversion of a coupled ocean-atmosphere-biosphere model is performed. The model contains an advective diffusive box model for the ocean--N and S

atmospheric and biospheric boxes. Observations for ^{12}C and ^{14}C are used to perform the inversion using the DAOP approach.

4.1 Reconciling Pre-industrial Sources and Sinks of CO_2

There has been much interest recently in the latitudinal distribution of the sources, sinks, and concentration of atmospheric CO_2. Much of this interest has been driven by the conclusions of a detailed study of meridional measurements of the atmosphere-ocean CO_2 flux (Tans et al., 1990). In that study Tans et al. used the measured fluxes, in conjunction with a model for atmospheric transport and distribution of carbon dioxide, to compare various source and sink scenarios for CO_2. Tans et al. concluded that the observed North-South inter-hemispheric gradient of CO_2 could only be explained if the Northern Hemispheric sink of CO_2 exceeded that in the Southern Hemisphere by about 2 GT C/yr. Since this sink is not in the oceans, as indicated by measurements of atmosphere-ocean flux, Tans et al. posited that there needs to be a terrestrial biospheric mid-latitude sink in order to balance the carbon budget. Enting and Mansbridge (1989) independently reached a similar conclusion through an earlier modeling study.

However, such a large northern biospheric sink is controversial because it does not agree with models of biospheric carbon uptake (Esser, 1992) and violates the observed 13C/12C gradient in the atmosphere (Keeling et al, 1989) In response to Tans et al. (1990), several modifications and corrections to their budget have been suggested, including carbon flux from rivers and rain (Sarmiento and Sundquist, 1992) and skin effect corrections for the air-sea exchange (Robertson and Watson, 1992). Another correction suggested is due to the effect of a carbon monoxide (CO) source (Enting and Mansbridge, 1991; Sarmiento and Sundquist, 1992). The magnitude of the CO source is quite different in the Northern and the Southern hemispheres and thus it has implications not only for the total CO_2 budget, but, more importantly, also for the inter-hemispheric gradient.

One of the implications of the current controversy is that it is quite important to determine the pre-industrial steady-state, especially the latitudinal asymmetry in the natural sources and sinks. It has been suggested by Keeling et al. (1989) that a large fraction of the northern hemispheric sink is part of a natural meridionally asymmetric pattern of oceanic uptake and transport. If the ocean transports net carbon from the Northern to the Southern Hemisphere as a part of its natural cycle, then the Tans et al. (1990) result of a high latitude biospheric sink would be reduced by twice that amount. Broecker and Peng (1992) provided an analysis of the pre-industrial oceanic uptake of CO_2 and which showed that in pre-industrial times the North Atlantic thermohaline circulation transported approximately 0.6 GT C from the Northern to Southern Hemisphere ocean. This transport was balanced by a reverse atmospheric gradient of CO_2 concentration, as was also suggested by Keeling and Heimann (1986); Pearman and Hyson (1980) reached a similar conclusion.. Broecker and Peng (1992) further suggested that measurement of the pre-industrial atmospheric gradient (from ice-core data) would provide confirmation of their analysis, and resolve at least a part of the Northern Hemispheric sink controversy.

The preceding discussion provides an important implication for modeling studies, which is that hemispherical disaggregation is quite essential for addressing many of the carbon cycle issues. However, until recently many modeling efforts focused on using globally averaged representations for the atmosphere (Oeschger et al., 1975; Enting and Pearman, 1987) . In the present work we use a hemispherically differentiated steady-state box model of the carbon cycle to examine various hypotheses regarding the pre-industrial carbon cycle. The inter-hemispheric gradient is defined as the difference between the atmospheric Northern (N) and Southern (S) hemispheric concentrations. A non-linear programming approach is used to determine maximum and minimum allowable values for inter-hemispheric atmospheric gradient (objective function) constrained by net hemispheric oceanic uptake and vice versa. We also utilize this formulation to determine the effect of inter-hemispheric gradients of CO and CH_4 and the inter-hemispheric asymmetry of oceanic CO_2 uptake on the atmospheric gradient of CO_2. The formulation accounts for the uncertainty in the parameters and observations since we specify ranges for the reservoirs, fluxes, and parameters of

the steady-state model as constraints. In addition the NLP formulation readily provides us with information regarding the sensitivity of the objective function with respect to the constraints.

The remainder of this section is organized in the following way. We first present the details of the steady-state model and the assumptions in the formulation, and then we discuss the choice of ranges for the model parameters(4.1.2). In section 4.1.3 we present the results of the non-linear optimization and sensitivity analysis. We conclude with some implications for the current understanding of the carbon cycle (4.1.5 & 4.1.6).

4.1.2 Hemispherically Disaggregated Steady-State Model

We formulate a hemispherically aggregated box model of the carbon cycle. This model is similar to other box models in the literature, such as Bacastow (1981), Emmanuel et al. (1984a, 1984b), and Sundquist et al. (1985). Figure 1 presents a pictorial overview of the model. Mathematically, the model is represented by the following set of coupled ordinary differential equations (1-7) :

$$\frac{dC_1}{dt} = -k_1C_1 + k_h(C_2 - C_1) + K_3C_3 - fq + fs + C_6/\tau_1 + C_8/\tau_2 \qquad (4.1.1)$$

$$\frac{dC_2}{dt} = -k_1C_1 + k_h(C_1 - C_2) + K_4C_4 - (1-f)q + (1-f)s + C_6/\tau_1 + C_8/\tau_2 \qquad (4.1.2)$$

$$\frac{dC_3}{dt} = k_1C_1 - k_3C_3 - k_5C_3 + k_7C_5 \qquad (4.1.3)$$

$$\frac{dC_4}{dt} = k_2C_2 - k_4C_4 - k_5C_3 + k_8C_5 \qquad (4.1.4)$$

$$\frac{dC_5}{dt} = k_5C_3 - C_5(k_7 + k_8) + k_8C_5 + d \qquad (4.1.5)$$

$$\frac{dB_n}{dt} = fq - fs - C_6/\tau_1 - C_8/\tau_2 - fd_1 \qquad (4.1.6)$$

$$\frac{dB_s}{dt} = (1-f)q - (1-f)s - C_7/\tau_1 - C_9/\tau_2 - (1-f)d_1 \qquad (4.1.7)$$

where

c1: amount of atmospheric carbon in the Northern Hemisphere
c2: amount of atmospheric carbon in the Southern Hemisphere

c3: amount of carbon in surface Northern oceans
c4: amount of carbon in surface Southern oceans
c5: amount of carbon in the deep ocean
Bn: amount of carbon in Northern biosphere
Bs: amount of carbon in the Southern biosphere.
k1, k2: N and S atmosphere to surface ocean transfer coefficients
k3, k4: N and S ocean to atmosphere transfer coefficients
k5, k6: N and S surface to deep ocean transfer coefficients
k7, k8: N and S deep to surface ocean transfer coefficients
q: Global biospheric carbon uptake
s: Global biospheric carbon release
f: fraction of uptake/release in the Northern biosphere
d: net oceanic uptake
c7, c8: N and S CH_4 concentrations
c8, c9: N and S CO concentrations
$\tau 1$: Lifetime of methane in the atmosphere
$\tau 2$: Lifetime of CO in the atmosphere
kh: Inter-hemispheric transfer coefficient.
All carbon amounts are in GTC, transfer coefficients in yr^{-1}, and fluxes in GTC/yr.

are the state variables and parameters of the system. The objective function is the inter-hemispheric gradient z = c1 - c2. The model has a number of "free" parameters corresponding to exogenous sources and sinks. These are the deep ocean uptake d, and the fraction of northern hemispheric transfer from land to the oceans f. These correspond to processes which equilibrate over time-scales much longer than the other processes, and are therefore, included as exogenous sources/sinks.[26] Thus, at equilibrium we are left with a set of algebraic equations. These equations serve as equality constraints in the optimization formulation.

At steady-state equations 1-7 are all set to zero. Additionally, there is a net transfer of carbon from the land to the oceans and d can be non-zero.[27] The net pre-industrial transfer from the ocean to the atmosphere ranged from 0.4-0.7 GT C/yr based on Sarmiento (1992).[28] The constraints on the model are provided in Table 1. Ranges on ocean/atmosphere and deep/surface ocean fluxes and reservoirs were chosen around the best estimates made by Bolin et al. (1981); they performed a constrained inversion of a steady-state 12 box ocean model. Biospheric flux

---

26 That is, at equilibrium, these terms do not cancel out. This choice was motivated by the discussion on time-scales in Sundquist (1985).
27 This implies that there is a net transfer of carbon from the terrestrial sections to the oceans, including transport from land to oceans via riverine flow.
28 That is, d1 + d2 ranged from 0.4 to 0.7

ranges were chosen according to Emanuel et al. (1984a) The hemispheric fraction of the biospheric source/sink was derived from the analysis by Bacastow and Keeling (1981). The total amount of carbon present in the atmosphere was chosen according to the range presented in the IPCC scientific assessment (IPCC, 1990). Pre-industrial concentrations and the gradient of CO were assumed to be from natural sources alone and obtained from Khalil and Rasmussen (1990). The pre-industrial concentration of methane was obtained from IPCC assessment and the N-S gradient was assumed to be the same as at present, as was the range for the methane lifetime.

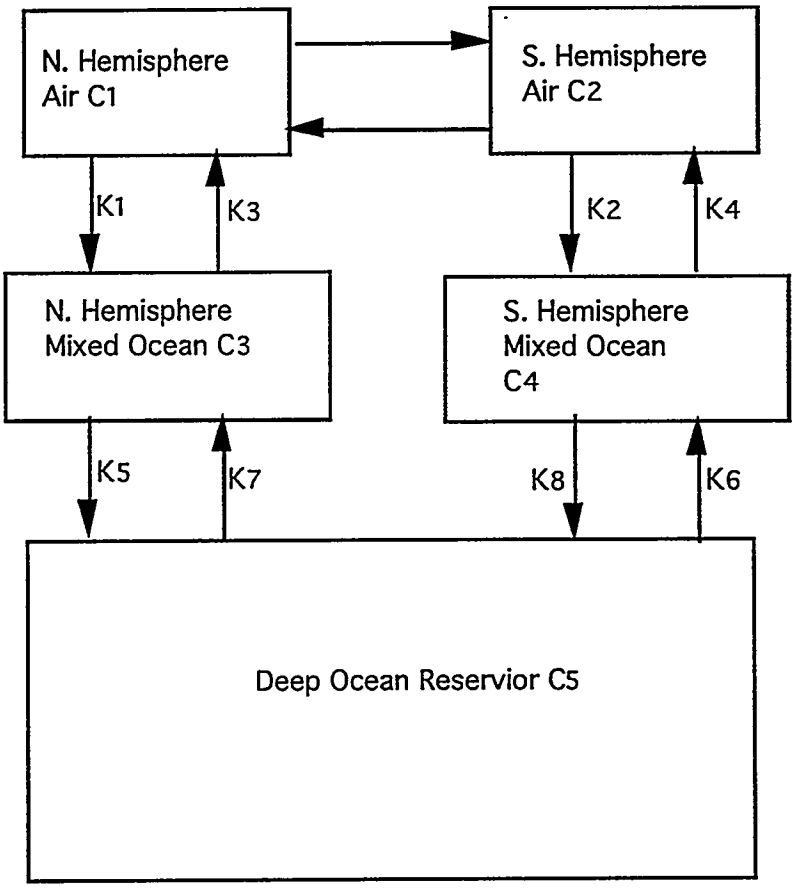

Figure 4.1.1 Schematic of the Hemispherically Disaggregated Carbon Cycle Model

Quantity (Description)	Lower Bound	Upper Bound
c1 + c2 (Total atmospheric Carbon)	610	620
c3 + c4 (Total Oceanic Carbon)	1200	1300
c5 (Deep Ocean Carbon)	35000	37000
c6 + c7 (Total Methane Carbon)	1.4	1.6
c6 - c7 (N-S Methane Gradient)	0.01	0.1
c8 + c9 (Total CO carbon)	0.8	1.28
c8 - c9 (N-S CO Gradient)	0.23	0.65
k1c1 + k2c2 (Total Atmosphere to Ocean Flux)	55	65
k3c3 + k4c4 (Total Ocean to Atmosphere Flux)	55	65
c5(k7+k8) (Total Deep to Surface Ocean Flux)	140	160
k5c3 + k6c4 (Total Surface to Deep Ocean Flux)	140	160
f (Biospheric Fraction in N. Hemisphere)	0.6	0.65
t (lifetime of methane)	8	12
q (total biospheric uptake)	120	130
s (total biospheric release)	120	130
kh (Inter-hemispheric transfer coeff.,1/yr)	1.4	1.6
d (Net riverine flux into oceans from land)	0.4	0.7

Table 4.1.1. Ranges for fluxes, concentrations, and other parameters--all concentrations are in GT C and fluxes are in GT C/year

4.1.3 Optimal Solutions and Sensitivity Analysis

We evaluate several scenarios--each scenario dealing with a particular hypothesis and associated data--as suggested in the literature. The maximum and minimum bounds (and hence the allowable range) for the inter-hemispheric gradient subject to the constraints are determined. The objective function in the optimization (max/min) is the difference between Northern and Southern atmospheric concentrations in the pre-industrial steady-state. The Broecker and Peng hypothesis (1992) that a net oceanic transport from the Northern to Southern hemisphere would necessarily lead to an inter-hemispheric atmospheric S-N gradient was examined.

Modifications to the global carbon budget suggested by Sarmiento and Sundquist (1992) were also used to determine the allowable inter-hemispheric carbon gradient. Sarmiento and Sundquist (1992) revised the budget of Tans et al. (1990) with the modifications suggested by Enting and Mansbridge (1991) and Robertson and Watson (1992); they also provided values for ocean-atmosphere flux of carbon disaggregated on a latitudinal basis. According to their calculations there is a net oceanic uptake of 0.86 GT C south of 15 S, and a net oceanic outflow of 1.70 GT C between 15N and 15S. If the outflux for this region were assumed to be equally distributed north and south of the equator, then the net southern ocean uptake would be close to zero. We evaluated the allowable range of the inter-hemispheric gradient for a number of southern oceanic uptake scenarios. The southern oceanic uptake was systematically varied from -0.6 GT/yr, to 0.6 GT C/yr in increments of 0.1 GT C/yr.[29] Finally, we evaluated the allowable range on southern oceanic uptake for prescribed values of inter-hemispheric gradients of 1.12 ppmv and 0.92 ppmv as suggested by Keeling et al. (1986) and Hyson et al. (1980), respectively.

In each case, the optimization was performed using the GAMS software. In addition to providing the value of the objective function and model variables and parameters, the procedure allows us to estimate the sensitivity of the objective function to the constraints and parameters of the model by providing a marginal value. This marginal value corresponds to the fractional change in the objective function F for a fractional change in the value of a parameter or a constraint x. The actual change in the objective function can be obtained by multiplying the marginal value with Dx, the magnitude of change in x.

4.1.4 Results

When a net transfer of 0.6 GT/yr, as suggested by Broecker and Peng (1992), was imposed on the model the optimization yielded an allowable range for the inter-hemispheric

---

[29] That is, the quantity k4c4 - k2c2 was varied from -0.6 to 0.6.

gradient of 0.52-0.75 GT. This corresponded to a concentration difference of 0.24-0.35 ppmv. In addition, the sensitivity of the maximum value of the N-S atmospheric gradient is not large enough to result in a positive N-S gradient for up to a 50% change in the value of the most sensitive constraint--which is the oceanic inter-hemispheric transport. Since the constraints themselves are defined over large ranges, the model-predicted inter-hemispheric atmospheric gradient is always from South to North, provided that there is oceanic inter-hemispheric transport of carbon for at least 0.3 GT /yr.

Figure 4.1.2 provides a graph of the envelope of allowable values for the inter-hemispheric S-N CO_2 gradient. The N-S gradient changes sign, i.e., has a positive maxima and a negative minima for all the scenarios where southern oceanic release is between 0.1 GT C/yr and 0.27Gt/yr. For these scenarios the sensitivity of the inter-hemispheric gradient to the other constraints and parameters in the model is important. Table 4.2.2 provides the optimal levels for variables and parameters of the model, and for minimization and maximization of the objective function when the southern oceanic release is fixed at 0.3 GT/yr.

In order to illustrate the sensitivity analysis we picked the scenario with a Southern oceanic release of 0.3 GT C/yr, since it provides for some interesting possibilities. The minimum value of the objective function is 0.012 GT implying a small gradient from south to north. Similarly, decreasing the southern ocean release by 10% from (0.3 GT/yr to 0.27 GT/yr) would cause the gradient to be reversed. Sensitivity analysis from each of the scenarios for southern oceanic uptake/release suggests that the inter-hemispheric gradient is most sensitive to (in decreasing order):

- The southern oceanic uptake/outflux,
- Inter-hemispheric gradient of carbon monoxide,
- The fraction of biospheric CO_2 uptake and release in each hemisphere,
-The inter-hemispheric transport time, and,
- The total amount of carbon monoxide in the pre-industrial atmosphere.

The concentrations and lifetime of methane do not have a significant effect because of the relatively long lifetime of methane in the atmosphere. In addition, the inter-hemispheric gradient is

not sensitive to the assumed ranges for reservoir concentrations, total ocean to atmosphere and atmosphere to ocean fluxes, surface to deep ocean fluxes, and global biospheric uptake and release.

Quantity (Units)	Minimum	Maximum
c1	307.8	305.6
c2	307.8	304.7
c3	649.7	643.9
c4	650.2	656.1
c5	35,142	35,040
c6	0.70	0.83
c7	0.69	0.82
c8	0..63	0.54
c9	0.40	0.26
k1	0.07	0.07
k2	0.05	0.11
k3	0.03	0.03
k4	0.045	0.046
k5	0.10	0.11
k6	0.110	0.106
k7	0.002	0.002
k8	0.002	0.002
q	130	130
s	128.1	128.6
z (= c2 - c1)	0.01	0.11

Table 4.1.2 Optimal values for model variables and parameters values for southern oceanic release of 0.3 GT C/year. Concentrations have units of GT C, fluxes of GTC/year, and transport coefficients have units of $year^{-1}$.

By forcing a positivity constraint on the inter-hemispheric gradient we determined a minimum value of southern oceanic release of 0.4GT C/yr, for which the gradient is always from south to north. This compares with 0.6 GT C/yr suggested by Broecker and Peng (1992). Using 0.6 GT C/yr for the net southern oceanic release leads to a South to North gradient range of 0.2 to 0.33 GT (0.09-0.16 ppmv). The Keeling et al. (1986) calculation of an atmospheric S-N gradient of 1.12 ppmv leads to values for southern oceanic release between 3.5 and 5 GT/yr. The Pearman and Hyson (1980) gradient of 0.92 ppmv leads to southern oceanic release values of 2.9 - 3.4 GT/yr. Both of these ranges are much larger than the estimates of either Broecker and Peng (1992) or Sarmiento (1992).

The budget proposed by Sarmiento and Sundquist will lead to a positive S - N atmospheric gradient, (i.e., with positive minimum and maximum values), only if the carbon release between 0 and 15 S is greater than 1.13 GT/yr.[30] If this release lies between 0.96 and 1.13 GT/yr; the inter-hemispheric gradient is from S to N, or vice versa (i.e., with a negative minimum and positive maximum) depending on the values of the other parameters in the model, most notably, the inter-hemispheric gradient of CO and the hemispheric fraction of biospheric uptake/release. A release of less than 0.92 GT leads to a negative S - N gradient. The S to N gradient proposed by Hyson and Pearman (0.92 ppmv) and Keeling and Heimann (1.12 ppmv) is not compatible with the results of this model.

4.1.5 Accounting for Covariance Between Transport and CO_2 Seasonality

As pointed out by a reviewer[31] the model in section 4.2 does not include an important aspect of the inter-hemispheric distribution of the global carbon cycle. In constructing the model the assumption was made that a zero concentration gradient implies a net zero inter-hemispheric flux. However, this assumption is only partly correct because it ignores the covariance between

---

30 Assuming that the oceans south of 15S take up 0.86 GT/yr.

31 The paper was sent to the Journal Tellus -B.

seasonality of inter-hemispheric advection of air and the seasonal cycle of atmospheric carbon concentration. In the northern hemispheric winter the mean meridional transport tends to be southward, between 20.5 N and 20.5 S, at low altitudes (0-4 km), with air returning to the northern hemisphere at high altitudes (7-15 km). The process reverses itself in the northern hemispheric summer (Newell et al., 1974; Hyson et al., 1980). Since seasonal concentrations are higher in the northern hemispheric winter than in the summer, the resultant net flux of carbon is from north to south. This could explain the discrepancy between the results of our model and those of Pearman and Hyson (1980) and Keeling and Heimann (1986a).

In order to explore the implications of seasonal carbon transport for this analysis, the box model in section 4.1.2 was modified by adding an annually averaged seasonal transport term to equations 1 and 2. The concentration in each hemisphere was assumed to be of the form:

$$C_{i\{i=1,2\}}(t) = C_i + C_{si}Sin(2\pi * t / T) \qquad (4.18)$$

The inter-hemispheric transfer coefficient was assumed to be of the form

$$K(t) = K_h + K_1 Sin(2\pi * t / T + \phi) \qquad (4.1.9)$$

Where C_i, C_{si}--(C1 and C2 in the model equations specified earlier)--are annual mean and maximum seasonal concentrations, respectively. K_h, K_1 are the annual average and effective seasonal components of the inter-hemispheric transfer coefficient, respectively; ϕ is the phase lag between seasonality of carbon concentration and seasonal transport; and T is equal to one year. Therefore, the annual average north-south flux is given by :

$$\int_0^T K(t)\{C_N(t) - C_S(t)\}dt \qquad (4.1.10)$$

This is equal to $K_h(C_1 - C_2) + 0.5K_1(C_{s1} - C_{s2})cos(\phi)$.

Accounting for the seasonal cycle therefore requires an additional term $0.5K_1(C_{s1} - C_{s2})Cos(\phi)$ in the mass balance equations 1 and 2. Note that if K(t) and C(t) are out of phase by p/2 rads the seasonal cycle has no effect on the inter-hemispheric flux.

The analysis carried out in section 4.1.3 was repeated with the correction for seasonal transport described above. Since seasonal transport and carbon concentration have been found to covary significantly, f was allowed to range between 0 and $\pi/6$ rads. The choice of seasonal transfer component K_1 poses a problem. Without greater geographic detail and the use of a well established tracer model it is not possible to accurately estimate its value. The analysis that follows, therefore is carried out using a plausible range of values for K_1. The effective seasonal mixing time ranged from 3 to 4 months, leading to a range for K_1 of 4 to 3 yr^{-1}. Figure 4.1.3 shows the maximum and minimum values of the inter-hemispheric gradient as a function of southern oceanic release for several values of the seasonal mixing time. For comparison, inter-hemispheric gradient estimates from Pearman and Hyson (1980) and Keeling and Heimann (1986) are shown. The inclusion of seasonal effects makes the results of this analysis come out closer to their calculations. The inter-hemispheric gradient is always from South to North for a large range of values for the southern oceanic release. The gradient ranged from 2.43- 0.85 ppmv to 3 - 1.22 ppmv when the southern oceanic release varied from 0.6 to -0.6 GT/yr. The Keeling et al. (1986) calculation of an atmospheric S-N gradient of 1.12 ppmv leads to values for southern oceanic release between -5.2 to 0.4 GT/yr. The Pearman and Hyson (1980) gradient of 0.92 ppmv leads to southern oceanic release values of -4.52 to 0.27 GT/yr. It is apparent from these results and from a comparison of figures 4.2.2 and 4.2.3 that a good estimate of the effective seasonal mixing time K_1 is key to finding a more narrow range for the inter-hemispheric gradient. A more effective analysis--which would help narrow down the pre-industrial inter-hemispheric gradient from a modeling effort of the sort described in this work--would require greater geographical disaggregation with three boxes (N, S, Tropics), for atmosphere and surface ocean, and a more formal procedure, perhaps the use of a detailed tracer model to estimate seasonal transfer coefficients.[32]

---

32 This work is underway and will be completed before the article is resubmitted to the journal.

4.1.6 Conclusions

The goal of the analysis was to examine and compare the current hypotheses regarding the inter-hemispheric asymmetry in the pre-industrial sources and sinks of CO_2. Given that the data are uncertain, determining allowable ranges for the inter-hemispheric gradient and southern hemispheric oceanic uptake allows us to make conclusions that are robust even after accounting for these uncertainties. The steady-state analysis, done without the inclusion of seasonal effects shows that a South-North atmospheric gradient, implies a southern oceanic release of at least 0.27 GT/yr and a corresponding net northern oceanic uptake of -0.27 GT/yr. Therefore, if a South to North gradient of atmospheric CO_2 can be detected from ice core records, the magnitude of the biospheric Northern sink proposed by Tans et al. (1990) would be reduced by 0.54 GT/yr. However, if a South - North gradient is not clearly indicated, a net oceanic transport of carbon is still possible, although its magnitude would be lesser than the range indicated above.

When seasonal effects are included the inferred inter hemispheric gradient critically depends upon the covariance between the seasonal cycle of atmospheric carbon and the seasonality of meriodinal advection. A more detailed analysis of this phenomena is required before any conclusions can be drawn regarding the inter-hemispheric gradient and, hence, the missing sink of carbon. Such an analysis is in progress.

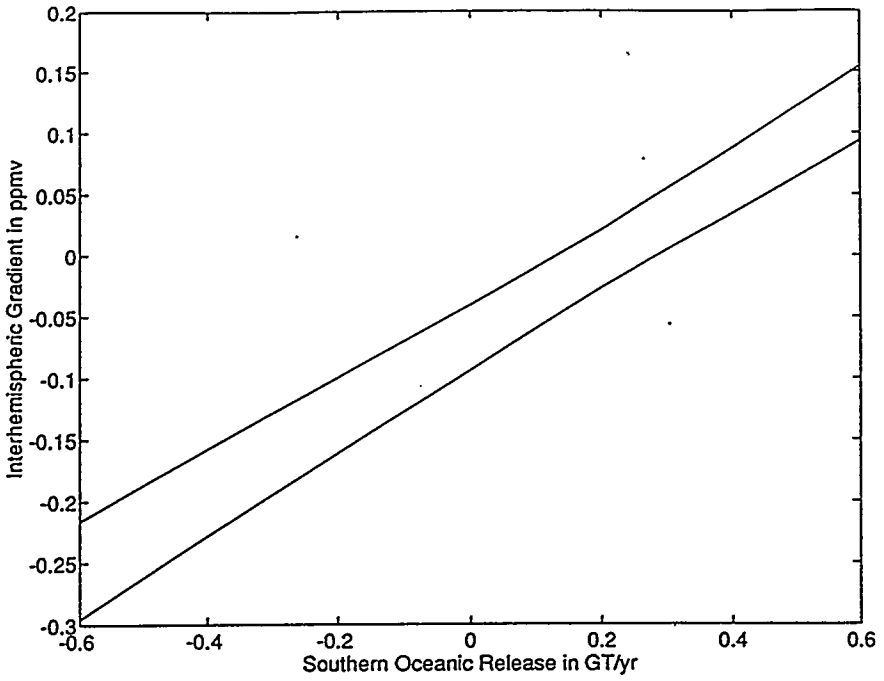

Figure 4.2.1: Inter-hemispheric gradient as a function of Southern Oceanic Uptake (without Seasonality)

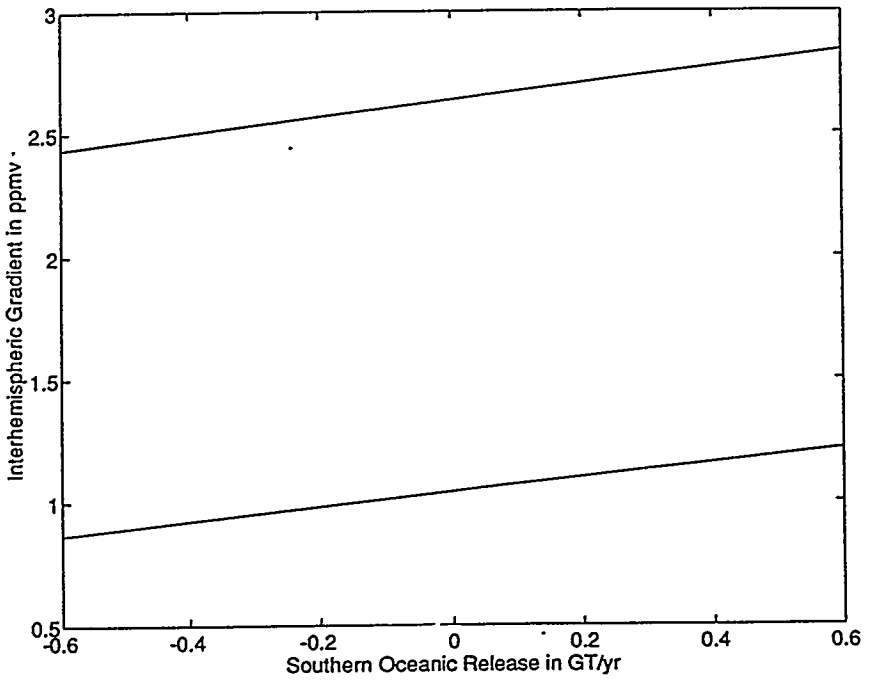

Figure 4.2.2: Inter-hemispheric Gradient as a function of Southern Hemispheric Uptake (with Seasonality)

4.2 Inversion of a Dynamic Model of the Carbon Cycle.

Quantifying natural and anthropogenic sources and sinks is critical to the prediction of future atmospheric concentrations of CO_2 and the consequent implications for global climatic change. Wigley (1993) provides an analysis of the implications of these uncertainties in predictions of future carbon concentrations. There is much debate in scientific circles on various aspects of the oceanic carbon cycle (Sarmiento, 1992). In particular, the atmosphere to surface ocean flux is difficult to quantify because of its dependence upon surface phenomena such as wind speeds and temperature. The role of marine biota is also a matter of dispute, with some scholars suggesting a prominent role (Longhurst, 1992; Banse, 1992), and others strongly disagreeing (Broecker, 1992) . The key issue, however, in balancing the global carbon budget deals with the uptake/release by terrestrial biosphere. Estimates for the source term associated with deforestation and other land use changes, both at present and over the past century, have changed significantly in the past decade. Additionally, as a result of regrowth and/or carbon fertilization the biosphere may be taking up carbon.

Emissions from the combustion of fossil fuel account for most of atmospheric carbon emissions, an estimated 6 GT/yr of carbon was released into the atmosphere in 1990. The IPCC (1990) estimated that the ocean acts as a net sink for 2.0±0.8 GTC yr-1. However, they concluded that known sources (fossil fuel combustion and land-use change) and sinks (uptake by the oceans) were out of balance with observed rates of increase in atmospheric carbon, suggesting a "missing" sink of 1.6 -1.4 GTC/yr (IPCC, 1990; 1992). Inference from modeling studies (Tans et al., 1990; Enting and Mansbridge, 1989; 1991) and observed temporal and spatial distributions of 13C/12C (Keeling et al., 1989; Quay et al., 1992) suggest that this missing sink is stronger in the Northern Hemisphere than in the Southern Hemisphere. Based on a detailed analysis of measured surface atmosphere-ocean fluxes coupled with a model of atmospheric transport, Tans et al. (1990)

concluded that the ocean sink for CO_2 is at most 1 GTC; this implies a very large sink in the terrestrial biosphere. As discussed in the previous section this sparked controversy and led to a re-evaluation of the sources and sinks of carbon. Dixon et al. (1994) have suggested that with current forest ecosystem inventories the best estimate of the missing sink is now about 1 Gt/yr. The gap in the carbon budget is not eliminated.

Coupled ocean-atmosphere carbon models provide estimates of oceanic carbon uptake, thus allowing one to infer the biospheric source. Available ocean - atmosphere models range from large-scale, dynamic, three-dimensional models of global ocean circulation and atmospheric transport to one-dimensional, box-diffusion models of exchanges. Atmospheric transport models solve the continuity equation for trace gases in the atmosphere and include ocean and biosphere exchanges as surface fluxes of carbon. Typically, tracer models are forward "steady-state" models in that they capture the geographical distribution of CO_2 atmospheric concentrations, given sources and sinks for a particular year. Best guess values are chosen depending on how closely the observations meet the model output. Pioneering tracer studies of two-dimensional, atmospheric models for CO_2 have been performed by Pearman and Hyson et al. (Pearman and Hyson, 1980). Three-dimensional GCM wind driven models have been built and studied by Fung et al. (1983) and Heimann et al. (1986). Enting and Mansbridge (1989, 1991) used a 2-D advective-diffusive, atmospheric model for explicit inversions of carbon sources and sinks.

Diffusion models have traditionally provided much of the insight regarding oceanic uptake of atmospheric carbon (Oeschger et al., 1975; Seigenthaler, 1987; Enting and Pearman, 1987). One and two-dimensional box-diffusion models of ocean exchange with a well-mixed at-atmospheric reservoir have been reviewed by Bjorkstrom (1986). One-dimensional box models can be formally calibrated using inversions techniques and the effect of alternate assumptions can be easily studied (Seigenthaler, 1983). The key to building box models lies in determining important processes and evaluating model parameters making use of available information from analogous processes. Most models of the carbon cycle use ^{14}C as a tracer.

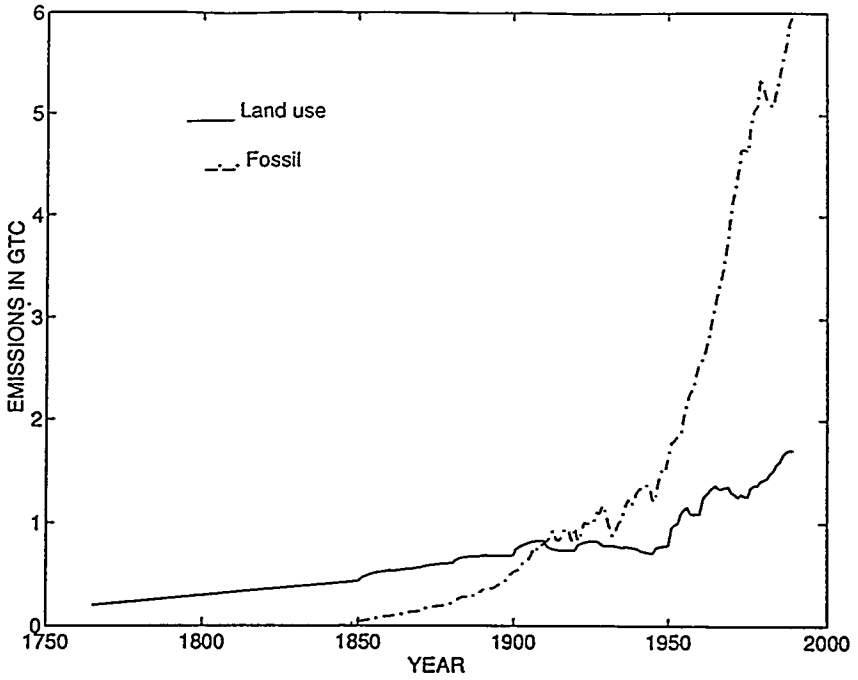

Figure 4.2.1 Historic Fossil and Land Use Change Emissions of Carbon

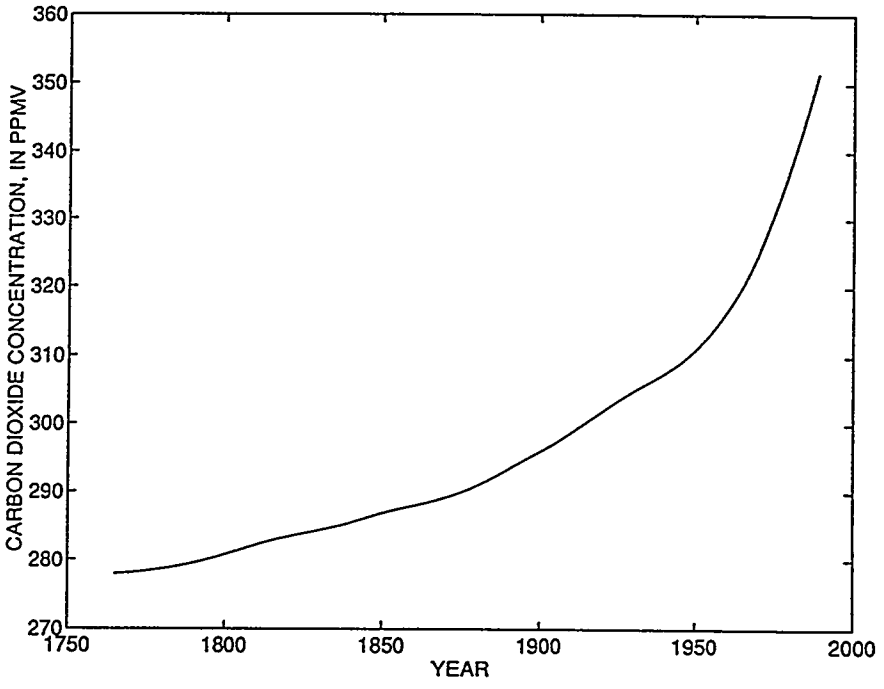

Figure 4.2.2. Carbon dioxide concentration from pre-industrial times (1765) to present day (1990)

Background concentration of ^{14}C in the atmosphere and the oceans occurs due to cosmic ray radiation. Since ^{14}C is a radioactive isotope and decays over time (time constant--8267 years), steady-state distributions of ^{14}C and ^{12}C concentrations can be used to determine parameters for oceanic transport processes. These parameterizations are valid over long time scales (~1000 years). Additionally, above ground testing of nuclear weapons in the late 1950s/early 1960s, resulted in a large ^{14}C forcing of the atmosphere. This ^{14}C was taken up by the oceans and the biosphere. By following the ^{14}C bomb peak in the ocean model parameters for oceanic transport over shorter time scales can be obtained. Most models of the carbon cycle are calibrated by using ^{14}C because its behavior as a tracer most closely approximates that of ^{12}C. Thus, most models tend to have similar shortcomings in terms of availability of data and modeling assumptions. A more detailed discussion of this issue can be found in Moore (1992).

In this work a box diffusion model for the global carbon cycle is built and calibrated with available data for ^{12}C and ^{14}C isotopes of carbon. A description of the model is provided in section 4.2.2. The calibration of the steady-state version of the model is discussed in section 4.2.3. The dynamic problem is posed as a Differential Algebraic Optimization problem. Details of the methodology and application to the model are provided in section 4.2.4. Results of the analysis, including estimates of oceanic and biospheric carbon uptake/release and values for model parameters are presented in section 4.2.5. Conclusions and implications for the global carbon cycle are provided in section 4.2.6.

4.2.2 A Box Diffusion Model for the Carbon Cycle

Since much of atmosphere carbon eventually is taken up by the deep ocean, the modeling of transport from the surface to deep oceans is a critical part of carbon cycle modeling. Box diffusion models for the carbon cycle were introduced into the literature by Oeschger et al. (1975) for studying the cycling of carbon between oceans and atmosphere; and in particular, the fate of

anthropogenic CO_2. The box diffusion model of Oeschger et al. (1975) was one-dimensional and the variation of vertical transport rates with latitude was not accounted for. Because the vertical exchange between surface and deep ocean layers is rapid at high-latitudes, a model that uses only diffusion may significantly underestimate oceanic carbon uptake. Seigenthaler (1983) modified the box-diffusion model with assumption that the transport from the outcrop at the surface to the deep ocean is infinitely fast. The outcrop provides a direct ventilation of deep water in the high-latitudes. The Outcrop Diffusion ocean model takes up more CO_2 than the earlier box-diffusion models.[33] and provides a better representation of the oceanic mixing processes includes the assumption for instantaneous mixing of atmospheric carbon with the deep ocean. A more realistic way to incorporate fast exchange in the high latitudes is to model the transfer of carbon from the cold surface to the cold deep ocean. Enting and Newsman (1987) were the first to explicitly model the phenomena as such. Subsequently, a High-Latitude Exchange/Interior Diffusion-Advection (HILDA) model was devised by Shaffer and Sarmiento (1992) and has been used to study inversion of the carbon cycle by Seigenthaler and Joos (1992). HILDA consists of two surface boxes of height hm--one a well-mixed, cold surface box in high latitudes and the other a well-mixed, warm surface box in low latitudes. These surface boxes occupy 16% (Ac = 0.16A) and 84% (Aw = 0.84A) of total sea surface area ($A = 3.62*10^{14}$ m^2), respectively. A well-mixed, high-latitude deep water box and an advective-diffusive interior box, both of height hd-hm, constitute the lower oceans. The model in this paper is similar to HILDA in that it has a very similar structure with one difference--the low and high-latitude boxes are equally divided into two boxes, one each for the N and S hemispheres. Additionally, in this model an attempt is made to incorporate marine biology, albeit in a highly aggregated manner. Figure 4.2.3 provides a schematic of the model.

---

33 Ocean models with surface reservoirs exchanging carbon with the atmosphere and with a deep-sea box. have been used by Knox and McElroy (1984), Sarmiento and Togweiler (1984), and Siegenthaler and Wenk (1984) for studying the importance of high-latitude oceanic processes for natural CO_2 variations.

The net air-to-sea flux of carbon is driven by the difference between atmospheric CO_2 concentration C_a and the partial pressure of carbon dioxide in surface-waters pCO_2. The air sea flux is given by the fickian diffusion equation $F_{as} = -F_{sa} = U(C_a - pCO_2)$, where U, the transfer velocity, depends on temperature and wind speed. The surface pCO_2 is related to the total amount of inorganic carbon in the surface water through the relationship in equation 4.2.1, where α is the solubility of carbon dioxide in water, A is the salinity of water, and K is the dissociation constant for the equilibrium reaction between water and CO_2 :

$$pCO_2 = \frac{(2\Sigma CO_2 - A)^2}{K\alpha(A - \Sigma CO_2)} \qquad (4.2.1)$$

Equation 4.2.1 results from the ionic balance of chemical reactions in sea surface water. Details are available in Broecker (1974). Typically, in models of the carbon cycle the relationship between total inorganic carbon and pCO_2 is expressed in terms of the Revelle factor, ξ, which is the normalized first order Taylor's series coefficient $\left\langle \frac{\partial pCO_2 / \partial \Sigma CO_2}{pCO_{2,0} / \Sigma CO_{2,0}} \right\rangle$ where the subscript 0 denotes the equilibrium value.

The transfer of carbon from the surface to the deep ocean takes place through three mechanisms. In mid-latitude, deep ocean box a downward Eddy Diffusion flux (with Diffusivity K) of carbon is used to approximate turbulent diffusion. At the same time upwelling of water at mid-latitude sites transfers carbon from deep ocean to the surface. Correspondingly, in the cold oceans transfer of carbon from the surface to the well-mixed interior boxes in the form of down welling of cold water is modeled as an advective process.

Another important mechanism for the transfer of carbon from the surface to deep oceans is the transport of organic carbon as detrital flux, via particulate (POC) and dissolved organic carbon (DOC). Organic carbon gets remineralized by zooplankton and bacteria as it settles, leading to a net flux of inorganic carbon from the surface to the deep oceans. There is controversy regarding the relative contributions of DOC and POC to the organic carbon cycle (Carlson et al., 1994).

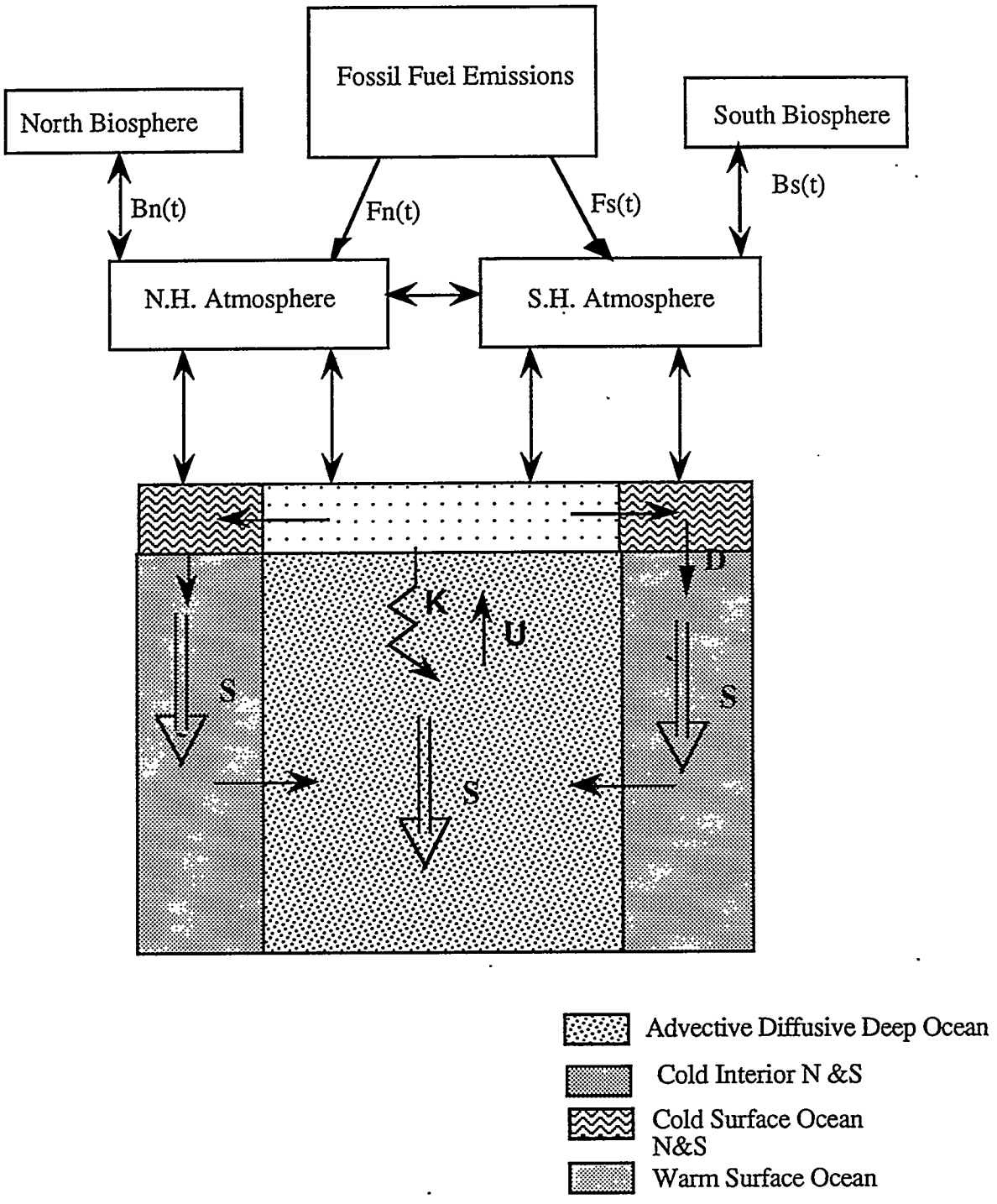

Figure 4.2.3 A schematic for the Global Carbon cycle model

. In addition to this "soft" pump of organic carbon, a carbonate pump also transfers carbon from the surface to the deep oceans. In this paper the assumption was made that organic detritus is produced in the surface oceans and is remineralized uniformly in the deep ocean.

The atmospheric concentration C_a is given as:

$$\frac{dC_{ai}}{dt} = K_h \Delta C_{ai} - U_i C_{ai} + U_j \frac{pCO_{2,0j}}{C_{S,0j}}(C_{S,0j} + \xi(C_{Sj} - C_{S,0j})) + F_i(t) + B_i(t) \qquad (4.2.2)$$

where the subscript i = {N,S} denotes the Northern and Southern hemisphere, j = {N,S,M) denotes the North and South cold and the mid-latitude warm ocean surface boxes. F(t) and B(t) are the net annual releases to the atmosphere from fossil fuels and the biosphere. Additionally, it was assumed that the Northen Hemisphere contributes 90% of all fossil emissions and 65% of all biospheric emissions/uptake. ΔC_{ai} is the inter-hemispheric concentration gradient and K_h is the inter-hemispheric transfer coefficient (0.8 yr^{-1})

Surface concentration in the cold, high-latitude boxes is given by $C_{S,j}(t)$ (j = N,S) :

$$\frac{dC_{S,j}}{dt} = U_i C_{ai} - U_j \frac{pCO_{2,0j}}{C_{S,0j}}(C_{S,0j} + \xi_j(C_{Sj} - C_{S,0j})) + v_{m,j} C_{S,m} - v_{j,d} C_{S,j} - S_j, \qquad (4.2.3)$$

where $v_{m,j}$ is the velocity of advective flow from the mid-latitude, warm surface ocean to the high-latitude, cold surface box. $v_{j,d}$ is the advective velocity of downwelling from the high-latitude, cold surface box to the high-latitude, deep ocean. S_j is the detrital flux in box j. If the total ocean detrital flux is given by S, then the detrital flux for each high-latitude box is equal to $S\frac{A_C}{2A}$.

The surface concentration in the warm, mid-latitude box $C_m(t)$ is given by

$$\frac{dC_{s,m}}{dt} = U_m C_{ai} - U_m \frac{pCO_{2,0m}}{C_{S,0m}}(C_{S,0m} + \xi_m(C_{Sj} - C_{S,0m})) - K\frac{\partial C}{\partial z}\Big|_{z=h_m} - S_m \qquad (4.2.4)$$

The Eddy flux from the warm mid latitude surface box to the interior ocean is given by $K\frac{\partial C}{\partial z_{|z=h_m}}$, h_m is the height of the mixed layer (75m) and K is the Eddy Diffusion constant. Detrital flux S_m is equal to $S\frac{A_m}{A}$

The concentration of carbon in the interior ocean $C_I(z,t)$ ($h_m \leq z \leq h_d$) is given by

$$\frac{\partial C_I(z)}{\partial t} = K\frac{\partial^2 C_I(z)}{\partial z^2} - v_u C_I(z) + S(z) \qquad (4.2.5)$$

v_u is the upwelling velocity in the interior box. S(z) is the remineralized detrital flux, assumed to vary linearly with depth, and is given by $S(z) = S\frac{z}{(h_d - h_m)}$. The boundary conditions for equation (4.2.5) are given by $C_I(z = h_m) = C_m$ and $K\frac{\partial C_I}{\partial z}_{|z=h_m} = 0$. The deep interior ocean was divided into 6 boxes of equal depth. The partial differential equation in (4.2.5) is converted into a set of ordinary differential equations by using a centered differencing scheme (i = 1,...6)

$$\frac{\partial^2 C_I(z_i)}{\partial^2 z_i} = \frac{\frac{C_I(z_{i+1}) - C_I(z_i)}{z_{i+1}} - \frac{C_I(z_i) - C_I(z_i - 1)}{z_i}}{\frac{1}{2}(z_{i+1} + z_i)}. \qquad (4.2.6)$$

where, $z_0 = h_m$, $z_i = h_m + i*(h_d - h_m)/6$. The Eddy Diffusivity is assumed to be linearly dependent with depth $K = K_0 + K_1 z$.

Carbon concentration in the high latitude deep ocean $C_{D,j}(t)$ is given by

$$\frac{dC_{D,j}}{dt} = -v_{m,j}C_{S,m} + v_{j,d}C_{S,j} + S_{D,j} \qquad (4.2.7)$$

where $S_{D,j} = S\frac{A_C}{2A}$.

For the biospheric boxes the mass balance in each hemisphere is given by

$$\frac{dR_i}{dt} = \frac{R_i}{\tau} - NPP_i + B_i(t), \tag{4.2.8}$$

where R_i (i = N,S) is the amount of biospheric carbon in each hemisphere and τ is the biospheric turnover time. The initial amount of carbon in the biosphere was fixed at 2000 GTC. Assuming an NPP (Net Primary Productivity) of 60 Gt/yr, the turnover time τ was calculated to be 33.3 years.

For carbon-14 the equations are identical with some key exceptions. The equation for carbon-14 in the atmosphere is given by:

$$\frac{dC^{14}{}_{ai}}{dt} = K_h \Delta C_{ai} - U_i C^{14}{}_{ai} + U_j \frac{pCO_2{}^{14}{}_{2,0j}}{C^{14}{}_{S,0j}} (C^{14}{}_{S,0j} + \xi(C^{14}{}_{Sj} - C^{14}{}_{S,0j})) + B_i{}^{14}(t) + \Omega + \eta * Bomb(t) - \lambda C_{ai}{}^{14}(t) \tag{4.2.9}$$

Cosmic ray radiocarbon flux, which is responsible for background levels of ^{14}C in the atmosphere, is given by Ω, Bomb (t) is the tonnage of above ground atomic tests (in Megatons), and η is a conversion factor. In each of the other equations, an additional term accounting for radioactive decay is required, i.e., an additional term λC (t) has to be subtracted from the RHS of the equations above, where C(t) is variable of interest and λ is the decay constant for ^{14}C (1/8267 yr^{-1}).

Calibration of the model equations proceeds in two steps. First, the model was calibrated using the available steady-state (pre-bomb) measurements of carbon 14 in the atmosphere and the oceans. This allows us to determine one set of values for model parameters. In Bayesian terms, these values serve as prior values, which get updated/refined by the time trajectory of atmospheric and oceanic measurements of ^{12}C and ^{14}C. Once the steady-state model is calibrated, its results can be used in two ways. First, the model can be run in the "forward" mode to determine the time trajectory of oceanic uptake of ^{12}C carbon by forcing the model with fossil and land use releases.

By comparing the model results with the observed atmospheric concentration of carbon a trajectory for the biospheric source can be inferred. The second stage of the analysis uses the results from the first as initial conditions to dynamic inversion of the carbon cycle. Here the inversion is used to calibrate the model simultaneously to time-stamped atmospheric and oceanic measurements of ^{12}C and ^{14}C. In particular, the model attempts to reproduce the observed oceanic uptake of bomb ^{14}C.

4.2.3 Steady-state Calibration of the Carbon Cycle

The calibration of the steady-state model of the carbon cycle requires the solution of the set of equations $G(N^{12}(0), N^{14}(0), p) = 0$, where G is the R.H.S. of the equations defined in the previous section, N(t)[34] is the amount of ^{12}C and ^{14}C carbon in each of the models 14 reservoirs, and p is the vector of model parameters. The calibration of the steady-state requires one to simultaneously determine the initial conditions of model variables N(0) and the parameter vector p. Since the steady-state model has 28 variables and 12 parameters constrained by 28 equations (14 for each of the two isotopes), it is clearly an under-determined problem. Additionally, the non-linearities in the model can give rise to multiple solutions, even if the model were to be exactly determined.

As outlined in chapter 2, model calibration requires more information about the magnitude of the individual reservoirs and/or the parameters. The ^{12}C isotope of carbon was assumed to have a uniform concentration in the pre-industrial ocean C_{pre} of 2.053 ± 0.2 mol/m^3. Fractionation of ^{14}C concentration for the pre-industrial ocean was derived pre-bomb GEOSECS data. The compilation by Seigenthaler and Joos (1992) was used. This information is incorporated as least squares objective function, which is minimized subject to the steady equations as constraints. Specifically the optimization formulation is:

---

34 N(t) = C(t)*V, where C(t) is the species concentration in a reservior and V is the reservior volume

$$\min \quad \sum_{i=1}^{14} \left\langle \frac{(N_i^{12}(0) - C_{pre}V_i}{0.1 * C_{pre}V_i} \right\rangle^2 + \left\langle \frac{(N_i^{12}(0) / N_i^{14}(0) - r_i}{0.1 * r_i} \right\rangle^2$$

$$\text{s.t.} \qquad G(N^{12}(0), N^{14}(0), p) = 0$$

$$p^l \leq p \leq p^u \qquad (4.2.10)$$

where r_i is the pre-industrial fractionation of ^{14}C in reservoir i of volume V_i, $r_i = (1 + \frac{\delta^{14}C}{1000})$, and p^l and p^u are, respectively, the lower and upper bounds on the model parameters. Multiple solutions for the error minimization problem were detected. The solution which had the minimum error was chosen to be the "correct" solution. In table 4.2.1 the initial conditions of the model ^{12}C and ^{14}C state variables corresponding to this solution are shown. The corresponding parameter values are shown in table 4.2.2. Additionally, the model provides a good fit to the observed 14C fractionation ratio in the deep oceans. (Figure 4.2.4).

The model integration in the forward mode was carried out using the initial conditions and parameter values specified in table 4.2.1. The model was forced with carbon released from fossil fuels and land-use change. The inferred biospheric release is shown in figure 4.2.5.

4.2.4 Differential Algebraic Optimization Approach to Model Inversion

The problem of estimating parameters and forcings of a dynamic system can be posed as follows:

$$\min \sum_i (y(t_i) - \mu)^T W (y(t_i) - \mu)$$

$$\text{s.t.} \quad \dot{y} = G(y, \theta, f(t)) \qquad (4.2.11)$$

The objective function defines a minimum mean squared error between model predictions y(t) and a vector of observations m, and the matrix W is a covariance matrix of observations. The

optimization attempts to determine the values of the parameter vector θ and the forcing function f(t) which minimizes the error.

Traditionally, the problem of determining optimal values for θ and f(t) is solved by minimizing and using the sensitivity equations approach which is a feasible path approach where the estimated parameters always satisfy the model. Here, an unconstrained optimization method is carried out in the outer loop; the evaluation of the objective function and its gradients is done by numerical integration of model differential equations in the inner loop. One problem with this approach is that intermediate parameters during the optimization can often make the system stiff and the numerical integration inefficient. Additionally this approach cannot directly handle system constraints other than bounds on the parameters. An alternative is to pose the inversion as a differential algebraic optimization problem (DAOP). The solution technique proceeds by discretizing the set of differential-equations G(y), defining the model using orthogonal collocation on finite elements. The resulting set of non-linear algebraic equations are treated directly as constraints in the minimization of the weighted least squares objective function. Thus the problem becomes a constrained least-squares problem, where the discretized model equations act as constraints. The result is a set of algebraic equations that can be embedded directly into the optimization together with any other system constraints. Thus, the problem becomes a constrained non-linear least-squares problem. A brief description of the orthogonal collocation approach is now provided. Consider the equation $G(y) = f(y,t)$. Here G(y) is the differential operator. In general the solution of this equation can be written as the combination of series of known basis functions β(t) and unknown coefficients a_i.

$$y(t) = \sum_{i=1}^{N} a_i \beta(t) \qquad (4.2.12)$$

as N becomes very large the equation 4.2.12 tends to the exact solution. Since β(t) are known basis functions, the problem of solving for y(t) is equivalent to finding the coefficients a_i. One way of determining a_i is to minimize a function of the residual

$$R(a_i,t) = G(\sum_{i=1}^{N} a_i\beta(t)) - f(\sum_{i=1}^{N} a_i\beta(t),t).$$

In general the approach calls for solving the equation

$$\int R(a_i,t)w(t)\,dt = 0, \qquad (4.2.13)$$

w(t) being a weighting function. This approach is called the Method of Weighted Residuals (MWR). There are many possible weighting functions--(remember that we want to find the best approximation to the solution). If $w(t) = \frac{\partial R(a_i,t)}{\partial a_i}$, then the MWR approach is equivalent to the weighted least squares approximation. The least squares method can become very cumbersome for solving differential equations. An alternative is to use the differential weighting function $\frac{\partial G(y(t))}{\partial a_i}$. Consequently, the polynomials β(t) may be chosen to be orthogonal to the residual $R(a_i,t)$ then equation 4.2.13 is satisfied. This is called the Galerkin approach and is theoretically the most efficient approach for determining y(t) (Villadsen and Michaelsen, 1978).

The orthogonal collocation method uses a delta function for w(t), such that

$$w(t) = \delta(t - t_k) \qquad (4.2.14)$$

where t_k are called the collocation points. This is equivalent to saying that the residual goes to zero at every collocation point. If the collocation points t_k are selected to be zeros of an orthogonal polynomial then y(t) approaches the Galerkin approximation (Villadsen, 1970). Collocation approach is easier to implement that the Galerkin approximation and, hence, has been extensively used. Details of the implementational aspects of the collocation method can be found in Cuthrell and Beigler (1986) and Diwekar (1994).

In this work, Lagrange polynomials were used for the basis functions β(t). The collocation points t_k were chosen to be roots of a second order Legendre polynomial. When the profile of

state functions is non-smooth, the collocation approach requires a large number of collocation points to meet a reasonable level of accuracy. One way of getting around this is to make a piece-wise polynomial approximations using finite elements. Time domain is discretized using finite elements and the solution within each finite element is obtained using the lagrange polynomial approximation. The location of the interior points of the finite elements is based on the profile of the experimental data; regions with steep gradients are approximated using more elements and vice versa. Thus the end points of the finite elements correspond to the time instant of a measurement and the residuals within each finite element go to zero at the collocation points within the length of the element. The optimization was carried out using Successive Quadratic Programming, an efficient, constrained optimization technique.

The calibration of the dynamic version of the carbon cycle was carried out by forcing the model with parameters determined from the steady-state analysis for initial estimates. Fossil emissions were taken from the compilation provided in the CDIAC data base (Trends, 1991). Emissions from land use change were taken from the specifications of the IPCC working group 1 (Enting,I., 1993). These are similar to the revised estimates provided by Houghton (1992). Estimates of bomb release were taken from Enting (1985) and aggregated on an annual basis. The data used for calibrating the model is given in table 4.2.3. Values for the atmospheric ^{12}C concentrations were taken from CDIAC data base (Trends, 1991). Atmospheric ^{14}C concentration data was taken from the compilation by Tans et al. (1981). Oceanic measurements from the GEOSECS experiment were adapted from the compilation by Seigenthaler and Joos (1992). The model was forced from 1860 to 1990. The time axis was partitioned into seven finite elements of 50, 48, 3, 2, 10, 8, and 9 years. The measured data at each end point of the finite elements were used for model calibration.

Reservoir	Amount of Carbon (GT)	^{14}C fractionation
N. H. Air	297	-10
S.H. Air	297	-10
ColdOcean Surface(N)	55.3	-40
Cold Ocean Surface(S)	55.3	-40
Warm Ocean Surface(M)	597	-70
Cold Deep Ocean (N)	2712	-130
Cold Deep Ocean (S)	2712	-130
Interior Ocean(1)	4770	-100
Interior Ocean(2)	4740	-140
Interior Ocean(3)	4720	-160
Interior Ocean(4)	4720	-180
Interior Ocean(5)	4730	-190
Interior Ocean(6)	4760	-190
Biosphere	2200	0

Table 4.2.1 Steady-state conditions for the carbon cycle model

Parameter Description	
K_{as}	0.11 yr^{-1}
K_{am}	0.10 yr^{-1}
K_{ma}	0.10 yr^{-1}
K_{sa}	0.11 yr^{-1}
Constant Diffusivity K_0	2700 m^2/yr
Variable Diffusivity K_1	0.6 m/yr
Upwelling Velocity Vu	$8*10^{-4}$ m/yr
Surface Advection	$4*10^{-3}$ m/yr
Downwelling Velocity Vd	$9.6*10^{-2}$ m/yr
^{14}C Natural Flux	570 mol yr^{-1}
Detrital Flux S	5.1 GT/yr
Revelle Factor (Cold)	14
Revelle Factor (Warm)	9

K_{as} = N and S Atmosphere to cold ocean transfer coefficient ($U_{i=N,S}$)in yr^{-1}

K_{sa} = Cold Ocean to Atmosphere transfer coefficient ($U_i \frac{pCO_{2\ 2,0i}}{C_{\ S,0i}}$ i = N,S)in yr^{-1}

Kam = N and S Atmosphere to warm mid-latitude ocean transfer coefficient ($U_{i=M}$)in yr^{-1}

Kma = Cold Ocean to Atmosphere transfer coefficient ($U_i \frac{pCO_{2\ 2,0i}}{C_{\ S,0i}}$ i = M)in yr^{-1}

Table 4.2.2. Parameters for the Steady State Calibration.

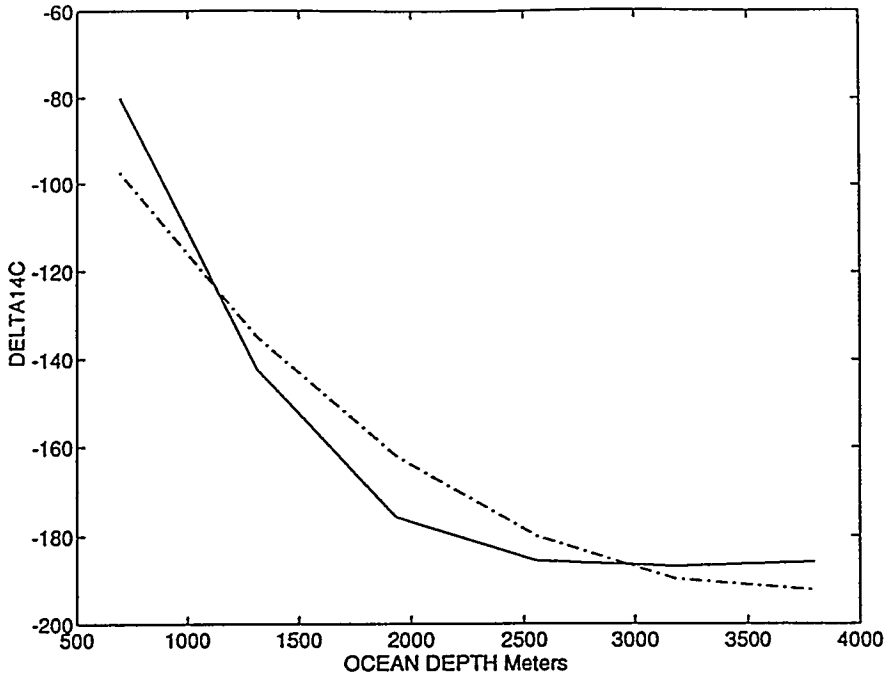

Figure 4.2.4 Observed and model-predicted 14C for the pre-industrial deep ocean. Dashed (predicted), solid line (observed).

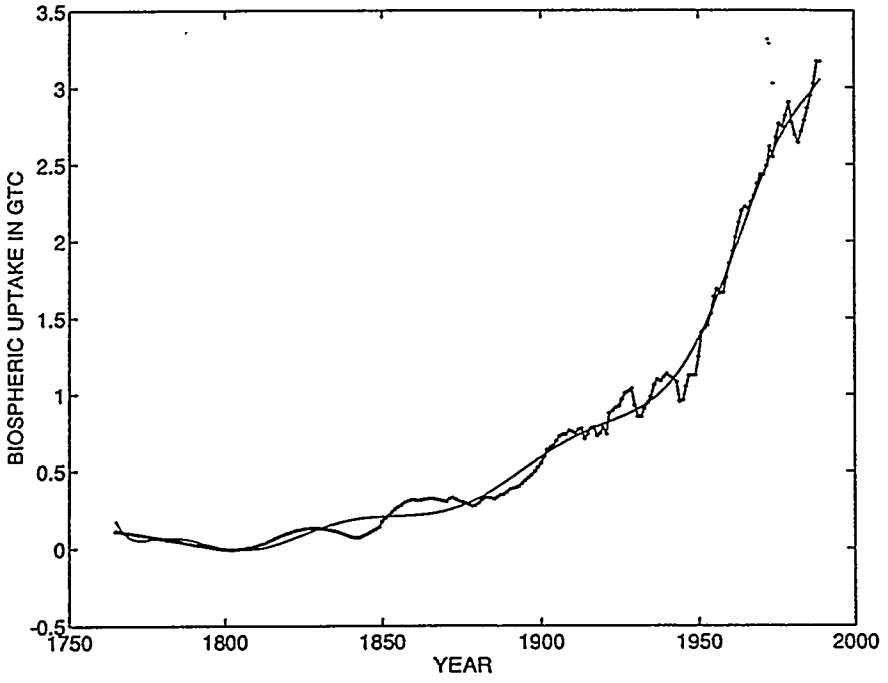

Figure 4.2.5 Biospheric uptake inferred from the steady-state model of carbon cycle

4.2.5 Model Results: Discussion and Conclusions

The results of the model calibration for the dynamic model are provided in tables 4.2.3 and 4.2.4. The optimal values of the model parameters (table 4.2.4) for the calibration of the dynamic model are significantly different from those of the steady-state calibration for the atmosphere ocean--surface exchange terms, the Eddy Diffusivity of the interior ocean, and the detrital flux. The Eddy Diffusivity is higher for the dynamic calibration--which leads to a faster uptake of atmospheric carbon--a requirement if the model has to closely reproduce bomb 14C uptake. In figure 4.2.6 the bomb uptake of carbon is shown. The model predictions are in close agreement with the observations; any discrepancies lie within the ± 10% error in the data.

The current (1990) value of the biospheric uptake from steady-state calculations is about 3 GT/yr (Figure 4.2.5) . This is higher than most inventory-based models of biospheric uptake, but in line with the observation that steady-state calibrations tend to underestimate the transfer of carbon from the atmosphere to the oceans. For example, the 1990 budget for the global carbon cycle, with a net forcing of 7.8 GT (6GT from fossils fuels, and 1.8 GT from land use change) using the steady-state calibration, would result in an oceanic uptake of 1.1GT/yr with the remaining 3.7 GT contributing to the atmospheric increase. .

The biospheric uptake inferred from the calibrated dynamic mode of the carbon cycle is about 1.9 GT/yr for 1990 (Figure 4.2.7). This implies a net oceanic uptake of 2.2 GT/yr. The model effectively suggests that the "missing" sink for carbon is hiding in the biosphere. These results are in fair agreement with a number of recent estimates of the biospheric uptake (Seigenthaler and Joos, 1992; and Sarmiento et al., 1992). The inferred biospheric uptake trajectory for the past 200 years indicates that the biosphere has been responsible for almost as much uptake of atmospheric carbon as the oceans. The total time integrated amounts of oceanic and biospheric uptake provide important insights regarding the relative roles of the two sinks (Fig 4.2.8). The total amount of carbon released to the atmosphere from 1760 to 1990 is about 360 GT, with 213 GT from fossil emissions and 47 GT from land use change. In this period the amount of

carbon in the atmosphere has increased by 157 GT. The remaining 203 GT of carbon uptake is partitioned into the biospheric and oceanic sinks. On the one hand, results from the steady-state calibration suggest that a greater fraction of this sink is biospheric -- 148 GT, as opposed to 55 GT for the oceans. The dynamic calibration, on the other hand, gives an almost even split between the two; the oceanic uptake of 103 GT is only slightly greater than the biospheric uptake of 100 GT.

If the biosphere is as important a sink for carbon important as the oceans, then long term carbon uptake depends upon the dynamics of this sink. Unfortunately, the current scientific understanding of carbon fertilization phenomena is unclear. Recent experimental evidence suggests that enhanced carbon uptake from fertilization may be possible in some ecosystems only with increased temperatures (Oechel et al., 1994). However, somemodeling studies show that increased temperatures may lead to an increase in respiration and attenuate the fertilization process (Sarmiento and Pacala, 1994). The long term implications of this for the carbon cycle are unclear at the present time.

While modeling results provide important insights, the models have significant limitations. Quite apart from the fact that they are highly abstracted versions of the actual processes, which may introduce some unknown biases, the model does not have a good mechanistic representation of two important processes. First, the modeling of marine biology is done in an ad-hoc sense, i.e., the detrital flux is assumed to lie in a particular range and the optimization calculates the best fit. A more process-based approach that links organic production and decay to observations would be required in order to better constrain the model. Second, the biospheric uptake is measured as a residual. More detailed modeling of the biosphere and links with inventories of biospheric uptake may constrain the biospheric sink further.

Year	Measured	Model Predicted
1910 Atmospheric Carbon GTC (N,S) Atmospheric $\delta^{14}C$ (N,S)	317, 317	316.6, 316.6
1958 Atmospheric Carbon GTC (N,S) Atmospheric $\delta^{14}C$ (N,S)	334.5, 334.04 140,140	334.2, 333.9 130,130
1961 Atmospheric Carbon GTC (N,S) Atmospheric $\delta^{14}C$ (N,S)	336.8, 336.4 240,240	336.8, 336.4 240,240
1963 Atmospheric Carbon GTC(N,S) Atmospheric $\delta^{14}C$ (N,S)	337.7, 337.1 750,750	337.6, 337.0 740, 740
1973		
Atmospheric Carbon GTC(N,S)	349.5, 347.5	349.8, 348.4
Atmospheric $\delta^{14}C$ (N,S)	560,570	550,550
Cold Ocean $\delta^{14}C$ (N,S)	10,10	10,10
Warm Ocean $\delta^{14}C$	110	90
Cold Deep Box $\delta^{14}C$	-120	-130
Interior Ocean $\delta^{14}C$ (For each of the six boxes)		
Interior Box (1)	20	30
Interior Box(2)	-150	-140
Interior Box(3)	-180	-180
Interior Box(4)	-190	-190
Interior Box(5)	-190	-190
Interior Box(6)	-190	-190
1981 Atmospheric Carbon GTC (N,S)	366.4, 358.6	367, 360
1990 Atmospheric Carbon GTC (N,S)	375.5,372.8	376, 373

Table 4.2.3. Measured and Model predicted values for atmospheric and oceanic ^{14}C and ^{12}C amounts.

Parameter Description	Value
K_{as}	0.104 yr^{-1}
K_{am}	0.095 yr^{-1}
K_{ma}	0.095 yr^{-1}
K_{sa}	0.104 yr^{-1}
Constant Diffusivity K_0	4995 m^2/yr
Variable Diffusivity K_1	0.4 m/yr
Upwelling Velocity Vu	$6*10^{-4}$ m/yr
Surface Advection	$7.2*10^{-3}$ m/yr
Downwelling Velocity Vd	$4.8*10^{-2}$ m/yr
^{14}C Natural Flux	580 mol/yr
Detrital Flux S	1.3 GT/yr
Revelle Factor (Cold)	14
Revelle Factor (Warm)	9

Table 4.2.4. Best estimates of model parameters dynamic calibration

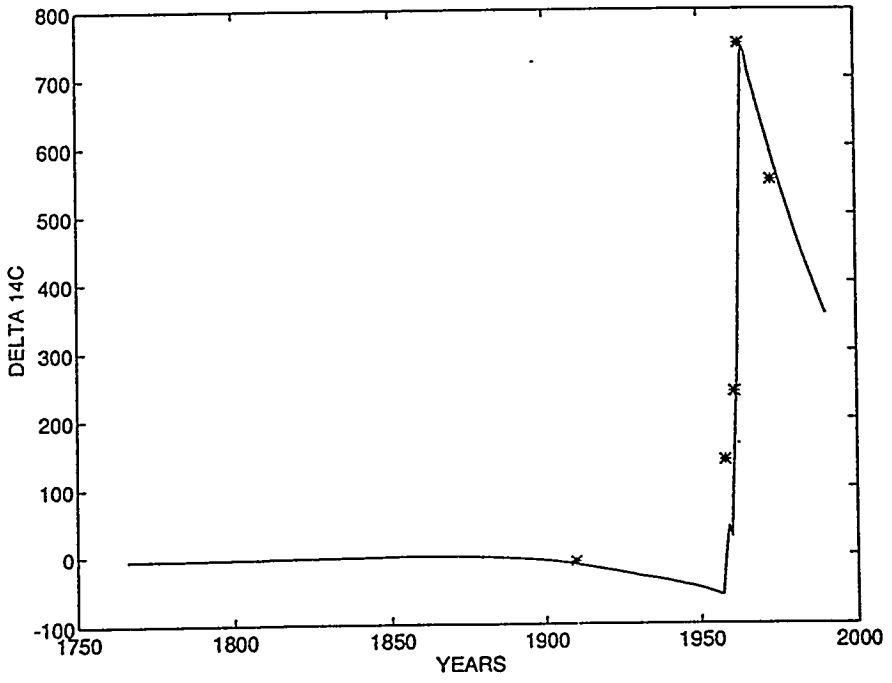

Figure: 4.2.6. Atmospheric fractionation of 14C. Notice the bomb carbon peak and subsequent oceanic uptake. Atmospheric observations are represented by *.

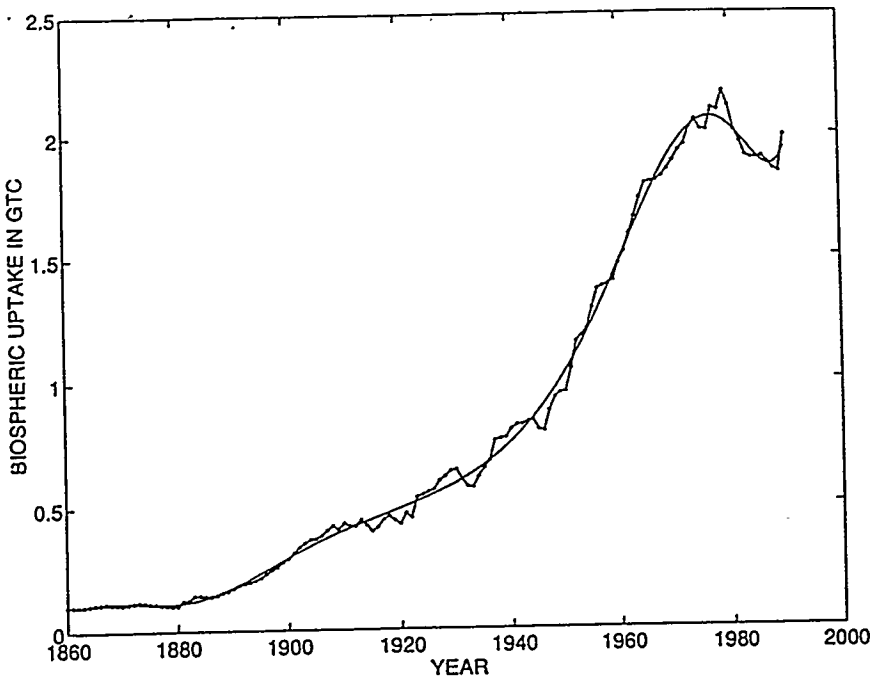

Figure 4.2.7 Biospheric Carbon sink inferred from the dynamic calibration

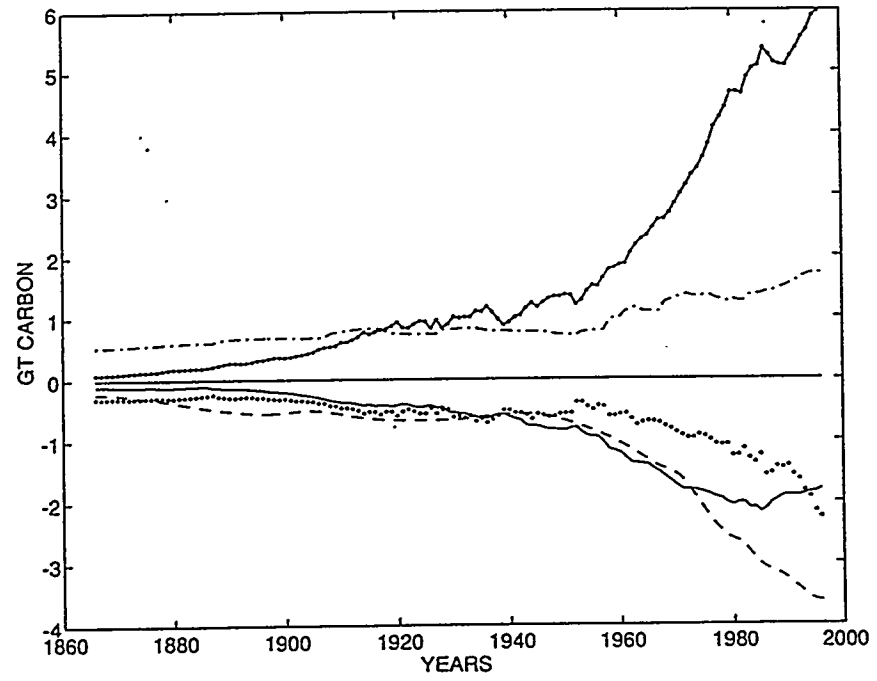

Fig 4.2.8. Relative contribution of sources and sinks of carbon. The top half shows sources and bottom half shows sinks. Legend for the top half : land use change(-·-·-), fossil fuel (—). Legend for the bottom half: Atmospheric increase(---), biospheric uptake (——), oceanic uptake (···).

An important aspect of model calibration which has not been discussed in this section deals with identification of model parameters. More precisely, while parameter estimation seeks to determine a best estimate for model parameters, parameter identification is aimed at determining the uncertainties in these estimates. As pointed out in chapter 2, ill-conditioned inverse problems may have large uncertainties in the estimates of model parameters. Few formal tools of parameter identification have been applied to models of the carbon cycle and a preliminary analysis suggests that the model of the carbon cycle is highly ill-conditioned. A detailed analysis that characterizes the identification of model parameters is in progress.

Chapter 5: Indices for Comparing Greenhouse Gas Emissions

5.1 Introduction

A key element of possible policy responses to global climate change is the abatement of emissions of radiatively active gases. There has been considerable interest in viewing the emissions abatement problem as one involving multiple gases and not CO_2 alone. Comprehensive abatement strategies were proposed by the US Government (USDJ, 1991) based on the rationale that all greenhouse gases contribute to climate change. Under a comprehensive plan greenhouse gas abatement must be carried out where "it costs least to do so" (Stewart, 1992). In such an approach, a minimum cost solution would require the control of multiple gases. More recently, comprehensive abatement has moved into an implementation phase with methane abatement being an important part of the Clinton Administration's proposal to meet emissions reduction targets (DOE, 1994).

It has been argued that a comprehensive abatement strategy requires the formulation of a greenhouse gas index that would allow for an evaluation of tradeoffs between greenhouse gases in a number of possible abatement contexts, including:

1. The evaluation of tradeoffs between gases in a comprehensive abatement strategy.

2. Comparison of investments in abatement projects made toward mitigating climate change.

3. Comparing the current and future emissions responsibility of nations.

Such a greenhouse gas index would require the dynamic representation of the greenhouse forcings, as well as the global cycles of individual gases. The most widely discussed metric is the

Global Warming Potential (GWP) (Lashof and Ahuja, 1990; Houghton et al., 1990). A number of scientific problems have been identified with the formulation and use of GWPs (Enting and Rodhe, 1991; Hammond et al., 1991; Handel, M., 1991a). Attempts have been made to provide alternatives (Hammond et al., 1991) and modifications (Harvey, 1992) to GWPs.

Additionally, "GWPs do not account for the time variation in the economic opportunity costs of an increment of radiative forcing," (Eckaus, 1992). Consequently, they do not provide any insights for abatement policy formulation. Damages linked to climate change and abatement costs associated with emissions reductions are both time varying quantities, and consequently, need to be explicitly included in the calculation of a metric that determines gas-by-gas greenhouse responsibility.

Optimal control and dynamic optimization models have been extensively used in natural resource economics (see for e.g., Kamien and Schwartz, 1981). Optimal control models have also been used to study greenhouse gas abatement policies (Nordhaus, 1992; Peck and Tiesberg, 1993; Falk and Mendelsohn, 1993). Reilly and Richards (1993) have used an economy-climate optimal control model to estimate greenhouse gas indices based on the relative economic impact of BAU greenhouse gas emissions assuming specific damage functions. Kandlikar and Patwardhan (1993) describe an analytical optimal control framework to evaluate trace gas indices.[35] In this paper the optimal control framework is used to further this analysis and estimate trace gas indices for greenhouse gases using more detailed science. The paper will examine the role of alternative problem formulations and uncertainties in these calculations.

Recognizing that in practice the specification of a dynamic damage function and abatement costs is a daunting task, we also formulate a cost-effectiveness framework, where climate change and damage information is included through constraints on model variables. First, cost-effective trace gas indices based on IPCC emissions scenarios are determined, while recognizing that these scenarios have been developed under different assumptions regarding future expectations of

---

35 Schmalensee (1993) arrives at similar results based on comparing damages from unit emmisions of trace gases.

technological diffusion and damages from climate change. Second, the optimal abatement problem for a multiple gas abatement strategy involving methane and carbon dioxide is solved numerically, assuming costs of abatement and climate damages presented in the literature. While trace gas indices are evaluated for other trace gases, nitrous oxide, and HCFC-22, the focus of this paper is on methane. Next to CO_2, Methane is the second most important greenhouse gas; the instantaneous radiative forcing due to a unit mass of methane is 58 times that of a unit mass of CO_2. This, coupled with the possibility of low costs of abatement, makes methane an attractive short-term abatement option.

The analysis in this paper includes both direct and indirect effects of trace gases on greenhouse forcing. Indirect radiative forcing effects of trace gases resulting from byproducts of tropospheric chemical interactions are considered. Other global (Stratospheric Ozone) or regional (Tropospheric Ozone) environmental effects are not considered. Additionally, we do not consider the uncertain benefits of CO_2 fertilization. While this may affect the trace gas index for other greenhouse gases, the effect on methane will not be large since each molecule of methane oxidizes to CO_2 in the atmosphere. If the benefits of carbon fertilization vary linearly with concentration then each unit of methane will lead to the same benefit as would a unit of CO_2.

The cost benefit (C-B) analysis formulation is set up in section 5.2. Trace gas indices, defined as the cost of abating the next unit of a non CO_2 trace gas (relative to CO_2), are analytically determined using a general form of damage function. In section 5.3, a similar analysis is carried out using the cost-effectiveness (C-E) framing, and scenario-based trace gas indices are determined using IPCC scenarios. In section 5.4, indirect radiative forcing effects resulting from chemical interactions of methane are calculated. Section 5.5 deals with the numerical estimation of the optimal index for the two gas strategy. This is followed by a discussion of the results and the policy implications of this work.

5.2 Trace Gas Indices Using Cost-Benefit Framing

In this section we briefly describe the optimal control framework developed in Kandlikar and Patwardhan (1993). We restrict out analysis to two gases--CO_2 (referred to as gas 1) and a non-CO_2 gas (referred to as gas 2)--since the analysis can be easily generalized to more than two gases. In a cost benefit framing, the costs abatement and minimizing damages due to climate change are minimized. The optimal control problem can be stated as:

$$\text{min.} \quad \int_0^t \left\{A_1(a_1(t)) + A_2(a_2(t)) + D(c_1(t),c_2(t))\right\} e^{-rt} dt \tag{5.1}$$

$$\text{St.} \quad \frac{dc_1}{dt} = -\gamma_1 c_1(t) + \beta\,(s_1(t) - a_1(t)) \tag{5.2}$$

$$\frac{dc_2}{dt} = -\gamma_2 c_2(t) + (s_2(t) - a_2(t)) \tag{5.3}$$

Equation 5.1 is the cost objective function, while 5.2 and 5.3 are trace gas mass balance equations. A $_{1,2}$, $a_{1,2}$, $c_{1,2}$, $s_{1,2}$, $\gamma_{1,2}$ are the costs of abatement, levels of abatement, atmospheric concentration and Business-As-Usual emissions, and atmospheric lifetimes of gases 1 and 2, respectively. β is the atmospheric airborne fraction of CO_2 and $D(c_1,c_2)$ is the damage function due to climate change. The Hamiltonian H is given by

$$H=\left\{A_1(a_1(t)) + A_2(a_2(t)) + + D(c_1,c_2)\right\} e^{-rt} +$$
$$\lambda_1(t)[-\gamma_1 c_1(t) + \beta(s_1(t) - a_1(t))] + \lambda_2(t)[-\gamma_2 c_2(t) + (s_2(t) - a_2(t))] \tag{5.4}$$

The first order necessary conditions are given:

$$\frac{\partial H}{\partial a_i} = 0 \tag{5.5}$$

$$\frac{\partial H}{\partial c_i} = -\lambda_i \tag{5.6}$$

This leads to

$$\lambda_1 = \frac{1}{\beta} * \frac{\partial A_1}{\partial a_1} e^{-rt} \quad \text{and} \quad \lambda_2 = \frac{\partial A_2}{\partial a_2} e^{-rt} \tag{5.7}$$

$$\dot{\lambda}_1 = \gamma_1 \lambda_1 - \left[\frac{\partial D(c_1, c_2)}{\partial c_1}\right] e^{-rt} \quad \text{and} \quad \dot{\lambda}_2 = \gamma_2 \lambda_2 - \left[\frac{\partial D(c_1, c_2)}{\partial c_2}\right] e^{-rt} \tag{5.8}$$

Equation 5.7 is the static optimality condition that relates the shadow price of the emissions constraint to the cost of abatement. Equations 5.7 and 5.8, in conjunction with equations 5.2 and 5.3 and initial conditions on c_i (e.g., the current value of atmospheric concentrations), and final conditions on λ_i represent a two point boundary value problem that can be solved numerically. The quantities $\frac{\partial A_1}{\partial a_1}$ and $\frac{\partial A_2}{\partial a_2}$ are the marginal costs of abatement for gases 1 and 2 and are subsequently denoted M_1, M_2. Assuming that the air-borne fraction β for CO_2 is a constant,[36] we can eliminate λ_1 and , λ_2 and $\dot{\lambda}_1$ and $\dot{\lambda}_2$ from 5.7 and 5.8 and obtain

$$\dot{M}_1 = (\gamma_1 + r) M_1 - \beta \left[\frac{\partial D(c_1, c_2)}{\partial c_1}\right] \quad \text{and} \quad \dot{M}_2 = (\gamma_2 + r) M_2 - \left[\frac{\partial D(c_1, c_2)}{\partial c_2}\right] \tag{5.9}$$

Equation 5.9 is a key equation that expresses the economic optimality condition - that the marginal costs of abatement of each gas is equal to the marginal damages from climate warming, if that unit of gas is left unabated. It contains the greenhouse gas attributes we need to capture- the gas lifetimes ($1/\gamma_1$, $1/\gamma_2$) , marginal costs of abatement (M_1, M_2), marginal climate damages ($\frac{\partial D}{\partial c_1}$, $\frac{\partial D}{\partial c_2}$)and discount rate, r. We now need to consider the specification of physically realistic damage functions. Typically damages due to climate change will be a function of particular climate

36 For details on the limitations of this assumption see Enting and Newsam (1990).

variables. In the simplest case, the damage function is assumed to be a function of the mean global temperature T(t)[37]. Thus we can write:

$$\frac{\partial D(c_1,c_2)}{\partial c_{i(i=1,2)}} = \frac{\partial D}{\partial c_i} = \frac{\partial D}{\partial T} * \frac{\partial T}{\partial c_i} . \qquad (5.10)$$

The terms $\frac{\partial T}{\partial c_1}$ and $\frac{\partial T}{\partial c_2}$ depend on the temperature trajectory T(t), which is the response of the climate system to radiative forcing, $R(c_1(t),c_2(t))$. A simple model to evaluate T(t), which treats the climate system as linear, is the convolution integral:

$$T(t) = \int_0^t R(C_{i=1,2}(t))H(t-\tau)d\tau. \qquad (5.11)$$

where H(t) is the impulse response of the climate system. Models with linear system approximations of the climate system have been formulated by Dickinson (1981) and Schneider and Thompson (1981), and also used for policy analysis (Houghton et al., 1990; Nordhaus, 1992). We further assume that the radiative forcing $R(c_1(t),c_2(t))$ is linearly separable, i.e., $R(c_1(t),c_2(t)) = R_1(c_1(t)) + R_2(c_2(t)$.[38]

From 5.8, 5.10, and 5.11 the marginal cost of abatement for gas i is given by

$$M_i(t) = \int_t^{T_h} \frac{\partial D(T(t))}{\partial T(t)} * \left\{ \int_0^t \frac{\partial R(C_i(t))}{\partial C_i(t)} * H(t-\tau) * F_i(\tau)\, d\tau \right\} e^{-rt} dt, \qquad (5.12)$$

---

37 We limit ourselves to damage functions that are dependent on the instantaneous value of temperature. In reality, damages will depend not only on the instantaneous value, but also on the time trajectory of temperature and other climatic variables, as well as on human adaptation activities. For a more detailed discussion of dynamic damage functions, see Dowlatabadi, Kandlikar, and Patwardhan (1994).

38 While this assumption does not hold for gases with significant overlap, such as CH_4 & N_2O, it is reasonable in most cases.

where $F_i(\tau)$ is the impulse response of the atmospheric concentration of gas i to its emission. The ratio of the marginal costs of abatement of a non CO_2 gas with that of CO_2 is defined as the trace gas index I. At the economic optimum I is equal to the ratio of damages caused per unit emissions of each gas. This index is evaluated at time t=0, which is set nominally at 1990.

$$I = \frac{\left[\int_0^{T_h} \frac{\partial D(T(t))}{\partial T(t)} * \left\{\int_0^t \frac{\partial R(C_i(t))}{\partial C_i(t)} * H(t-\tau) * F_i(\tau)\, d\tau\right\} e^{-rt} dt\right]_{i=2}}{\left[\int_0^{T_h} \frac{\partial D(T(t))}{\partial T(t)} * \left\{\int_0^t \frac{\partial R(C_i(t))}{\partial C_i(t)} * H(t-\tau) * F_i(\tau)\, d\tau\right\} e^{-rt} dt\right]_{i=1}} \qquad (5.13)$$

In the above equation, $F_i(\tau)$ is the additional increase in future concentration per unit of the source released at time (τ=0). If the trace gas cycle is approximated by a linear system this term is equal to the impulse response of atmospheric concentration to source emissions.[39]

$H(t-\tau)$ is equal to the change in global mean temperature at future time t for small change in the radiative forcing at time τ, $0 < \tau < t$. This captures the inherent lag in the climate response to an increase in radiative forcing. $\frac{\partial R(C_i(t))}{\partial C_i(t)}$ is the instantaneous radiative forcing of gas i, i.e., it is the increase in radiative forcing due to a unit increase in the atmospheric concentration of the gas.[40] $\frac{\partial D(T(t))}{\partial T(t)}$ describes how climate damages may change with temperature. There is much evidence and concern that climate damages measured in physical units (for example, sea level rise due to temperature change or soil moisture) or in corresponding economic units (damages from coastal

39 Although the trace gas cycles of CO_2 and CH_4 have non-linearities, it is routine to use linear approximations for the purposes of prediction. Impulse responses have been derived for most trace gases.

40 Relative to CO_2, most other trace gases have high values of instantaneous radiative forcing.

erosion and storms or loss in agricultural yield) are likely to be non-linear and convex, i.e., the rate of increase in damages may increase with increasing temperature (RFF, 1993).

We can obtain the GWP from equation (5.13) by making the following simplifying and arbitrary assumptions:

1. Assume that damages are a *linear* function of temperature, i.e., the term $\frac{\partial D(T(t))}{\partial T(t)}$ from equation 4 can be replaced by a constant.

2. Assume that the climate lag time (i.e., the time constant for the oceanic response) is *zero.*, i.e, the function $H(t-\tau)$ is set equal to $\delta(t)$, the Dirac delta function.

This effectively replaces the integral inside the curly brackets with the term $\frac{\partial R(C_i(t))}{\partial C_i(t)} * F_i(\tau)$. In addition to assumptions 1 and 2, if the discount rate is set equal to zero, then equation (5.13) reduces to

$$I = \frac{\left[\int_0^{T_h} \frac{\partial R(C_i(t))}{\partial C_i(t)} * F_i(\tau)\, d\tau\right]_{i=2}}{\left[\int_0^{T_h} \frac{\partial R(C_i(t))}{\partial C_i(t)} * F_i(\tau)\, d\tau\right]_{i=1}} \qquad (5.14)$$

which is exactly the definition of the Global Warming Potential (GWP). Thus the GWP is an optimal trace gas index under unrealistic scientific and economic assumptions, although for different reasons than those put forth by Reilly and Richards (1993). This analysis does not require that shadow price of emissions be a constant in order for an index exclusive of economic damages to be optimal. Additionally, the index devised by Reilly and Richards can be derived from equation (5.13) by setting the oceanic response time to zero. In general, optimal trace gas indices defined in equation (5.13) have to be numerically evaluated by solving the two point boundary value problem

described by equation (5.9); this and would involve specifying costs of abatement and greenhouse damages. This numerical exercise is carried out for methane in section 4. However, the relative costs of greenhouse abatement and damages from climate change are a subject of much controversy. Costs of abatement vary from the relatively high "top down" estimates from energy-economic modeling, to the low "bottom up" estimates from engineering feasibility studies. Similarly, damage estimates vary greatly, as do expert judgments regarding them (Nordhaus, 1993). In order to capture these different expectations, an alternative approach to the calculation of trace gas indices would be to specify scenarios for future temperature trajectories and directly evaluate equation (5.13), assuming different functional forms for the damage functions. This approach is termed here as a cost-effectiveness approach. Note that in the cost-effectiveness approach it is sufficient to specify only the functional dependence of greenhouse damages on global mean temperature; the index does not depend on a scale factor for conversion into economic units. In the next section (5.3), the cost-effectiveness analysis is described and trace gas indices are calculated for a variety of emissions/abatement scenarios.

5.3 Cost-Effectiveness Analysis

A cost-effectiveness analysis is often regarded as a plausible alternative to cost benefit analysis when benefits are uncertain or unknown or when value of the benefit stream from a set of actions cannot be explicitly quantified (Tietenberg, 1991). A desirable and obtainable objective is selected--with the implicit assumption that the investments/decisions are worthwhile--but a formal cost-benefit criterion is not applied (Morgan and Henrion, 1990). A cost-effectiveness analysis has several potential advantages. First, from the perspective of negotiating a climate treaty, several contentious issues dealing with determining costs and damages are replaced by politically negotiated choices on climatic variables and trajectories.[41] Second, constraining physical variables

[41] Indeed, the guidelines for greenhouse abatement in the Framework Convention on Climate Change (UNCED, 1992) seek to*"acheive stabilization of atmospheric carbon at a level and in a*

can allow us to implicitly value the preservation of natural systems--something most estimates of greenhouse damages[42] fail to do.

The cost-effectiveness analysis is formulated by minimizing the total costs subject to a constraint on the global mean temperature trajectory of the form T(t) = T*(t), where T*(t) is an exogenously specified temperature trajectory. Following Kandlikar and Patwardhan (1993), it can be easily shown that the trace gas index is same as that in equation (13), where the term $\frac{\partial D(T(t))}{\partial T(t)}$ is evaluated at T(t) = T*(t). The resultant trace gas index has been evaluated for two different scenarios; the IPCC scenarios A and D reflecting business as usual, and high abatement situations.

Index evaluations were carried out for methane, nitrous oxide, and HCFCs for the time horizon T_h of 100 years. CFCs were omitted because their role in net radiative forcing is considered to be small due to offsetting effects of ozone depletion (Ramaswamy, 1992). With the exception of CO_2, greenhouse gas impulse responses $F_i(\tau)$ were constructed using a single exponential lifetime (See table 5.1). For CO_2 a single lifetime model is inadequate to accurately represent the oceanic uptake (Enting and Newsam, 1990), hence, the multiple exponential model devised by Meier-Reimer and Hasselman (1987) is used. Additionally, biospheric sources and sinks of CO_2 are assumed to be equal. Concentration dependent radiative forcing was determined by using the Wigley-Raper relationships provided in the IPCC scientific assessment. A simple climate model with climate sensitivity of (ΔT for CO_2 doubling) of 3 °C and an ocean response time of 30 years was used. Calculations were carried out for damages that are linear, quadratic, and cubic functions of temperature; they were carried out for discount rates of 0%, 3%, and 6%. The corresponding values for global warming potentials, which are independent of the emissions scenarios, are also presented.[43] All index calculations are based on direct radiative forcing; indirect effects of methane resulting from tropospheric interactions have not been included.

---

time frame sufficient to: 1) allow ecosystems to adapt naturally to climate change, 2) to ensure that food production is not threatened, and 3) to enable economic development to proceed in a sustainable manner."

42 For a critical assessment of greenhouse damages, see Ayres and Walters (1991).

43 The values for methane and nitrous oxide are higher than those provided in the 1992 IPCC supplement . The difference is due to the spectral overlap between Methane and Nitrous oxide (not included here), which reduces radiative forcing of methane by 15-20%. Additionally, the assumed

In table 5.1 we provide for reference the assumed lifetime, current values for instantaneous radiative forcing (relative to CO_2), and the global warming potentials for methane, nitrous oxides, and HCFC-22--a representative halocarbon . Table 5.2 provides trace gas indices derived from this analysis for each of the emissions and damage scenarios at an assumed discount rate of 2%. In table 5.3 we capture the effect of discount rates on the scenario-based trace gas index for methane. For gases that are short-lived relative to CO_2, i.e., Methane and HCFC-22, the trace gas index decreases with increasing non-linearity of the damage function. This is simply due to the monotonic dependency of the indices upon the temperature trajectory and climate-derived temperature change which accumulates with time, thus de-emphasizing gases with lifetimes shorter than CO_2. Conversely, Nitrous oxide has a higher effective lifetime relative to CO_2 and, hence, the value of index increases with increasing non-linearity of the damage function.

The effect of emissions scenarios A and D, on trace gas indices is slightly more complicated. The temperature trajectories resulting from the IPCC emission scenarios A and D deviate significantly from one another on time scales greater than the lifetimes of short-lived gases. Since the marginal damages due to the realized temperature change increase monotonically with temperature, the difference in indices for the two scenarios results primarily from differences in temperature trajectories on longer time scales. Thus a gas with a short lifetime has a smaller index for scenario A (high future temperature trajectory) than for Scenario D (low future temperature trajectory) and vice versa.

From table 5.2 it is seen that trace gas indices are more sensitive to the level of non-linearity in the damage function than they are to that in the emissions scenario. Scenarios A and D capture very different, opposing views--ranging from a coal intensive energy supply for scenario A to a renewable and nuclear intensive energy supply for scenario D--of the expected future energy mix. This suggests that index calculations are reasonably robust over a wide range of possible outcomes of energy supply futures. From table 5.3 it is apparent that trace gas indices depend critically upon the choice of the discount rate. A higher discount rate reduces the impact of future damages from

---

lifetime for nitrous oxide and HCFC-22 in this analysis were slightly different than those in the IPCC, 1992 supplement.

trace gases with longer lifetimes and leads to an increase in the value of the index for species that are short-lived relative to CO_2. Conversely, for a species that is long lived relative to CO_2, higher discount rates lead to an decrease in its trace gas index.

These results may differ from the corresponding ones given by Reilly and Richards (1993) for several reasons. This analysis includes a representation of the lagged oceanic response to radiative forcing not included in their work. The ocean lag tends to increase the amount of time between emissions of the trace gas and the resulting damages. Therefore, the inclusion of more realistic science in the form of oceanic lag tends to increase the value of the trace gas index for shorter lived gases and vice versa. Second, this analysis includes realistic representations of the relationship between radiative forcing and trace gas concentrations. Finally, we use a more representative oceanic carbon cycle model; a single exponential model, such as that used by Reilly and Richards (1993), tends to underestimate predicted concentrations of CO_2.

5.4 Indirect Radiative Forcing Effects of Methane

In addition to directly trapping heat in the atmosphere, chemical interactions of methane in the atmosphere lead to the formation of other trace species that can in turn trap heat. The chemistry of methane in the troposphere is complex and involves dozens of trace species. For a detailed account see Wuebbles and Tamaseris (1993). Uncertainties in the modeling of these interactions arise from the short lifetimes of the chemical constituents involved and emissions uncertainties (Kanikadou and Crutzen, 1993; Guthrie and Yarwood, 1992). Although the uncertainties are large, the inclusion of "best guess" indirect effects in trace gas index calculations is appropriate. As is shown in this section the inclusion of indirect effects can increase the value of the trace gas index as much as 50%. The key mechanisms that result in indirect radiative forcing of the atmosphere are the increased concentration of tropospheric ozone, increased concentration of

stratospheric water vapor, and changes in the lifetime of methane resulting from its non-linear, atmospheric interactions, also called the CH_4-OH feedback effect.

Following Lelieveld et al. (1993), the indirect effects of methane can be calculated by modifying the instantaneous radiative forcing term to include indirect radiative forcing. This is readily achieved by replacing the direct radiative forcing term $\frac{\partial R(C_i(t))}{\partial C_i(t)}$ in equation (5.14) with

$$\frac{\partial R(C_i(t))}{\partial C_i(t)} = \frac{\partial R(C_i(t))}{\partial C_i(t)} + \sum_j \frac{\partial R(C_j(t))}{\partial C_j(t)} * \frac{\partial C_j(t)}{\partial C_i(t)}, \qquad (5.15)$$

where the terms inside summation represent a first order approximation for the indirect radiative forcing. The subscript j refers to the trace species formed in the atmosphere due to chemical interactions of trace gas i, in particular for methane, j refers to ozone and water vapor.

The sensitivity terms $\frac{\partial C_j(t)}{\partial C_i(t)}$, the amount of trace species j produced per unit amount of methane, were determined from model-based calculations. The formation of tropospheric ozone from methane depends upon the concentration of nitrous oxides (NOx) in the atmosphere. For regions of high NOx a single molecule of methane yields about 3.7 molecules of ozone, while in regions of low NOx each molecule of methane leads to -1.7 molecules of ozone (Wuebbles and Tamaresis, 1993). Model results suggest that the net effect of low and high NOx emissions will be an increase in the concentration of ozone. The influence of methane on stratospheric water vapor is not well known. Model results for excess molecules of water vapor from one molecule of methane vary from 0.05 to 0.3 (Wuebbles, 1989). For the purpose of this analysis we chose 0.05 derived from calculations by Lelieveld et al. (1993). The instantaneous forcing for trace species $\frac{\partial R(C_j(t))}{\partial C_j(t)}$ were derived using the Wigley-Raper relationships presented in IPCC (1990).Another mechanism by which tropospheric interactions affect the trace gas index of methane is through changes in its lifetime. Increasing concentrations of methane are expected to deplete the atmospheric abundance of the hydroxyl radical, which is the main sink for methane,

and thus lead to an increase in the lifetime of methane. Hence the lifetime of methane depends on the particular emissions scenario.[44] Assuming a current lifetime of 10.5 years, and using the simple relationships derived by Osborn and Wigley (1994), the time dependent lifetime for methane was determined for each scenario and used to calculate the indirect effect of changing methane lifetime. Indirect trace gas indices calculated from equation 14 are presented in table 5.4.

The inclusion of indirect effects leads to a 50% increase in trace gas index for methane. Much of this increase is attributable to ozone (30%) with stratospheric water vapor contributing to a small increase (5%). The effect of changing methane lifetime on atmospheric trace gas indices is between 5 and 10%, depending on the emissions scenario; the high number corresponds to the high emissions scenario, and vice versa for the low number. As mentioned earlier, all these numbers must be treated with caution because of the current uncertainties in model predictions especially those that arise from a lack of spatial detail in atmospheric chemistry models (Lelieveld et al., 1993).

Index	Cubic Damages		Quadratic Damages		Linear
	IPCC-A	IPCC-D	IPCC-A	IPCC-D	Damages
Direct	8.5	10	12	13	19
Ozone	2.5	3.0	3.6	3.8	5.7
Water Vapor	0.4	0.5	0.6	0.65	0.95
OH Feedback	1.2	0.8	1.7	1.0	2.6
Net	12.6	14.2	17.9	18.3	27.8

Table 5.4 Scenario-based trace gas indices for methane, including indirect effects (Integration time of 100 years, discount rate of 2%).

44 In reality the lifetime depends on NOx, carbon monoxide, and non-methane hydrocarbon concentrations. However, it is possible to fit an accurate response surface to the lifetime using methane concentrations alone. The equation $T(t) = T(0) * (C(t)/C(0))^{0.238}$, where T(t) is the time varying lifetime at time t , T(0) is the current lifetime, and C(t) is the concentration trajectory, provides a good fit to model outputs (R^2 = 0..98) (Wigley and Osborne, 1994).

Trace gas	Instantaneous forcing CO_2 =1	Life time (years)	GWP*
Carbon Dioxide	1	See Text	1
Methane	58	10.5	11
Nitrous Oxide	206	150	290
HCFC-22	5440	15	1500

Table 5.1: Key Scientific Attributes of Trace Gases.
*GWP Integration time is 100 years.

Trace gas	Cubic Damages		Quadratic Damages		Linear Damages
	IPCC-A	IPCC-D	IPCC-A	IPCC-D	
Methane	8.5	10	12	12.9	19
Nitrous Oxide	289	286	282	280	269
HCFC-22	1284	1466	1706	1811	2445

Table 5.2: Scenario based trace gas indices for trace gases (Integration time of 100 years) for a discount rate of 2%. Note that for damages that depend linearly on temperature, the index is independent of damage function and emissions scenario.

Discount rate	Cubic Damages		Quadratic Damages		Linear Damages
	IPCC - A	IPCC - D	IPCC - A	IPCC - D	
r = 0%	6.4	7.6	8.5	9.3	13.3
r = 2%	8.5	10	12	12.9	19
r = 6%	15	16	20.6	21	27.7

Table 5.3: The effect of discount rate on trace gas index for methane

5.5 Estimation of Optimal Index for Methane

In the previous section numerical values for trace gas indices were determined under scenarios for future greenhouse warming. Since the emissions trajectories were exogenously specified, the calculation did not require an explicit characterization of the costs of abating greenhouse emissions. In section 2 it was noted that an optimal trace gas index could be determined if costs of abatement for greenhouse gases and damages from climate change were specified. Here the calculation of such an optimal index is presented on the basis of estimates of greenhouse abatement costs and damages available in the literature. A note of caution needs to be added before one presents a cost-benefit analysis for climate change policy, indeed as one should when attempting any such analysis over century long time scales. Despite recent efforts, greenhouse damage estimates remain sketchy at best. The estimates by Nordhaus (1992) suggest a rather benign impact of climate change on the human economic system. Ayres and Walters (1991) and Cline (1992), among others, tend to disagree with this assessment and suggest much larger values for benefits of greenhouse abatement. Lave and Vickland (1989) argue that developing countries may be more vulnerable to climate change and could face large damages. Additionally, non-market/ecosystem damages of global temperature rise remain largely unknown. On the cost side, engineering estimates of carbon abatement costs differ greatly from those derived from macro-economic energy modeling. For example, one study cites that estimates for a 20% percent reduction in current emissions the marginal costs vary from 120 $/tC to 50 $/tC across models (Wilson and Swisher, 1993).

Bearing in mind the above uncertainties, the analysis that follows should be treated as purely illustrative. Greenhouse damages are specified as a fraction (1.3%) of an exogenous global GDP, based on Nordhaus (1992), with the global GDP following the Nordhaus no-controls scenario. The lack of an explicit economy growth model means that economic feedbacks are not modeled. If climate damages are large this could lead to an underestimate of total damages compared to a model where economic feedbacks are explicitly modeled.

Costs of abatement for CO_2 were taken from Falk and Mendelsohn (1993), whose estimates for the cost curve are based on work by Nordhaus. The costs used in the analysis, therefore, reflect the energy economic "top down" view of CO_2 abatement. The costs of abatement for methane are extremely sketchy, and estimates vary over a wide range. Adams et al. (1992) estimate costs of abatement for agricultural activities in the US ranging from $500 to $4000 per ton. The NAS report on policy implications of greenhouse warming (NAS, 1992) suggest far lower US costs of 50-100 $/tC. Additionally the NAS report estimates landfill emissions control costs as low as 20-30 $/tc. To reflect this variation two scenarios were chosen for the costs of abatement for methane relative to CO_2. One scenario, where the cost of abatement for the two gases is equal for the same level of abatement, i.e., $A_1(e_1) = A_2(e_2)$ when $e_1 = e_2$--(Scenario 1)-- and a second scenario, where costs of abating methane are an order of magnitude higher, i.e., $A_1(e_1) = 0.1*A_2(e_2)$ when $e_1 = e_2$--(Scenario 2).

The trace gas index for methane was determined by solving the optimal control problem for the costs and damages described above. Trace gas and climate models were the same as those described in section 3. The formulation requires the specification of a Business As Usual (BAU) scenario which was taken from the IPCC Scientific Assessment. The problem was solved as a dynamic, non-linear optimization problem. The control profile was approximated as a time dependent polynomial, whose coefficients were estimated by optimization. In order to obtain physically realistic solutions, the abatement activity of methane was limited to its anthropogenic emissions.

The analysis was carried out for linear, quadratic, and cubic damage functions and for discount rates of 0%, 2%, and 6%. The scenario-based optimal indices for methane are presented in Table 5.4. The optimal temperature trajectories resulting from the solution of the optimal control problem, are shown in Figure 5.1.

Discount rate	Cubic Damages		Quadratic Damages		Linear Damages
	Scenario 1	Scenario 2	Scenario 1	Scenario 2	
r = 0%	9	9.65	12.2	12.9	19.6
r = 2%	11.9	12.8	17.0	18	28
r = 6%	20.8	22.6	30	31	42.6

Table 5.4 Optimal values of trace gas index for Methane (including indirect effects)

As observed from figure 5.1, the optimal temperature trajectories for the two scenarios of methane abatement costs do not differ significantly. When the costs of methane abatement are low (Scenario 1), the high per unit instantaneous radiative forcing of methane results in significant early methane abatement. This causes the temperature trajectory to deviate from the BAU case at t = 1990. For high costs of abatement (Scenario 2) this deviation takes place later in time. Additionally, the two trajectories do not differ sufficiently enough to cause significantly different marginal damages. Hence, the indices for the two scenarios do not differ significantly, suggesting that accurate costs of abatement for methane may not be critical in trace gas index calculation. As in the previous section, the degree of non-linearity in the damage function continues to be a more critical determinant of the trace gas index than the temperature trajectory. The discount rate also continues to be the most important parameter in the calculation of the optimal trace gas index.

Much of the early discussion on trace gas indices, particularly GWPs, revolves around the choice of an appropriate time horizon for integration. This is particularly problematic because there is no clear way to choose an integration time. When the problem is cast into an economic framing the choice of time horizon is converted into a choice of an appropriate discount rate. The choice of a discount rate is then linked to expectations of future economic growth, and, in turn to the degree of optimism that a decision-maker has regarding future outcomes. More optimistic outcomes would imply higher discount rates. The analysis by Lave and Dowlatabadi (1993) suggests that future expectations and decision criteria of decision-makers may be the most important determinants of

climate change policy decisions. Hence, the fact that the choice of a discount rate may be key to climate change policy decisions is also reflected in the value of trace gas indices.

Scientific uncertainty plays an important role in determining trace gas indices, particularly for methane. Uncertainties in tropospheric interactions and resulting indirect effects and uncertainties in the lifetime of methane continue to plague trace gas index calculations (IPCC, 1992). Sensitivity analysis performed on model parameters shows that methane lifetime is a key parameter; varying the lifetime of methane from 8 to 12 years (best estimate 10.5 years) could change the index by up to 50%; the index for methane was less sensitive to uncertainties in the carbon cycle. Uncertainties in climate models were the least important.

From the analyses in sections 2 and 4 we can draw some conclusions regarding the relative importance of the various economic and scientific uncertainties in trace gas index calculation for methane. We list them below in order of importance:

- Social Discount Rate
- Uncertainty in Methane lifetime
- Non linearity in Damage Functions
- Costs of abatement for Carbon

5.6 Conclusions

Comprehensive abatement strategies are based on the rationale that a minimum cost abatement strategy would require the control of multiple gases. This calls for the use of trace gas indices that allow for trading off between gases in a variety of possible abatement policies. This paper provides an evaluation of trace gas indices based on an optimal control framing. The analysis suggests that robust greenhouse gas indices require a better knowledge of non-linear greenhouse damage functions and greenhouse gas lifetimes. Uncertainties in costs of carbon abatement are less

important. Additionally, the choice of an appropriate discount rate has an important bearing on the outcome of index calculations.

The key issue of side benefits/costs of CO_2 abatement has been left out of the analyses on trace gas indices. To be sure, carbon abatement strategies will be accompanied in many cases by reductions in Sulfate, NOx and TSP emissions. The subsequent side benefits may have a net present value exceeding the benefits from damages avoided by carbon abatement. However, carbon abatement will also lead to a reduction in aerosol emissions and a subsequent increase in atmospheric radiative forcing.

Although an economics based approach, such as that presented in this paper, has several advantages compared to a purely scientific index, much of the debate on trace gas indices continues to be dominated by GWP, in spite of its scientific and conceptual flaws. If damages from climate change are highly non-linear then the use of GWPs may result in an overestimate of the benefits of greenhouse abatement projects involving non CO_2 trace gases. It is therefore important for approaches incorporating economics in calculations of greenhouse indices to gain more currency in the policy debate.

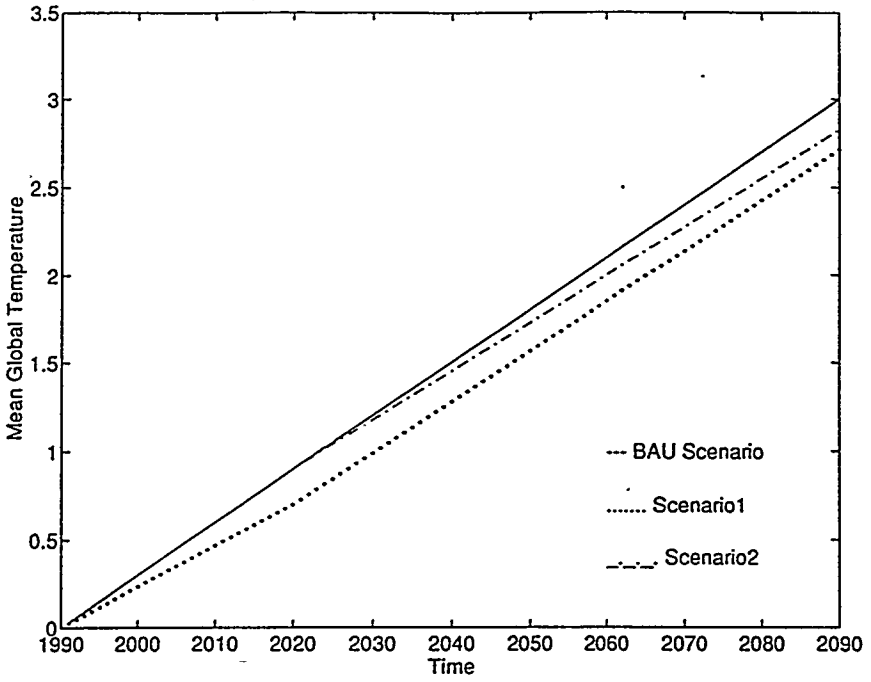

Figure: 5.1 Optimal global temperature paths with comprehensive abatement

Chapter 6: Concluding Remarks

In this chapter the main substantive contributions of this thesis are summarized and its limitations are discussed. Implications of this thesis for greenhouse science and policy and topics for future research are provided.

The central theme of this thesis was the use of available data in constructing consistent models for use in scientific and policy analysis. In chapter 1 of this thesis an ambitious claim was made--that reinterpreting and integrating available data will provide new insights. Clearly, the task at hand was a difficult one since the problems addressed have been well studied within a large scientific community of researchers. However, bringing together tools of modeling and data reconciliation for greenhouse problems where uncertainty is paramount has provided some new insights. Two broad insights emerge. First, analyses that explicitly incorporate uncertainty will go a long way towards attempting to answer important scientific and policy questions. Systematic inverse analysis would have revealed the large uncertainties in the biospheric source of carbon, well before the hypothesis of the missing sink by Tans et al. (1990). The lack of such analyses in the literature is a reflection of the fact that explicit characterization of uncertainties has never been a priority among biogeochemists. Curiosly, biogeochemists deal with uncertainties on a regular basis. Most biogeochemistry text books provide tables with ad-hoc uncertainty ranges; taking the analysis one step further and checking for consistency with observations may have substantial payoffs -- both in terms of reducing the uncertainties as well as providing research directions. The second insight that emerges deals with measurement, modeling and observation programs. Global change research is seldom informed by explicit decision theoritic framings where reducing uncertainties is an important outcome. We would not like to argue that research allocation should

be driven by "value of information" analyses[45]; however, performing such analyses may provide a baseline for discussion of alternative strategies for research. Systematic uncertainty analyses may have the added benefit of making explicit the subjective utilities of scientists for different research activities. Indeed, a recent debate on the oceanic carbon cycle and the JGOFS measurement program illustrates the need for such exercises. The emphasis of JGOFS on the role of marine biota in the oceanic carbon cycle is a subject of much controversy. Biological oceanographers have ascribed it a prominent role (Longhurst, 1992), while chemical oceanographers have strongly disagreed (Broecker, 1992). A systematic analysis of all the uncertainties in the ocean carbon cycle before the JGOFS program was made operational might have paved the way for a consensus. It must be added that much needs to be done in the area of research prioritization before it can meaningfully inform climate change policy choices. It is a field of inquiry that will continue to challenge scientists and decison theorists/policy analysts alike.

The application of chance constrained and bayes monte carlo techniques to the global methane cycle yielded budgets for methane which are consistent with observations and source-sink flux measurements. Global budgets for methane have been typically presented in an ad-hoc manner, without careful attention being paid to the uncertainties in individual sources and their consistency with observations. It is hoped that this analysis will draw attention to the need for researchers to provide a statistical interpretation of uncertainties in their observations, and also to the need for researchers to effectively integrate uncertainties into modeling.

The carbon cycle modeling efforts made in this work attempted to pin down the "missing sink" of carbon. The quantification of the missing sink has been the preoccupation of much recent research on the carbon cycle since the missing sink has some major implications for policy. Admittedly, this thesis has not provided any path-breaking new insights into the problem; this is to be expected given the current level of scientific interest in the problem, and given that the limited data has been interpreted by several prominent researchers. The results from the dynamic inversion presented in this thesis add to the growing body of evidence indicating that the biosphere may be

[45]Such Bayesian framings assume a complete characterization of the world. A luxury that most scientists can ill afford.

currently taking up around 2 GT of carbon per year. One important piece of work that could make a significant contribution to the literature involves the question of parameter identification and data worth; the analysis for this work is underway. The steady-state analysis may provide some important clues; however, in its current form the model has not adequately accounted for the covariance between the seasonality of carbon concentrations and atmospheric transport. Efforts to correct this discrepancy are in progress.

Finally, this thesis deals with the important policy question of comparing abatement measures for different greenhouse gases. The problem stands at the interface of science and economics. Not surprisingly the scientists have treated the economics in an ad-hoc manner, or have not treated it all, and the economists have treated the science as though it were a necessary evil--which they included, but without essential detail. This thesis has shown that a careful analysis of the scientific and economic factors determining the complex tradeoffs between greenhouse gases gives new insights into the relative roles of scientific and economic uncertainties in determining trace gas indices. Additionally, it shows that there is no single number for the index. The answer is tied to larger questions of economic valuation and technological growth. While this may make some uncomfortable, it is the task of the policy analyst to lay out the space for decision-making under uncertainty, with the hope of informing the policy process. Uncertainties cannot be wished away for the purpose of psychological comfort. That said, the analysis could be further enhanced to include side benefits of greenhouse gas abatement. It is entirely possible that in some cases the side benefits of abatement may well exceed the benefits of damages avoided. That would certainly make the choice of alternative abatement policies more transparent.

References

Adams, R.M., Chang C.C., McCarl B.A., Callaway J.M., 1992. The role of agriculture in climate change: A preliminary evaluation of emissions control strategies, in Economic issues in Global Climate Change, pp.273-287,Westview Press.

Ahuja, D.R. 1992. Estimating National Contributions to Greenhouse Gas Emissions, in J.K. Mitchell, Ed., Global Environmental Change, 22, pp 83-87.

Asselman, I., P.Crutzen, 1989. Global distribution of natural freshwater wetlands and rice paddies: their primary productivity, seasonality and possible methane emissions, *J. Atmos. Chem.*, 8, 307:358.

Augenstein D.C., 1990. Greenhouse Effect contributions of U.S. Landfill Methane, GRDCA 13th annual lanfill gas symposium, Lincolnshire, IL.

Ayres R.U., Waters J., 1991. Greenhouse effects: Damages, Costs and Abatement, Environmental and Resource Economics, 1:237:270.

Ayres, R.U., 1984. Limits and possibilities of large-scale long-range societal models, *Technological forecasting and Social Change*, 25, 297-308.

Bacastow, R 1981. Numerical evaluation for the In: *Carbon Cycle Modeling* ed. B. Bolin SCOPE 16. Wiley, 95-101.

Bacastow, R., & Keeling, C. 1981. Hemispheric airborne fractions difference and the hemispheric exchange time. In Bolin., B. Ed., *Carbon Cycle Modeling*, pp.241-246. SCOPE 16, John Wiley, New York.

Bachelet, D., Neue H.U., 1993a. Methane emissions from wetland rice areas of Asia, *Chemosphere*, Vol 26, 1-4, pp 219-238

Bachelet, D., Neue H.U., 1993b. Sources and Sinks of Methane: Working Group Report in

Banse, K., 1991. *Global Biogeochemical Cycles*, 5-4, 305-307.

Bard, Y., 1974. *Non linear Parameter Estimation.* Academic Press, New York.

Bartlett, K., Harris C., 1993. Review and assessment of Methane emissions from wetlands, Chemosphere, Vol 26, 1-4, 261-320.

Bartlett, K.B., P.M. Crill, J.A. Bonassi, R.L. Sass, R.C. Harriss, N.B. Dise, 1992. Methane flux from the Amazon River Floodplain : Emissions during rising water, *J. Geophys. Res.*, 95, 16773-17788.

Beck, L.L., S.D Piccot, D.A. Kirchgessner, 1993. Industrial Sources, in *The Atmospheric Methane Cycle: Sources, Sinks and Role in Global Change*, M.A.K. Khalil, ed., Springer Verlag, Berlin.

Bevington, P.R. 1969. *Data Reduction and Error Analysis for the Physical Sciences*, McGraw-Hill, New York.

Bingemer, H.G., and Crutzen, P.J., 1987. The production of Methane from solid wastes, *Journal of Geophysical Res* , 92, 2181-2187.

Bjorkstorm, A.., 1986. One and Two Dimensional Ocean Models for Predicting the Distribution of CO_2 between the Ocean and the Atmosphere, in the *Changing Global Carbon Cycle: A Global Analysis*. J. Trabalka, D.E. Riechle, Eds. Springer-Verlag.

Blake, D.R., and Rowland F.S., 1988. Continuing worldwide increase in tropospheric Methane, 1978 to 1987, *Science*, 239,1129-1131

Bolin, B., Bjorkstrom, A., Holmen, K., & Moore, B. 1983. The simultaneous use of tracers for ocean circulation studies. *Tellus*, 35B, 206-236.

Bolle, H.J., W. Seilar, B. Bolin, 1986. Other Greenhouse gases and Aerosols in *The Greenhouse Effect, Climatic Change, and Ecosystems* B.Bolin, ed., John Wiley and Sons, New York, 157-203.

Boyer, C.M., J.R. Kelafant, V.A. Kuuskra, K.C. Manger, D. Kruger, 1990. Methane emissions from coal mining: issues and opportunities for reduction, *EPA report no: 400/9-90/008*, U.S. E.P.A., Washington, D.C.

Broecker, W. S. and Peng, T.-H. 1982. *Tracers in the sea* Eldigio Press, Lamont-Doherty Geological Observatory, Palisades, N.Y.

Broecker, W. S., 1991. Keeping Global Change Honest, *Global Biogeochemical Cycles*, 5-3, 191-192,

Broecker, W., & Peng, T.-H. 1992. Interhemispheric transport of carbon dioxide by ocean circulation. *Nature, 356*, 587-89.

Brook, A., Kendrick, D., & Meerhaus, A. 1988. *GAMS: A Users's Guide*. Scientific Press, Redwood City, CA.

Bryson, A.E., Y. Ho 1975, Applied Optimal Control, Hemisphere Publishing Co., New York.

Carlson, C.A., H.W.Ducklow, A.F. Michaels, Annual Flux of Dissolved Organic Carbon from the euphotic zone in the Northwestern Sargasso Sea, *Nature*,371, 405-408.

Cass, G.R., and McRae G.J., 1983. Source Receptor reconciliation of routine air monitoring data for trace metals: An emissions inventory assisted approach, *Environ. Sci. Technol*, 17, 129-139.

Charlson, R. J., Schwartz, S. E., Hales, J. M., Cess, R. D., Jr, J. A. C., Hansen, J. E. and Hofmann, D. J. (1992). Climate Forcing by Anthropogenic Aerosols. *Science* 255(5043): 423-430.

Charnes, A., W.W. Cooper, 1960, Normal deviates and chance constraints, *J. Am. Stat. Assoc*, 52, 134-148.

Cicerone, R.J., 1991. *Environment*, March 1991.

Cicerone, R.J., Oremland R.S., 1988. Biogeochemical aspects of atmospheric Methane, *Global Biogeochemical cycles,* 1988, 2, 229-327.

Cline, W 1992, *The Economics of Global Warming*, Institute for International Economics, Washington D.C.

Crutzen P.J., I. Asselman, W. Seiler, 1986. Methane production by domestic animals, wild ruminants, and other herbivorous fauna and humans. *Tellus*, 38B, 271-280.

Crutzen, P.J., 1988 . Tropospheric Ozone: An Overview in *Tropospheric Ozone: Regional and Global scale interactions* , I.S.A Isaksen., Ed., D. Reidel , Boston, MA.

Crutzen, P.J., 1991. Methane's sinks and sources, *Nature*, 350, 380-381.

Cuthrell, J.E., L.T. Beigler 1987, On the Optimization of Differential- Algebraic Systems, *AIChE J.*, 33, 1257-1280.

D. Freeman, R. Egami, N. Robinson,J .Watson, A Method for Propogating Measurement Uncertainties Through Dispersion Models, *Journal of the Air Pollution Control Association*, 36, 246-253.

Dickinson, R.E. 1981, Convergence Rate and Stability of Ocean-Atmosphere Coupling Schemes with a Zero-Dimensional Climate Model, Journal of Atmospheric Sciences, **38**, pp 2112-2120.

Diwekar, U. 1994. Batch Distillation, Taylor and Francis.

DOE 1994, The Climate Change Action Plan: Technical Supplement, U.S. Department of Energy, Washington, D.C.,

Dowlatabadi, H., Kandlikar, M., Parwardhan, A. 1994, Dynamic forms for Greenhouse Damage Functions, Paper presented at the AWMA conference on Global Climate Change Science and Policy, Phoenix, Az, April 1994.

Dowlatabadi, H., M.G. Morgan, 1993. A model framework for the integrated studies of the climate problem, *Energy Policy*, March 1993, 209-221.

Eckaus, R, 1992, Comparing the effects of greenhouse gas emissions on global warming, The Energy Journal, 13, 1, 25-25

Ehhalt, D.H., 1974. The atmospheric Cycle of Methane, *Tellus,* 26B, 58-70.

Emanuel, W., Killough, G., Post, W., & Shugart, H. 1984a. Modeling terrestrial ecosystems in the global carbon cycle with shifts in carbon storage capacity by land-use change. *Ecology,* 65, 970-983.

Emanuel, W., Killough, G., Post, W., Shugart, H., & Stevenson, M. 1984b. Computer implementation of a globally averaged model of the world carbon cycle. Tech. rep. DOE/NBB-0062, TR 010, ORNL/DOE, Washington, D.C.

Enting, I., & Mansbridge, J. 1989. Seasonal sources and sinks of atmospheric CO_2: Direct inversion of filtered data. *Tellus, 41B,* 111-126.

Enting, I., & Pearman, G. 1987. Description of a one-dimensional carbon cycle model calibrated using techniques of constrained inversion. *Tellus, 39B,* 459-76.

Enting, I., 1985a. A classification of Inverse problems in geochemical modeling, *Tellus*, 37B, 216-229.

Enting, I., 1985b. Principles of Constrained inversion in the calibration of Carbon cycle models, *Tellus*, 35B, 1-27.

Enting, I., G. Newsam, 1990. Atmospheric Constituent Inversion Problems Implications for Baseline Monitoring, *J. Atmos. Chem.*, 11, 69-87.

Enting, I., J. Mansbridge, 1989. Seasonal sources and sinks of atmospheric Carbon: Direct inversion of filtered data, *Tellus*, 41B, 1991, 111-126

Enting, I., J. Mansbridge1991. Latitudinal distribution of sources and sinks of Carbon: Results of an inversion study, *Tellus*, 43B, 1989, 156-170.

Enting, I., Pearman, G., 1987. Description of a one-dimensional model of the Carbon cycle calibrated using techniques of constrained inversion,*Tellus*, 39B, 459-76.

Enting, I., Rodhe, H., 1991, Greenhouse Budgets, Nature, 349, pp 468.

Enting, I.G., Newsam G.N., 1990., Atmospheric Constituent inversion problems : Implications for Baseline monitoring, *J. Atmos.Chem*, 11, November 1990, pp. 69-87

Enting, I.G., Newsam G.N., 1990., Atmospheric Constituent inversion problems : Implications for Baseline monitoring, J. Atmos.Chem, 11, November 1990, pp. 69-87

Enting,I. 1993. Personal Communication.

Enting,I., & Mansbridge, J. 1991. Latitudinal distribution of sources and sinks of CO_2: results of an inversion *study. Tellus, 4~B,* 156-170.

EPA, 1990. *Methane emissions and opportunities for control*, EPA/400/9-90/007, September 1990.

Esser, G. 1992. *The Role of the Tropics in the Global Carbon Budget: Impacts and Possible Developments, pp.* 241-252. Advances in Life Sciences. Birkhauser/Verlag, Basel, Switzerland.

Falk I., R. Mendelsohn 1993, The Economics of Controlling Stock Pollutants: An Efficient Strategy for Greenhouse Gases, Journal of Environmental Economics and Management, **25**, pp-76-88

Fung, I., John J., Matthews E., Prather M., Steele L.P., Fraser, P.J., 1991. Three dimensional model synthesis of global Methane cycle, *J. Geophys. Res*, 96, 13033-13065.

Fung, I., K.Prentice, E. Matthews, M. Prather, G. Russell, 1983. Three Dimensional Model of the Global Carbon cycle, *J. Geophys. Res.*, 96, 13033-13065.

Gelb, A. 1988. *Applied Optimal Estimation*, MIT Press, Cambridge, MA.

Ginn, T.R., and Cushman J.H., 1990 . Inverse methods for subsurface flows: A critical review of stochastic techniques, *Stochastic Hydrol.Hydraul*, 4, 1-26

Grubb, M.J., D.G. Victor, Hope W.C., 1991. Pragmatics in the greenhouse, *Nature*, 354, 348-350.

Guthrie, P. Yarwood G., 1991. Analysis of the IPCC future Methane simulations, *SYSAPP-91/114, Systems Application International*, San Rafael, CA.

Hammersley, J.M., D.C. Hanscomb, 1964. *The Monte Carlo Method*, Pergamon, Oxford.

Hammond B, Moomaw, L., Rodenburg, E. 1991, Greenhouse Budgets, Nature, 349, pp 468

Hammond B, Moomaw, L., Rodenburg, E., 1990, Calculating National Accountability for Climate Change, Environment, Vol **33**,, Number 1, 11-33.

Handel, M 1991, Greenhouse Budgets, Nature, 349, pp 468

Harris, R., A. Thompson, M. Gibbs and K. Hogan, 1992. The Future of Atmospheric Methane in *The Atmospheric Methane Cycle: Sources, Sinks and Role in Global Change*, M.A.K. Khalil, ed., Springer Verlag, Berlin.

Harvey, 1993, A Guide to Global Warming Potentials, Energy Policy, Jan. 1993, pp 24-33.

Heimann, M., & Keeling, C. 1986a. Meridional eddy diffusion model of the transport of atmospheric carbon dioxide l. seasonal carbon cyle over the tropical pacific ocean. *Journal of Geophysical Research, 91* D7, 7765-81.
Henrion, M., Fischoff, B., 1986. Assessing the uncertiainty in physical constants, *American Journal of Physics*, 54-9, 791-798.

Hogan, K., J. Hoffman, A. Thompson, 1991. Methane on the greenhouse agenda, *Nature*, 354, 181-182.

Hyson, P., P.J. Fraser, G.I. Pearman, 1980. A two dimensional transport simulation model for trace atmosheric constituents, *J. Geophys. Res.*, 85, 4443-4455.

IPCC 1990, Greenhouse gases and aerosols in Climate Change, The IPCC Scientific Assessment. Cambridge University Press, 1990, 7-40

IPCC 1992, Greenhouse gases and aerosols in Climate Change 1992, The Supplementary Report to The IPCC Scientific Assessment. Cambridge University Press, 1992, 51-67

Johnson, D.E., T.M. Hill, G.M. Ward, K.A. Johnson, M.E. Branine, B.R. Carmean, D.W. Lodman, 1993. Ruminants and other animals, in *The Atmospheric Methane Cycle: Sources, Sinks and Role in Global Change*, M.A.K. Khalil, ed., Springer Verlag, Berlin.

Judd, A.G., R.H. Charlier, A. Lacroix, G. Lambert, C. Rouland, 1993. Minor Sources of Methane, in *The Atmospheric Methane Cycle: Sources, Sinks and Role in Global Change*, M.A.K. Khalil, ed., Springer Verlag, Berlin.

Kamien, M.I., N.L.Schwartz 1981, Dynamic Optimization: The Calculus of Variations and Optimal Control in Economics and Management, North Holland, Amsterdam.

Kammen, D.M., Marino B.D., 1993. On the origin and magnitude of pre-industrial anthropogenic CO_2 and Methane emissions, *Chemosphere*, Vol 26, 1-4, pp 69-86.

Kanakidou, M., Crutzen, P.J., 1993 Scale problems in global tropospheric chemistry modeling: comparison of results obtained with a three-dimensional model, adopting longitudinally uniform and varying emmisions of NOx and NMHC, Chemosphere, Vol. 26, Nos. 1-4, 787-803.

Kandlikar, M., Patwardhan, Optimal Control Framework for Trace Gas Index Calculations, Preseneted at the 32nd Hanford Regional Conference on Health and the Environment, Richland, WA, October 1993.

Keeling, C. D, Piper, S C and Heimann. M. 1989b. A three dimensional model of atmosphcnc CO_2 transport based on observed winds: 4. Mean annual gradients and interannual variations *Ceophysical Monograph 55* 305-363

Keeling, C., & Heimann, M. 1986. Meridional eddy diffusion model of the transport of atmospheric carbon dioxide 2. mean annual carbon cycle. *Journal of Geophysical Research, 91* D7, 778296.

Keeling, C., Piper, S., & Heimann, M. 1989. *Aspects of Climate Variability in the Pacific and the Western Americas*, pp. 305-363. Geophysical Monographs, 55. American Geophysical Union, Washington, D.C.

Keeling. C. D Bacastow, R. B., Caner, A F, Piper, S. C Whorr, T. P., Heimann, M., Mook, W G and Roelorrzen, H. 1989a. A three dimensional model of atmospheric CO2 transport based on observed winds: 1. Analysis Or obsenational data *Geophysical Monograph 55* 165-236

Khalil, M., & Rasmussen, R. 1990. The global cycle of carbon monoxide: Trends and mass balance, *Chemosphere*, 201-2, 227-242.

Khalil, M.A..K., and Rasmussen R.A., 1990, Constraints on global mass balance and an analysis of recent budgets, *Tellus* , 42B, 229-236, 1990.

Khalil, M.A.K. , 1992. A Statistical Method for Estimating uncertainties in the total global budgets of atmospheric trace gases, J. Environ. Sci. Health, A27, 3 , 755-770.

Khalil, M.A.K., and Rasmussen R.A., 1983. Sources, sinks and seasonal cycles of atmospheric Methane, *J. Geophys. Res*, 88, 5131-5144.

Khalil, M.A.K., and Rasmussen R.A., 1990. Atmospheric Methane: recent global trends, *Envrion. Sci. Technol.*, 24, 549-53.

Khalil, M.A.K., R.A. Rasmussen, J.R.J. French, J.A.Holt, 1990. The influence of termites on atmospheric trace gases - CH_4, CO_2,$CHCl_3$, N_2O, CO, H_2 and light hydrocarbons. *J. Geophys.Res.*, 95, 3619-3634.

Khalil, M.A.K., R.A. Rasmussen, M.J., Shearer, S. Ge, J.A. Rau, 1993. Methane from coal burning, *Chemosphere*, Vol 26, 1-4, 473-478

Khalil, M.A.K., Rasmussen R.A., 1993. Decreasing trend of Methane: unpredictability of future concentrations. *Chemosphere*, Vol 26, 1-4, 803-814

Kirchgessner, D.A., Piccot S.D., Winkler J.D., 1993. Estimate of global emissions from coal mines, *Chemosphere*, Vol 26, 1-4, 453-473

Knox, F. and McElroy, M. B. 1984. Changes in atmospheric CO_2: influence of the marine biota at high latitudes. J. *Geophys. Res. 89* 4629-4637

Kvenvolden, K., 1988. Methane Hydrate: A major reserve of carbon in the shallow geosphere, in *Origins of Methane in the Earth* , M.Schoell, ed., 10:223-243.

Kvenvolden, K., 1988. Methane hydrates and global climate, *Global Biogeochemical cycles*, 2, 221-229.

Lacroix, A.V., 1993. Unaccounted for sources of fossil and isotopically enriched Methane and their contribution to the emissions inventory: a review and synthesis,*Chemosphere*, Vol 26, 1-4, 507-559

Lambert, G., Scmidt S., 1993. Revaluation of oceanic flux of Methane: uncertainites and long term variations *Chemosphere*, Vol 26, 1-4, 579-590.

Land, K.C., S.H. Scheider, 1987. Forecasting in the social and natural sciences: An overview and analysis of isomorphisms, *Climatic Chan*ge, 11, 7-31.

Lashof and D.R. Ahuja 1990, Nature, **344**, 529-531.

Lave L.B., Dowlatabadi, H., 1993. Climate change policy: The effects of personal beliefs and scientific uncertainty. *Environ. Sci and Tech.*, 27-10, 1962-1972.

Lave, L., Dowlatabadi, H., 1993, Climate Change : Effect of personal belief and scientific uncertainty, Environ. Sci. Technol, **259**, pp-1381

Lave, L., Vickland K.H., *Risk Analysis*, 9, 283-91.

Lawson, C.L and Hanson, R.J., 1974. *Solving Least Squares Problems*, Prentice Hall, Englewood Cliffs, NJ.

Lelieveld, J., P.J. Crutzen, C. Bruhl 1993, Climate effects of atmospheric methane, *Chemosphere*, Vol. 26, Nos. 1-4, 739-769.

Levine, J.S., W.R. Cofer, J.P. Pinto, 1993. Biomass Burning, in *The Atmospheric Methane Cycle: Sources, Sinks and Role in Global Change*, M.A.K. Khalil, ed., Springer Verlag, Berlin.

Levine, J.S.. ed., 1991. *Global Biomass Burning : Atmospheric, Climatic and Biospheric Implications*, MIT press, Cambridge, MA.

Lieleveld, J., P.J., Crutzen, C. Bruhl, 1992. Climatic effects of atmospheric methane, *Chemosphere*, 26, 1-4, 739-768.

Logan, J.A., M.J. Prather, S. C. Wofsy, and M.B. McElroy, 1981. Tropospheric Chemistry: A Global Perspective, *Journal of Geophysical Res* , 86, 7210-7254.

Longhurst, A.R., 1991. A Reply to Broecker's Charges, *Global Biogeochemical Cycles*, 5-4, 315-316.

Luckacs, 1960. *Characteristic functions*, Charles Griffin, London.

M.B. Beck, 1987. Water Quality Modeling: A Review of the Analysis of Uncertainty, *Water Resources Research*, 23, 1392-1442.

Maier-Reimer, E. and Hasselman, K., 1987, Transport and Storage of CO_2 : An Inorganic Ocean Circulation Carbon Cycle Model, Climate Dynamics, 112, 63-90.

Marland, G. 1989. Fossil fuels CO_2 emissions *CDIAC Communicalions Winter 1989*. Carbon Dioxide Information Analysis Center, Oak Ridge National Laboratory, Oak Ridge, TN. 1-3.

Martius, C., R. Wassman, U. Thien, A. Bandeira, H. Renneneberg, W.Junk, W. Seiler 1993. Methane emission from wood feeding termites in Amazonia, *Chemosphere*, 26, 1-4, 623-632.

Mathews, E., I. Fung, 1987. Methane emissions from natural wetlands: Global distribution, area and environment of characteristics of sources, *Global Biogeochemical Cycles*, 1, 61-86

Mathews, E., I. Fung, J. Lerner, 1991. Methane emissions from rice paddies : Geographic and seasonal distribution of cultivated areas and emissions, *Global Biogeochemical Cycles*, 5, 3-24.

Matthews, E., 1993. Wetlands, in *The Atmospheric Methane Cycle: Sources, Sinks and Role in Global Change*, Springer Verlag, Berlin.

Morgan M.G., H. Dowlatabadi, 1994. What have we learnt from Integrated Assessments of climate change ?, to be submitted.

Morgan, M G., Henrion, M.1990 , Uncertainty : A guide to dealing with uncertainty in quantitative risk and policy analysis, Cambridge University Press, Cambridge.

Newell R.E., G.J. Boer, J.W. Kidson, 1974. An estimate of the interhemispheric transfer of carbon monoxide from tropical general circulation data, *Tellus*, 26, 103-107.

Nordhaus W.D 1992., An optimal transition path for global climate policies, *Science* 258, 1315-1319 .
Oechel W.S., S. Cowles, N. Grulke, S.J. Hastings, 1994. Transient Nature of CO2 fertilization in Arctic Tundra, *Nature*, 371, 500-503.

Oeschger, H, Siegenthaler, U., Schotterer, U. and Gugelmann, A. 1975. A box dilrusion model to study the carbon dioxide exchange in nature. *Tellus* 27, 168-192.

Oeschger, H., Siegenthaler, U., Schotterer, U., & Gugelmann, A. 1975. A box diffusion model to study the carbon dioxide exchange in nature. *Tellus*, XXVII2, 168-192.

Orlich, J, 1990. Methane emissions from landfill sites and waste water lagoons, Proceedings of the International Workshop on methane emisiosn from natural gas systems, coal mining, and waste management systems. U.S. EPA, Washington, D.C.

Osborne, T.J., Wigley, T.M.L., 1994, A simple model for estimating methane concentration and lifetime variations, Climate Dynamics, 9:181-193.

Papoulis, A. 1984. *Probability, Random Variables and Stochastic Processes*, McGraw Hill,

Patwardhan, A., Small, M., Bayesian Methods for Model Uncertainty Analysis with Applications to Future Sea Level rise, *Risk Analysis*, 124, 513-523.

Pearman, G.I., D. Etheridge, F. de Silva and P.J. Fraser, 1986. Evidence of changing concentration of atmospheric CO_2, N_2O and Methane from air bubbles in the Antarctic ice, *Nature*, 320, 248-250.

Pearman, G.I., P. Hyson 1980. Activities of the global biosphere as reflected in atmospheric carbon dioxide records, *J. Geophys. Res.*, 85, 4468-4474.

Pearman, G.I., P. Hyson, P.J. Fraser, 1983. The global distribution of atmospheric carbon dioxide:1 Apects of observations and modeling, *J. Geophys. Res.*, 88, 3581-3590.

Peck, S.C., Teisberg, T., 1993, CO_2 Emmisions Control: Comparing Policy Instruments, The Energy Journal,Vol **21**,No.**3**, 222-230.

Peer R.L., Thornsloe S.A., Epperson, D.L., 1993. A comparison of methods estimating global Methane emissions from landfills, *Chemosphere*, Vol 26, 387-401.

Peng, T., Broecker, W., Freyer, H., Trumbore, S. A deconvolution of tree-ring based d13C record, *Journal of Geophysical Res,* 88C, 1983, 3609-20.

Prinn, R., D. Cunnold, P. Simmonds, F. Alyea, R. Boldi, A. Crawford, P. Fraser, D. Gutzler, D. Hartley, R. Rosen, R. Rasmussen, 1992. Global average concentration and trend for hydroxyl radicals deduced from ALE/GAGE trichloroethane data for 1978-1990, *J. Geophys. Res*, 97, 2445-2461.

Prinn, R., D. Cunnold, R. Rasmussen, P. Simmonds, F. Alyea, A. Crawford, P. Fraser, R. Rosen, 1987. *Science*, 238, 945-95037.

Quay, P.D., S.L. King, J. Stutsman, D.O. Wilbur, L.P. Steele, I.Fung, R.H.Gammon, T.A. Brown, G.W. Farrel, P.M. Grootes, F.H. Schmidt, 1991. Carbon isotopic composition of of atmospheric Methane: Fossil and biomass burning source strengths, *Global Biogeochemical Cycles*, 5, 25-47.

Quay, P.D., Tilbrook, B., C.S. Wong, 1992. Oceanic Uptake of Fossil Carbon: Carbon-13 Evidence, *Science*, 256, 74-79.

Ramaswamy, V., Schwarzkopf M.D., Shine K.P., 1992, Nature, 355, 810-812.

Rasmussen, N. 1975. Reactor Safety Study, Technical Report, WASH-1400, U.S. Nuclear Regulatory Commission.

Raynaud, D., Chappelaz J., Barnola J.M., Koretkevich Y.S., Lorius C., 1988. Climatic and Methane cycle implications of glacial interglacial Methane change in the Vostok ice core, *Nature* , 333, 655-657.

Reilly, J., Richards K.R. 1993. Climate Change and Trace gas index issue, Environmental and Natural Resource Economics, **3**:41-61.

Rennenberg, H., R. Wassman, H. Papen, W. Seiler, 1992. Trace Gas exchange in Rice cultivation, *Ecological Bulletins*, 42.

Robertson, J., & Watson, A. 1992. Thermal skin effect of the surface ocean and its implications for CO2 uptake. *Nature, 358,* 738-40.

Rouland, C., A. Brauman, M. Labat, M. Lepage, 1993. Nutritional factors affecting methane emissions from termites, *Chemosphere*, 26, 1-4, 617-622.

Rubin, E., M. Small, C. Bloyd, M. Henrion, An Integrated Assessment of Acid Deposition Effects on Lake Acidification, 1992a. *Journal of Environmental Engineering, A.S.C.E.*, 118, 120-134.

Rubin, E.S, R.N. Cooper, R.A. Forsch, T.H. Lee, G. Marland, A.H. Rosenfeld, D.D Stine, 1992b. Realistic Mitigation Options for Global Warming, *Science*, 257, 148-266

S.C. Peck and T.Teisberg, 1991. Global Warming Uncertainties and the Value of Information: An Analysis using CETA, Electric Power Research Institute, 1991.

Safley, L.M., M.E. Casada, J.W. Woodbury, K.F. Roos, 1992. , Global methane emisisons from livestock and poultry manure, EPA/400/1-91/048, U.S.E.P.A., Washington, D.C.

Sarmiento, J., & Sundquist, E. 1992. Revised budget for the oceanic uptake of anthropogenic carbon dioxide. *Nature, 356,* 589-593.

Sarmiento, J., and Pacala, S., 1994. Terresterial Uptake of Antropogenic Carbon, Submitted to *Nature.*

Sarmiento, J., Orr, J. C. and Siegenthaler. U 1992. A perturbation simulation of CO_2 uptake in an Ocean General Circulation Model., *J. Geophys Res* , 97, 3621-3645

Sarmiento, J.L., Toggweiler, J.R, 1984 A new model for thc role of thc oceans in determining atmospheric pCO_2, *Nature,* 308, 621-624

Schmalensee, R. 1993, Comparing Greenhouse Gases for Policy Purposes, *Energy Journal* 141, 245-255.

Schneider, S.H., S.L. Thompson 1981, *J. Geophys Res* , 86, 3135-3150.

Schutz, H., W. Seiler, H. Rennenberg, 1990. Soil and land use related sources and sinks of methane in the context of the global methane budget, in *Soils and the Greenhouse Effect,* A.F. Bouman ed., J. Wiley and sons, N.Y., 29-63.

Shearer, M.J., Khalil, M.A.K., 1993. Rice Agriculture: Emissions, in *The Atmospheric Methane Cycle: Sources, Sinks and Role in Global Change*, M.A.K. Khalil, ed., Springer Verlag, Berlin.

Shlyakhter, A.I., D.M. Kammen, 1992. Sea level rise or fall, *Nature*, 357- 6373, 25.

Siegenthaler,U. 1983. Uptake of excess CO_2 by an outcrop-diffusion model or the ocean. *J. Geophys. Res.,* 88, 3599-3608.

Siegenthaler, U. 1987. Carbon dioxide: its natural cycle and anthropogenic perturbation. In: *The role of air-sea exchange in geochemical change* , P. Buat-Menard ed., Reidel, 209-247.

Siegenthaler, U. and Wenk, T. 1984. Rapid atmosphenc CO_2 variations and ocean circulation. *Nature,* 308, 624-625.

Siegenthaler, U., & Joos, F. 1992. Use of a simple model for studying oceanic tracer distributions and the global carbon cycle. *Tellus,* 441-454, 186-207.

Simon, H. 1990, Prediction and prescription in systems modeling, *Op. Res.*, 38-1, 7-14.

Smale, S. 1976. On the differential equations of species in competition, *J. Math. Bio,* 35.

Stevens, C., 1993. Isotopic Abundances in the Atmosphere and Sources, in *The Atmospheric Methane Cycle: Sources, Sinks and Role in Global Change*, M.A.K. Khalil, ed., Springer Verlag, Berlin.

Stewart, R.B 1992, Comprehensive and Market Based Approaches to Global Climate Policy, in in Economic issues in Global Climate Change, pp.24-40,Westview Press.

Sundquist, E. 1985. Geological perspectives on carbon dioxide and the carbon cycle. In W.S., Broecker,& Sundquist, E. Eds., *The Carbon CycleandAtmospheric CO_2: Natural Variations Archean to Present, pp.* 5-61. American Geophysical Union, Washington, D.C. Geophysical Monographs 32.

Tans, P. P, Fung, I., and Takahashi, T., 1990. Observational constraints on the global atmosphcric CO_2 budget, *Science,* 247, 1431-1438.

Tans, P. P. 1981 A compilation of bomb-^{14}C data for use in global carbon cycle models. In: *Carbon cycle modelling,* ed B. Bolin. . SCOPE 16. Wiley, 131-158

Tans, P., Fung, I., & Takahashi, T. 1990. Observational constraints on the global atmospheric CO2 budget. *Science,* 247, 1431-8.

Taylor, K. and Penner, J. E. (1994). Anthropogenic aerosols and climate change. *Nature* 369: 734-737.

Thompson, A.M., R.J. Cicerone, 1986. Possible perturbations to Atmospheric CO, CO_2, and OH. *J. Geophys. Res*, 91, 10853-10864.

Thorneloe, S.A., M.A. Barlaz, R. Peer, L.C. Huff, L. Davis, J. Magino, 1993. Waste Management, in *The Atmospheric Methane Cycle: Sources, Sinks and Role in Global Change*, M.A.K. Khalil, ed., Springer Verlag, Berlin.

Tie, X., F.N. Aylea, D.M. Cunnold, C.-Y Jim Kao, 1993. Atmospheric Methane: A global three dimensional model study, *J. Geophys .Res.*, 96, 17339-17348.

Tietenberg, T.1991, Environmental and Natural Resource Economics, Harper Collins.

Trends, 1991. A compendium of data on global change. CDIAC, Oakridge National Labs., Oakridge, TN.

Trends, Eds. Boden T.A., Kancurik P., Farrel M.P., 1990 , *Trends 1990, A compendium on global change,* The CO_2 Information Analysis Center, Oakridge National Laboratory.

USDJ, 1991 , US task force on the the Comprehensive Approach to Climate Change, A Comprehensive Approach to Addressing Potential Climate Change, U.S. Department of Justice, Wash., D.C.

Vaghjiani, G.L., A.R. Ravishankara, 1991. New Measurement of the rate coefficient for the reaction of OH with Methane. *Nature*, 350, 406-409.

Vajda, S., 1970, Stochastic Programming in *Integer and Non-linear programming*, J. Abadie ed., North Holland Publishing Company, 1970, 321-337.

Victor , D.G, 1991, Limits of market based strtaegies for slowing global warming: The case of tradeable permits, Policy Sciences, November 1991.

Villadsen, J., M. L. Michaelsen, 1978. Solution of Differential Equations Models by Polynomial Approximation, Prentice-Hall.

Wassman, R., Papan, H., H. Rennenberg, 1993. Methane emissions from rice paddies and possibel mitigation strategies, *Chemosphere*, 26, 1-4, 201-218.